ABSTRACT

Title of Dissertation: PHYLOGENETIC EXPLORATION OF MATING SYSTEM EVOLUTION IN THE EASTERN NORTH AMERICAN LEIOBUNINE HARVESTMEN (OPILIONES: SCLEROSOMATIDAE)

Mercedes M. Burns, Doctor of Philosophy, 2014

Directed By: Dr. Jeffrey W. Shultz, Associate Professor,
Department of Entomology

Understanding the basis for the vast diversity in reproductive structures found within the animal kingdom is a perennial issue in evolutionary biology. Meanwhile, taxonomists have long capitalized on the substantial genital diversity in the eastern North American leiobunine harvestmen for identifying and delimiting species, but no attempts have been made to explore the functional or evolutionary significance of this variety. Past discussion of the evolution of reproductive heterogeneity attributes genitalic diversification to female preferences, although recent work has also emphasized the (potentially competing) importance of intersexual conflict leading to sexually antagonistic coevolution. Here I test the overarching support for diversification of reproductive structures in leiobunine harvestmen via female choice and sexual conflict mechanisms of sexual selection. My dissertation work consisted of 1) reconstructing the phylogeny of eastern North American leiobunine harvestmen using molecular characters, 2) mapping and simulating relevant discrete morphological features, and 3), using biomechanical and kinetic reproductive data to test whether the direction of evolutionary change in reproductive characters within and between sexes is consistent with increasing sexual antagonism through evolutionary time via a comparative approach. I found support for the monophyly of the eastern North American leiobunine harvestmen, as well as evidence for an evolutionary transition from enticement-based mating to conflict-based systems. My novel uses of phylogenetic comparative methods to quantify mating systems demonstrate that leiobunine species form a continuum of reproductive diversity ranging from specialization in female enticement to precopulatory antagonistic contexts, with correlations between male and female discrete and continuous traits, suggesting long-term sexual coevolution has occurred. I conclude that mating system evolution has occurred in the leiobunine harvestmen, with sexual selection as its ultimate driver, and I offer hypotheses as to the origins of sexual conflict in these temperate lineages.

PHYLOGENETIC EXPLORATION OF MATING SYSTEM EVOLUTION IN THE EASTERN NORTH AMERICAN LEIOBUNINE HARVESTMEN (OPILIONES: SCLEROSOMATIDAE)

By

Mercedes M. Burns

Dissertation submitted to the Faculty of the Graduate School of the
University of Maryland, College Park, in partial fulfillment
of the requirements for the degree of
Doctor of Philosophy,
2014

Advisory Committee:

Dr. Jeffrey W. Shultz, Chair
Dr. Sarah Bergbreiter
Dr. Daniel Gruner
Dr. David Hawthorne
Dr. Priscila Chaverri, Dean's Representative

© Copyright by

Mercedes M. Burns

2014

DEDICATION

The production of my dissertation work was supported by those outside of the scientific community as well as those within it. I dedicate this work to my parents, Thomas J. and Judith J. Burns, my brother, Simon Burns, my sister, Mary E. L. Burns, my friends Andrew Scott and Chad Barry, and my future husband James C. Barklage, for their love, support, and willingness to be my audience when I needed one. They knew I was studying something a little “different” but always received my psycho-babble with interest and good humor. Thanks.

ACKNOWLEDGEMENTS

In the preparation of this dissertation, I would foremost like to thank my adviser, Dr. Jeffrey W. Shultz, who has been a true mentor, colleague, and friend throughout my graduate career. Jeff pushed me to be a more effective writer, a more thoughtful speaker, and a more dynamic scientist. He is the first person I go to when sharing my research triumphs and tribulations. May those days continue!

I additionally show appreciation for my past and present committee members, Drs. Sarah Bergbreiter, Priscila Chaverri, Daniel Gruner, David Hawthorne, and Gerald Wilkinson for their assistance and flexibility in my dissertation process. Beatrice Mao, Dr. Julie Byrd-Hebert, Alex Forde, and Greg Hess must also be thanked for their various roles in my graduate career—friendship, stimulating discussion, qualifying exam preparation, and laboratory support, just to name a few. Finally, I would like to acknowledge the following persons and organizations that supported the research covered in each chapter:

Chapter 1: I thank Elizabeth Ingianni for use of images included in Figure 1.1.

Chapter 2: A version of this chapter was previously published in the journal Molecular Phylogenetics and Evolution (Elsevier Ltd.) and is reprinted here under author-retained rights for scholarly purposes. I thank my coauthors, Dr. Jeffrey W. Shultz of the University of Maryland (UMD) and Dr. Marshal Hedin of San Diego State University (SDSU). Funding was provided by a collaborative National Science Foundation (NSF) grant awarded to JWS (DEB-0640179) and MH (DEB-0640173). JWS was also supported by the Maryland Agricultural Experiment Station. MMB was supported by a NSF Graduate Research Fellowship (GRF). P. Chander, J. Deas, M. McCormack, and J. Underwood helped in the collection of molecular data. Many persons provided data/samples or collected specimens for sequencing, including: A. Bailey, M. Brewer, J. Cokendolpher, P. Miller, P. Nunez, K. Prestwich, J. Satler, S. Schwartz, J. Starrett, G. Stratton, B. Tomberlin, M. Walker, D. Wilgers, and R. Willemart. I acknowledge the comments made by two anonymous reviewers in the preparation of this manuscript.

Chapter 3: A version of this chapter was previously published in the open source web journal PLoS ONE. I reprint it here under the Creative Commons Attribution 2.5 Generic License. I thank my coauthors and together we thank Joe Warfel (Eighth-Eye Photography) for the use of his photo of mating *L. vittatum* and acknowledge Kasey Fowler-Finn and three anonymous reviewers for comments on the manuscript. Funding was provided by a collaborative National Science Foundation grant awarded to JWS (DEB-0640179) and MH (DEB-0640173). JWS was supported by the Maryland Agricultural Experiment Station. MB was supported by a NSF GRF and a NSF Doctoral Dissertation Improvement Grant (DDIG). The funders had no role in study design, data collection and analysis, decision to publish, or preparation of the manuscript.

Chapter 4: In the production of this work I was supported by an NSF GRF, DDIG, and a University of Maryland Ann G. Wylie Dissertation Fellowship.

Chapter 5: Specimen collection for this project was achieved in one summer with the generous help of Mary E.L. Burns, Jeffrey W. Shultz, and the attendees of the 2013 American Arachnological Society annual meeting, held in Johnson City, TN. This work was financially supported by a NSF DDIG, and a UMD Ann G. Wylie Dissertation Fellowship.

TABLE OF CONTENTS

Chapter 1: Introduction and Background to Dissertation

Chapter 2: Molecular phylogeny of the leiobunine harvestmen of eastern North America (Opiliones: Sclerosomatidae: Leiobuninae)

Materials and Methods

Results and Discussion

Chapter 3: Comparative Analyses of Reproductive Structures in Harvestmen (Opiliones) Reveal Multiple Transitions from Female Choice to Precopulatory Antagonism

Materials and methods

Results

Discussion

Chapter 4: Comparative analyses of biomechanical reproductive traits in harvestmen (Arachnida, Opiliones) support intersexual coevolution via simultaneous sexual selection mechanisms

Methods

Results and Discussion

Conclusions

Chapter 5: Variation in the mechanical properties of male genitalia in harvestmen is consistent with variation in mating strategies

Methods

Results and Discussion

Conclusions

LIST OF TABLES

LIST OF FIGURES

CHAPTER 1: Introduction and background to dissertation

Sexual Selection

Sexual selection theory was first postulated by Charles Darwin to explain the origin and perpetuation of sex-specific characters, particularly in males, which tend to be the most decorated “in their weapons, means of defence, and charms” (Darwin, 1871). Females typically invest more in reproduction than do males and so are expected to mate preferentially with males demonstrating qualities leading to either direct (Fisherian) benefits to the female (Hosken and Stockley, 2004; Daly and Wilson, 1983) or indirect benefits that may be manifested in progeny. Assuming genetic variation and heritability of these characters, features preferred by females should accrue rapidly in a population and may result in complex and costly male structures and displays (Eberhard, 1985). This logic has resulted in the widespread assumption that sexual selection is dominated by female choice, either overtly via precopulatory mechanisms or cryptically via postcopulatory mechanisms (Arnqvist and Rowe, 2005; Andersson, 1994).

Species-specific variation in genitalia and other reproductive structures is pervasive in arthropod evolutionary biology (Eberhard and Cordero, 2003; Eberhard, 1985), and many workers regard sexual selection via female choice as sufficient to explain the origin and maintenance of this variation. However, some workers have noted species displaying structures and behaviors that appear to increase male fitness through coercive mating rather than through enticement or appeasement of females (Vahed, 2007; Hosken and Stockley, 2004; Sakaluk et al., 1995; Thornhill and Sauer, 1991). The existence of male coercion may produce selective pressure for females to present more discriminatory or defensive phenotypes, which would be reciprocated by the evolution of additional coercive features in the male and so on. This escalating pattern of conflict is termed sexually antagonistic coevolution (Arnqvist and Rowe, 2002). Reminiscent of the Red Queen hypothesis (Van Valen, 1973) in which organisms continually adapt to new selective pressures simply to maintain fitness (Venditti et al., 2010), a “sexual arms race” describes continual selection for the development of armaments and strategies in the sexes to gain control of mating outcomes. Though traditional female choice theory capitalizes on the existence of a male trait that can be identified and a preference that can be exploited (ie: as in the sensory bias hypothesis; Vahed, 2007), because exploitative structures or behaviors are countered by the opposite sex, sexual arms races may be common but largely invisible processes shaping mating interactions in a population (Arnqvist and Rowe, 2005; 2002).

Early research into the organization of sex roles based on anisogamy underscored the likelihood that sexes would be in conflict regarding mating rates (Chapman, 2010; Parker, 1979; Trivers, 1972). A superficial survey of male-female interactions across the animal kingdom suggests that mating and subsequent sexual selection in many species involves some level of overt sexual conflict (Chapman, 2010; Arnqvist and Rowe, 2005). However, obtaining experimental evidence of sexual conflict is challenging, because examples of obvious male-female coevolution may escape detection (whether due to their inability to lead to overall mating rate change or due to the subtlety of their mechanism) (Arnqvist and Rowe, 2005; Pizzari and Snook, 2003) and the costs and benefits of behaviors and structures associated with sexual interaction (and, additionally, the plasticity of these characters given environmental effects) are numerous and cryptic (Cornwallis and Uller, 2010; Fricke et al., 2009). Also, some controversy remains as to the type of data necessary for analysis of sexual conflict (Chapman et al., 2003; Pizzari and Snook, 2003). Potentially coevolving features are described discretely (for example, the presence or absence of a female barrier to prevent coercive mating by the male), through the size and shape of features associated with reproduction in a species (Bergsten and Miller, 2007; Koene and Schulenburg, 2005), and through the amount or proportion of time a sex is observed engaging in persistent, or resistant mating behaviors (Arnqvist and Rowe, 2002). Caution must be taken particularly with analyses of complex morphological data, which are vulnerable to subjective interpretations of a coercive or resistant reproductive function from appearance or drawings (Arnqvist and Rowe, 2005; Arnqvist, 1992).

Sexual selection via sexual conflict is typically presented as an alternative to female choice (Eberhard and Cordero 2003), where males of a species compete for access to females, who control fertilization with overt or cryptic mechanisms (Andersson, 1994). These mechanisms should not be considered as a binary, but as occupying different parts of a spectrum of many possible mechanisms, including the sensory bias and “sexy sons” hypotheses (Vahed, 2007; Hosken and Stockley, 2004), which may work in tandem. These hypotheses contain an undercurrent of conflict even when female “choice” is assumed: sensory biases can exploit female willingness to mate by advertising male signals that may not be honest, sons of high fitness may be produced through Fisherian selection at the cost of a female's fitness and potentially that of her daughters, and even traditional female choice occurs only in a backdrop of conflict, where some males will be rejected even after producing costly morphological traits and/or direct benefits for female attraction.

The presence of sexual conflict within a species may be satisfactorily confirmed by demonstrating predicted in male and female structures and behaviors, but to identify macroevolutionary processes like sexual arms races, species-specific tests of sexual conflict must be extrapolated to an inter-specific level. This requires the definition of the additional parameters of history and directionality. Because we are unable to examine directly the history of a population, species or lineage, a phylogeny-based approach with taxonomically broad sampling is needed to establish the direction of evolutionary covariation, that is, whether the intensity of conflict has increased or decreased through evolutionary time. Heretofore phylogeny-based tests of sexual conflict have been aimed at removing phylogenetic effects in order to analyze covariation of structures or behaviors across samples of modern species (Bergsten and Miller, 2007; Rönn et al., 2007; Szekely et al., 2006; Koene and Schulenberg, 2005; Arnqvist and Rowe, 2002) or to explore speciation as a consequence of sexual conflict (Gavrilets and Hayashi, 2005; Arnqvist et al., 2000). These tests may establish covariation resulting from conflict, but they do not determine whether the covariation is established by evolutionary escalation or de-escalation.

Phylogenetic Comparative Methods

When comparing the characteristics of multiple species, phylogenies and statistical methods that consume phylogenies are necessary (Felsenstein, 2004). This is because species are not independent results of macroevolution—because they evolved on a phylogeny they have a shared evolutionary history. Thus, sister taxa have a higher likelihood of possessing common trait than one species and its more distant ancestor. The assumptions made by ignoring shared evolutionary history confer a star-phylogeny assumption on taxa for which there are comparative data, regardless of the actual relationships (Garland et al., 2005).

Phylogenetic comparative methods (PCMs) can be used in many interspecific studies, including evaluations of phylogenetic autocorrelation of a trait (Garland et al., 2005; Harvey and Pagel, 1991; Cheverud et al., 1985) and assessment of covariance of two traits across a phylogeny (Paradis, 2006; Martins and Hansen, 1997; Harvey and Pagel, 1991; Felsenstein, 1985). In order to test the hypothesis that evolution in male and female reproductive structures is directional and covariable, I use several types of PCMs in order to study correlation of male and female traits: 1) phylogenetic generalized least squares, to generate size-corrected residuals (Revell, 2009a) where body size is expected to co-vary with trait type, 2) multivariate methods in which traits are either simulated across a phylogeny, or a maximum likelihood estimate of the combined covariance of traits with a phylogeny is applied to the variance/covariance matrix in order to account for variance due to shared history, and 3) likelihood-based methods conditioned on the ultrametric (i.e. tips contemporaneous) phylogeny for the estimate of traits rates and their correlations (Pagel and Meade, 2006). For procedures of type #3, iterated Monte Carlo simulation procedures are frequently used to estimate evolutionary model parameters and likelihoods, which then are compared using a log-likelihood ratio test:

$$LR = -2 \ \log_e(\frac{L(I)}{L(D)})$$

where *L(I)* is the likelihood of the tree under a standard or null model (ex. instantaneous rates of evolution are independent) and *L(D)* is the alternative model likelihood (ex. a dependent model where one state is dependent on another state) (Pagel, 1994). I implement log-likelihood ratio tests for discrete character sets in the BayesTraits program (Pagel and Meade, 2006; Venditti et al., 2006; Barker and Pagel, 2005; Pagel et al., 2004; Pagel and Meade, 2004) where evolutionary models are nested, allowing ratio test significance to conform to a chi-squared distribution in which degrees of freedom are indicated by the difference in the number of estimated parameters (Pagel, 1994). Where log-likelihood ratio tests are deemed inappropriate (i.e. models are not nested, or several competing models are tested), I use Akaike Information Criteria calculated from log-likelihood scores (Burnham and Anderson, 2004).

Study System

The leiobunine harvestmen, or “daddy-long-legs,” of eastern North America consist of about 30 known species that form a monophyletic group

(Burns et al., 2012). The basic anatomy of reproductive structures in leiobunine harvestmen is depicted in Figure 1.1 and is fundamentally similar in males and females. The primary genitalia consist of a variably sclerotized, cylindrical penis in males and a segmented ovipositor in females. Both are housed within a pregenital chamber that is covered externally by a genital operculum located below the preoral chamber. The pregenital chamber opens anteriorly with levator muscles. Mating occurs face to face, with the male using his pedipalps to clasp the female at the coxal bases of her second and third pairs of legs. The penis is everted throughout the mating process and eventually gains entry into the female pregenital opening. Insemination occurs when the tip of the penis penetrates the terminal opening of the ovipositor, which is retracted in the pregenital chamber during mating. Both sexes mate multiply and are traditionally assumed to mate indiscriminately and without apparent courtship. Among the approximately thirty described species, there is considerable species-level distinction in the length, structure, and complexity of the male intromissive penis, which may bear distal nuptial gift-delivering sacs, or no sacs, as well as intermediate forms. In lieu of an enticing gift, species lacking sacs show modifications that appear to aid in enforcing copulation, whether by avoiding female barriers, improving grip on a female during courtship with the pedipalps, or by forcing open the female genital operculum.

Historically, arthropod taxonomy focused heavily on species-specific male reproductive organs (Song and Bucheli, 2010), and male genitalia is frequently used to assign species in many arthropods (Bond et al., 2003; Eberhard, 1985).

Male reproductive characters are often found to evolved rapidly and divergently, punctuating speciation events by way of prezygotic mating isolation (Song and Bucheli, 2010; Soto et al., 2007). In the eastern North American leiobunine harvestmen genital variation has been shown to be common (Davis, 1934; McGhee, 1970; 1977), although until recently variation was only characterized in males (especially the penis and pedipalps) of recognized species. Female structures are often unknown or assumed to display no species-specificity (Eberhard, 2004b). The taxonomic focus on male anatomy reflects a general assumption by systematists that male genitalia evolve very rapidly and that females show comparatively little variation.

Recent work by myself and Dr. Jeffrey W. Shultz has added important insights into harvestman reproduction, namely, that there is close-contact courtship in harvestmen that superficially resembles copulation. The male grasps the female and everts the penis but is stayed from penetrating the female genital chamber. During this precopulatory period, the male produces a fluid nuptial gift from ducts at the base of the penis which is imbibed by the female. The proximity of the openings to the preoral and pregenital chambers may have led to the confusion between courtship and mating by earlier workers. In the so-called ‘sacculate’ species, the male has a pair of distal penile sacs that contains a small reservoir of nuptial gift, and these sacs are inserted into the female’s preoral chamber upon contact. In sacculate species, the male tends to be substantially smaller than the female, the penis is short and weakly sclerotized, and the pedipalps are simple. The sacculate condition is apparently primitive for

Leiobuninae, but occurs in few species in eastern North America. In contrast, most leiobunines in the United States lack the distal sacs— these species are termed ‘lanceolate’, or ‘non-sacculate.’ Lanceolate species show less size dimorphism, the penis is elongate and sclerotized, and the pedipalps are elaborate, presumably improving mate-clasping. Among the sacculate species females have largely identical genitalia. However, within lanceolate species that do not have nuptial gift sacs, females have developed opercular sclerites and pivoting sterna that seem to be used to exclude male genitalia. Taken together, these behavioral and morphological observations suggest to us that the leiobunine harvestmen of eastern North America have experienced evolution in mating system, perhaps indicative of a sexual arms race.

Overview

This work marks the first attempt to utilize a phylogeny-based approach to determine the existence *and* directionality of sexual selection mechanisms, rather than simply covariation of male and female armaments. Previous research on sexually antagonistic coevolution has been heretofore largely based on examinations of the qualities of individual species (Chapman et al., 2003). For example, many efforts have been made to explore the existence of intralocus sexual conflict (Bonduriansky and Chenoweth, 2008) under laboratory conditions (Pischedda and Chippindale, 2006; Rice et al., 2006; Fedorka and Mousseau, 2004) and in the wild (Foerster et al., 2007). These studies represent microevolutionary phenomenon that do not require the evolution of novel structures or behaviors, only changes in the frequency of genes controlling the relative intensity of existing behavior. While such inquiries may indeed uncover evidence of sexual conflict, there appears to be no way to accurately evaluate the existence of a sexual arms race without the use of phylogenetic trees to understand the character states of closely related groups and ancestral runners in such an arms race. Results from species-specific tests of sexual conflict must be extrapolated to encompass many species to accurately portray a sexual arms race scenario that identifies the direction of escalation/de-escalation of conflict.

In chapter 2, I describe the production of the first phylogenetic reconstruction of eastern North American harvestmen, specifically to address the historical signal from a potential sexual arms race. A phylogenetic reconstruction provides an essential historical framework for testing hypotheses concerning long-term evolutionary trends (Arnqvist and Rowe, 2005). Previous work showed that the leiobunine harvestmen of eastern North America are monophyletic and more closely related to Mesoamerican congeners than to European or Asian clades (Hedin et al., 2012). Thus, eastern North American harvestmen present the ideal simplified system with which to apply the morphological indicators of sexual conflict to a phylogenetic reconstruction. While considered one of the major groups of “poorly studied” arthropods (Coddington et al., 1990), harvestmen are exceedingly common in the eastern North America. The Appalachian region of the United States is known to be a center of opilionid diversity, characterized largely by male genitalia up until recently (Davis, 1934; McGhee, 1970; 1977) and additionally, the genital structures of harvestmen are easily accessed and less complex than many arthropods used for investigations in sexual conflict.

In chapter 3, I produce an ultrametric phylogeny and use Bayesian likelihood- and parsimony-based techniques to evaluate the evolutionary trajectory, covariation and rate precedence of discrete, binary reproductive morphologies—the presence or absence of penile nuptial gift sacs and presence or absence of female pregenital barriers—in leiobunine harvestmen. Based on the results of this analysis, which supported the coevolution of male and female armaments, I postulated the existence of morphological syndromes. These collections of male and female reproductive characters develop and coevolve as a consequence of the dominate mechanisms of sexual selection at play in the mating systems of the species. In this chapter I additionally offer hypotheses as to the proximate conditions in which sexual conflict and female choice might operate to produce the syndromes described.

This work is among the first to use biomechanical approaches to assess the mechanics of copulation rather than inferring function from morphology. Although attempts have been made to diagnose sexual conflict from images of structures and the perception that the structures are actually used for the purpose of controlling mating success and frequency (Bertin and Fairbairn, 2005; Eberhard, 2004a), functional morphology alone is insufficient to prove that a given structure developed due to or is affected by sexual conflict. In contrast, genital biomechanical studies can be used to generate data that describe the actions and forces created by the genitalia for the purpose of influencing mating rate. By analyzing these continuous traits of genitalia, which are directly related to mating success, we can make inferences on the dynamics of mating system change based on contrasts independent from phylogeny. In Chapters 4 and 5, I examine the phylogenetic signal and evolutionary correlations of suites of reproductive biomechanical and genital force traits, and I make inferences on the contributions of female choice and sexual conflict to the morphological diversity of species via multivariate classification analyses.

Finally, in chapter 6 I revisit the apparent mutual exclusivity of sexual selection mechanisms as they continue to receive regular academic discussion, and I summarize the contributions of my work to this discourse. I conclude by describing the ongoing and future work in the fields of sexual selection and reproductive functional morphology.

Figures

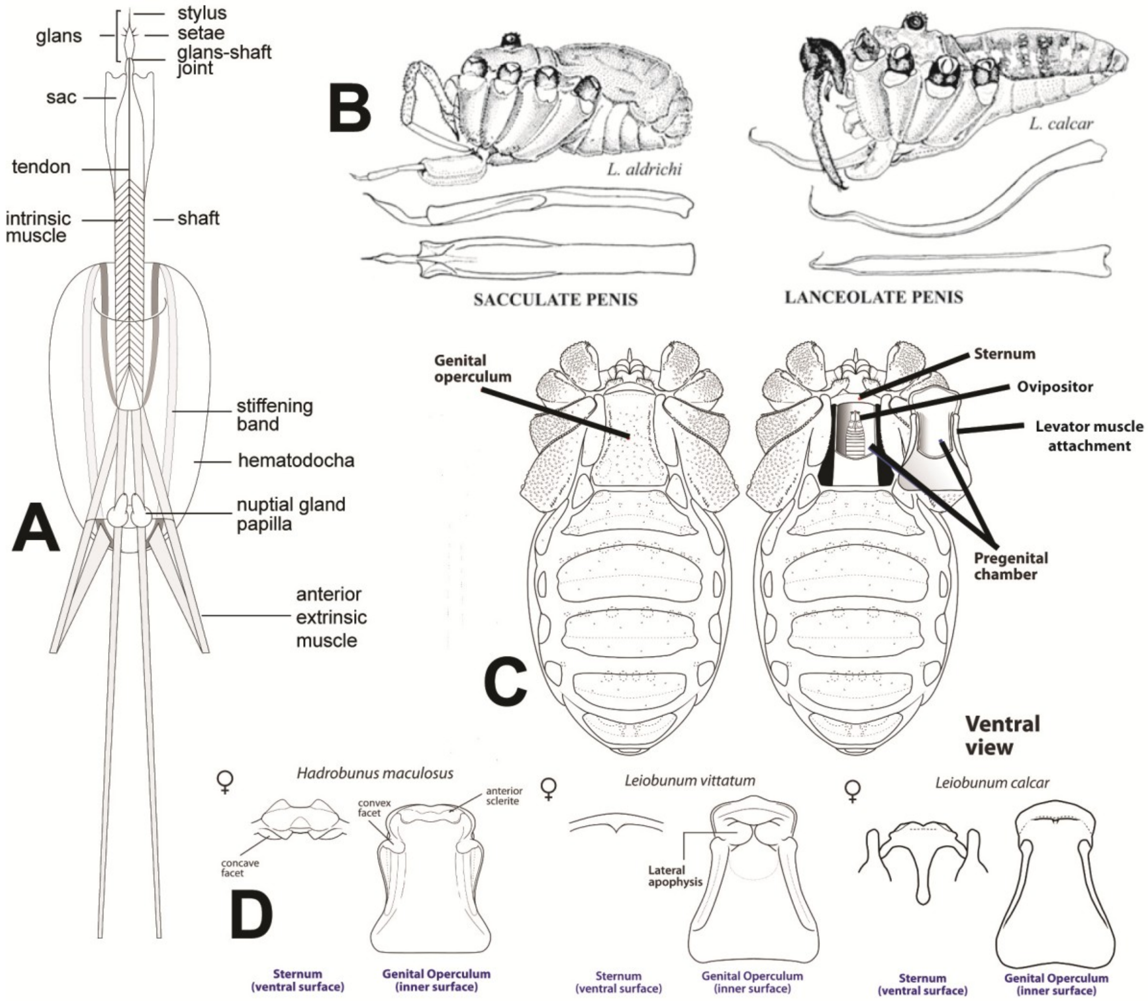

Figure 1.1: Leiobunine harvestman morphology. Genitalia of the sacculate male is diagrammed in (A). Examples of sacculate and lanceolate males (legs removed; from Bishop, 1949) are given in (B). Note penis length and curvature is strongly related to body shape and lanceolate male displays enlarged pedipalps. A ventral view of a sacculate female is shown in (C) with genital operculum removed. Elaborations of the female opercula and sterna forming pregenital barricades from the lanceolate *calcar* (courtesy of Elizabeth Ingianni)*, vittatum,* and *Hadrobunus* sp. lineages are identified in (D).

CHAPTER 2: Molecular phylogeny of the eastern North American leiobunine harvestmen (Opiliones: Sclerosomatidae: Leiobuninae)

Mercedes M. Burns, Marshal Hedin, Jeffrey W. Shultz

See Appendix 1 for supplementary tables (Tables S2.1 – S2.2) and figures (Figures S2.1) referenced in this chapter.

Abstract

Phylogenetic relationships among the leiobunine harvestmen or ‘‘daddy-longlegs’’ of eastern North America (*Leiobunum, Hadrobunus, Eumesosoma*) are poorly known, and systematic knowledge of the group has been limited largely to species descriptions and proposed species groups. Here we obtained mitochondrial (NADH1, 16S and 12S rDNA) and nuclear (28S rDNA, EF-1a introns and exons) DNA sequences from representatives of each genus, virtually all *Leiobunum* species from the USA and Canada, four western North American outgroup species and the distantly related *Phalangium opilio*. We applied Bayesian, maximum-likelihood and parsimony methods under various data-partition treatments to reconstruct phylogeny and to test taxonomy-based phylogenetic hypotheses. Results were largely congruent among methods and treatments and well supported by bootstrap and posterior probability values. We recovered *Leiobunum* as paraphyletic with respect to *Eumesosoma* and *Hadrobunus*. Most species were encompassed by five well-supported clades that broadly correspond to groups based on male reproductive morphology (*Hadrobunus* group, an early-season *Leiobunum* group, *L. vittatum* group, *L. politum* group and *L. calcar* group). Relationships within species groups were

often ambiguous or inconsistent with morphology, suggesting the presence of gene introgression or deep coalescence and/or the need for taxonomic revision.

Introduction

The harvestman or ‘‘daddy-longlegs’’ fauna of eastern North America (i.e., eastern and central USA and adjacent Canada) is dominated by the subfamily Leiobuninae (Sclerosomatidae), with four genera (*Leiobunum, Nelima, Hadrobunus, Eumesosoma*) encompassing about 35 described species. *Leiobunum* and *Nelima* are species rich genera that also occur in Mesoamerica, East Asia and the Euro-Mediterranean Region. *Hadrobunus* and *Eumesosoma* contain few species and are endemic to North America. Few explicit phylogenetic hypotheses have been proposed for these harvestmen, with most taxonomic treatments describing species and occasionally noting similarities among them (e.g., Roewer, 1923; Crosby and Bishop,1924; Bishop, 1949a; Davis, 1934; Edgar, 1966). The recognition of four genera is one of the few implicit phylogenetic hypotheses.

In a largely unpublished dissertation on the *Leiobunum* of the region, McGhee (1970, 1975) circumscribed several species groups based on male genitalia. He recognized three penis types (sacculate, bulbate, lanceolate) using the morphology of a bilateral pair of subterminal cuticular structures (Fig. 2.1). He did not explore the sacculate group beyond noting its heterogenous membership. Eight sacculate species were widely recognized at the time (*L. aldrichi, L. aurugineum, L. bimaculatum, L. cretatum, L. flavum, L. nigripes, L. ventricosum, L.verrucosum*), although *L. nigripes* is now considered a junior synonym of *L.*

verrucosum (Shultz, 2008b). The bulbate group encompassed three species (*L. politum, L. bracchiolum, L. holtae*), with *L. holtae* being a distinctive outlier (McGhee, 1975). However, the ‘‘bulbs’’ of *L. politum* and *L. bracchiolum* are simply sacs with reduced lateral walls and no ‘‘bulb’’ is apparent in *L. holtae* (orig. obs.). The lanceolate group contained species that lack penial sacs or ‘‘bulbs’’, and McGhee (1970) recognized two subgroups, the *calcar* and *vittatum* species groups. The calcar group was characterized by a gradually tapered, dorsoventrally compressed penis (Fig. 2.1) and male palpal tibiae specialized for clasping the female during mating (Table 2.1). It included five species (*L. calcar, L. nigropalpi, L. serratipalpe, L. hoffmani, L. cumberlandense*), although *L. serratipalpe* was later synonymized with *L. calcar* (Cokendolpher, 1981) and descriptions of *L. hoffmani* and *L. cumberlandense* were never formally published. A recent revision of the group (Ingianni et al., 2011) resurrected the *L. serratipalpe* concept under the name *L. euserratipalpe*, formally described *L. hoffmani*, and synonymized *L. cumberlandense* with *L. calcar*. In the vittatum group, males tend to have long palpal femora with a proventral row of spines, and the penis (Fig. 2.1) has an expanded basal portion and thinner, usually cylindrical distal shaft (Table 2.1). McGhee placed four species in this group (*L. vittatum, L. speciosum, L. crassipalpe, L. formosum*). However, *L. uxorium* and *L. relictum* should also have been included. Indeed, *L. speciosum sensu* McGhee seems to correspond to *L. uxorium* and the traditional view of *L. speciosum* (see Davis, 1934) appears to correspond to *L. vittatum*. The inclusion of *L. formosum* in the *vittatum* group was uncertain. The other widespread genus, *Nelima*, is characterized by the absence of pro- and retrolateral rows of coxal denticles but is otherwise similar to *Leiobunum*. The genus is represented in eastern North America by a single species, *N. elegans*, with clear affinities to *N. paessleri* and *L. exilipes* of western North America (Hedin et al., 2012).

The two endemic North American genera, *Eumesosoma* and *Hadrobunus*, differ from most *Leiobunum* and *Nelima* species in having relatively short legs and substantial dorsal armature. *Eumesosoma* contains six known species distributed in the southern and central United States (Cokendolpher, 1980). They are primarily ground-dwelling forms with a hard, tuberculate scutum and sacculate penes (Table 2.1). Hadrobunus includes three described species in eastern North America (*H. grandis, H. maculosus, H. fusiformis*), although the distinction between *H. grandis* and *H. maculosus* has never been clear. Two *Hadrobunus* species have been described from Mexico, the northeastern *H. knighti* and southwestern H*. davisi*, but the latter does not appear to belong to the genus (Shultz, 2010). *Hadrobunus* is currently united by having posteriorly curved (retrorse) spinules on the scutum. Many undescribed species of *Hadrobunus* are known to us, and the diversity of penial structure within the genus (Fig. 2.1) exceeds that of *Leiobunum*; there are sacculate and lanceolate types, and more commonly, massive chisel-like penes (Fig. 2.1: *H. maculosus*).

Until recently, there has been little understanding of the broader phylogenetic and biogeographic affinities of the Leiobuninae of eastern North America (but see Table 2.1; Cokendolpher and Lee, 1993). However, because non-leiobunine harvestmen from this region have close relatives in Europe, Mesoamerica and East Asia, it has long seemed possible (even likely) that leiobunines would also represent a phylogenetic mosaic with diverse biogeographic affinities. This expectation would seem to require any meaningful phylogenetic treatment of the group to include a significant representation of the entire holarctic leiobunine fauna, which would be an extremely daunting task. However, in a recent molecule-based phylogenetic analysis, Hedin et al. (2012) began to address this problem and showed that geographic proximity is often superior to current morphology-based taxonomy in predicting phylogenetic relationships among leiobunines. These authors found that *Leiobunum* and *Nelima* are polyphyletic syndromes that appear to have arisen independently in different geographic areas and that the leiobunines of eastern North America form a clade along with species from eastern Mexico. There is no evidence of any close relationship with Asian, European or even western North American clades. Indeed, among the eastern North American taxa, only *N. elegans* lies outside the clade. With this significant advance in our understanding of leiobunine phylogeny, a taxonomically meaningful phylogenetic analysis of eastern North American leiobunines can now be undertaken without intensive sampling of European, Asian or even western North American groups.

Materials and Methods

1. Taxon sample

The ingroup sample included all non-problematic species of *Leiobunum* from the eastern and central United States, except *L. cretatum* (see Tables 2.1

and 2.2). Taxonomically ambiguous species not represented in the analysis are *Leiobunum peninsulare* Davis, 1934 (probably a junior synonym of *L. bimaculatum*), *L. leiopenis* Davis, 1934 (probably a junior synonym of *L. formosum*), and *L. speciosum* (historically problematic and likely synonymous with *L. bimaculatum*). All specimens corresponding to *Leiobunum speciosum sensu* Davis (1934) were included as *L. vittatum*. *Leiobunum davisi* and *L. zimmermani* are probably synonymous with species included here; the original descriptions were poor, the types appear to have been lost, and type localities are historically well collected. Four species of *Hadrobunus* were sampled, including *H. maculosus* and three previously undescribed species. *Eumesosoma* was represented by *E. roeweri*. The Mexican *Leiobunum royali* was also included because Hedin et al. (2012) showed it to be closely related to USA and Canadian leiobunines. Outgroup sampling included four leiobunines from western North America (*Togwoteeus biceps, Leiobunum potosum, Leiobunum townsendi* and *Leuronychus pacificus*) as well as the distantly related phalangiid *Phalangium opilio.*

2. DNA extraction, amplification and sequencing

Total DNA was extracted using the DNeasy Blood and Tissue kit (QIAGEN, www.qiagen.com). Eight gene fragments were targeted, corresponding to mitochondrial genes (namely, NADH dehydrogenase 1, 16S ribosomal DNA, the 50 end of the 12S ribosomal subunit and their intervening tRNAs, leucine and valine), and the two nuclear genes 28S ribosomal DNA and elongation factor-1α (EF1α) exons and introns. Gene fragments were PCR amplified with 35 cycles (94° for 30 sec, 55° for 30 sec, 72° for 1 min). Primer sequences and combinations are presented in Table 2.3. PCR products were run out on a 1% low-melt electrophoresis gel with ethidium bromide added to visualize amplicons, and product bands were excised and purified using the Wizard Genomic DNA Purification kit (Promega, www.promega.com). Amplicons were fluorescently labeled and sequenced with a 3730_ DNA Analyzer (Applied Biosystems) under the Long50_Z protocol with KBbasecaller setting using the same primers.

3. Phylogenetic analyses

Sequences were manually edited using BioEdit v.7.0.1 (Hall, 1999) and aligned using the multiple alignment programs Clustal X (Larkin et al., 2007) and ProAlign (Löytynoja and Milinkovitch, 2003) to assess the effect of alignment method on results. Data were uploaded and exported into Nexus format using Mesquite (Maddison and Maddison, 2011). jModelTest (Posada, 2008) and MrModelTest (Nylander, 2004) were used to evaluate each gene for the appropriate likelihood models using the MrModelTest hierarchies and the Akaike Information Criteria (AIC) (Akaike, 1974) to select the best model. See Table S2.1 in the Supplementary Information for the best models per fragment. Separate analyses treating each partition scheme with a general time reversible model with an estimated proportion of invariable sites and a gamma distribution (GTR + I + Γ) were also applied to demonstrate the lack of difference between reconstructions used with this and other selected models (see Table S2.2). We applied maximum likelihood (GARLI-part-0.97; Zwickl, 2006) with 1000 bootstrap replicates to assess the relative robustness of taxon bipartitions and Bayesian likelihood inference methods (MrBayes v.3.1.2; Ronquist and Huelsenbeck, 2003; Huelsenbeck and Ronquist, 2001) to concatenated sequences modeled using one, three (mitochondrial DNA, 28S and EF-1α), or seven partitions (all genes and tRNAs). Bayesian analysis was performed using Markov-chain Monte Carlo with two independent runs of four Metropolis-coupled chains of ten million generations each, to estimate the posterior probability distribution. Topologies were sampled every 1000 generations, and a majority-rule consensus tree was estimated after discarding the first 250,000 generations. Maximum parsimony was applied to un-partitioned sequences using PAUP* v 4.0b10 (Swofford, 2002) or TNT (Goloboff et al., 2008) with 1000 bootstrap replicates. Table 2.4 gives GenBank accession numbers by sample.

Results and discussion

1. General findings

Analyses of alternative partitioning schemes of the complete concatenated data produced very similar topologies, and the tree derived from analysis of seven partitions (each having a separate program-tested model) was selected to illustrate this result (Fig. 2.1A). Findings from other analytical conditions are summarized in Table S2.2. Most nodes were strongly supported by bootstrap values and posterior probabilities, with lower values and poor resolution being limited primarily to several terminal nodes. Analyses differed in their relative placement of *Leiobunum bimaculatum* and *L. royali*, although their placement was weakly supported under all analytical conditions. The tree derived from nuclear genes (Fig. 2.1B) was largely congruent with that generated from the complete data but recovered fewer well-supported nodes, and these tended to correspond to major species groups. Taken together, these findings indicate that most of the phylogenetic signal within species groups was derived from the mitochondrial data.

Among the 15 species in our analysis that included multiple geographic examplars, only five were consistently reconstructed as monophyletic, namely Leiobunum *verrucosum, L. formosum, L. aldrichi, L. uxorium and L. nigropalpi*. Likely explanations for species non monophyly vary. For example, the apparent paraphyly of the widely distributed and/or morphologically diverse *Leiobunum vittatum* and *L. calcar* with respect to distinctive species *L. uxorium* and *L. hoffmani*, respectively, may reflect the need for more intensive taxonomic work. However, the recovery of morphologically apomorphic and geographically restricted species as polyphyletic (e.g., *Leiobunum holtae, L. relictum, L. crassipalpe*) probably reflects either problems in data quality, gene introgression, or deep coalescence impacting mitochondrial data. The latter factors likely explain non-monophyly of species in the *vittatum* group, where mixed species clades tend to cluster by geographic proximity. Deep coalescence may also account for results that are counter-intuitive from a morphological perspective, such as the apparent derivation of a sacculate species, *Hadrobunus* n. sp. 3, from a highly derived and paraphyletic *H. maculosus*. Similarly, results from the full data set recover the more generalized *L. nigropalpi* from the more derived *L.*

calcar, although the nuclear-only data resolves these taxa in a manner consistent with expectations derived from morphology. Thus, while the general phylogenetic structure of the Leiobuninae of eastern North America is well-supported, resolving relationships within species groups will require additional data, probably from rapidly evolving nuclear genes.

2. Taxonomic implications

2.1. Eastern North America *Leiobunum* is not monophyletic

Results from a recent molecular analysis of sclerosomatid harvestmen (Hedin et al., 2012) indicate that *Leiobunum*, the largest genus in Leiobuninae, is artificial. This conclusion will surprise few harvestman systematists. The genus is traditionally defined by the presence of long, thin legs without femoral nodules (pseudoarticulations), rows of coxal denticles at least on the prolateral surface of coxa I and retrolateral surface of coxa IV, and poorly armed dorsal cuticle. This combination of traits has evolved independently in different regions of the Northern Hemisphere, with the type species of the genus, *L. rotundum* (Latreille 1789), occurring in Europe. The ‘‘*Leiobunum*’’ of East Asia and North America are more closely related to other sympatric genera than to the European *Leiobunum*, and they will inevitably be transferred to new genera once the phylogenetic understanding of the group has stabilized. This situation is complicated further by the fact that regional ‘‘*Leiobunum*’’ appear to have given rise to new genera. Thus, aside from *L. rotundum* and its close relatives, *Leiobunum* is polyphyletic at deeper, intercontinental levels of leiobunine phylogeny and often paraphyletic at shallower, regionally restricted levels. These problems are well illustrated by the results of our analysis, where *Leiobunum* is clearly paraphyletic with respect to *Eumesosoma* and *Hadrobunus* in the east and *Leuronychus* in the west (Fig. 2.1).

2.2. The early-season *Leiobunum* group

This group encompasses five species (Fig. 2.1; Table 2.1) and was recovered under all analytical conditions with high support in analyses that include all mitochondrial and nuclear sequences. The early-season group has no obvious morphological synapomorphies, although its members appear to be unique in overwintering as juveniles rather than eggs and in reaching sexual maturity in the late spring and early summer rather than mid- to late summer. This aspect of the life cycle has been determined for *L. verrucosum, L. flavum, L.* n. sp. and *L. ventricosum* by original observation (JWS), but the life cycle of *L. holtae* has not been specifically investigated. McGhee (1975) noted that adult specimens of *L. holtae* are present from spring to fall, which suggests the life history of this species is similar to that of *L. ventricosum* in maturing in late spring and persisting as adults for several months.

With the exception of *L. holtae*, species in the early-season group have a pair of subterminal, distally opened sacs on the penis (Fig. 2.1: *L. verrucosum*, *L. ventricosum*) used to deliver a nuptial secretion to the female during mating (Shultz, 2005; Macías-Ordóñez et al., 2010; MMB and JWS, orig. obs.). Sacs are useful in identification but are symplesiomorphic for Leiobuninae. The penis in *L. holtae* (Fig. 2.1) lacks sacs and is otherwise highly specialized, with a long, thin, laterally compressed distal shaft and broad, somewhat dorsoventrally compressed proximal portion. Despite its unique male genitalia, *L. holtae* is similar to *L. ventricosum* in body size, relative leg length, and coloration. It is likely that *L. ventricosum* will eventually emerge as being paraphyletic with respect to *L. holtae*.

2.3. *Leiobunum vittatum* group

The *vittatum* group was recovered with high support under all analytical conditions (Fig. 2.1). Our analysis included three well delimited morphospecies, namely *L. uxorium, L. crassipalpe and L. relictum*. The taxonomic status of *Leiobunum vittatum* requires more thorough morphological and molecular study. This species occurs throughout the eastern and central United States and adjacent southern Canada (Cokendolpher and Lee, 1993) and shows considerable variation in color, relative leg length and male palpal armature. It is unclear whether the geographic variants reflect taxonomically objective boundaries. The problematic species *L. speciosum*, as described by Davis (1934), appears to correspond to one such *L. vittatum* variant; specimens in the type series are clearly *L. bimaculatum* (JWS, orig. obs.). Another distinctive species, *L. denticulatum*, is a heretofore unrecognized member of the group (JWS, orig. obs.) known from a few museum specimens from south-central Mexico. We were unable to obtain specimens for molecular work. The *vittatum* group is united by synapomorphic features associated with reproduction. The penis lacks all evidence of sacs or alae. The distal half to two-thirds of the penis shaft is a thin cylinder (broader in *L. crassipalpe*) and the proximal region is thicker (Fig. 2.1: *L. vittatum*). In all species except *L. relictum*, the femur and patella of the male pedipalp are long and a proventral row of spines extends along the femur, patella and tibia.

As noted above, the internal phylogenetic structure of the *vittatum* group recovered here does not match implicit taxonomic predictions*: L. vittatum* and *L. crassipalpe* are recovered as paraphyletic and *L. relictum* as diphyletic. A literal interpretation of our result suggests that the *L. vittatum* concept corresponds to a widespread ancestral form that has persisted and has also given rise to several distinctive, regional forms. However, the interpretation of nonmonophyly in the morphologically distinct and geographically restricted *L. crassipalpe* and *L. relictum* may stem from other factors, such as quality of the DNA templates, low phylogenetic signal (note low support values in Fig. 2.1 and Table S2.2), standing genetic variation, or deep coalescence of mitochondrial haplotypes. The latter factors are consistent with the geographic proximity of related terminals. Clearly, the internal structure of the *L. vittatum* species group, especially *L. vittatum*, demands a more thorough taxonomic and phylogenetic treatment.

2.4. *Leiobunum politum* group

This group contains two named species, *L. politum* and *L. bracchiolum*. They are united by a pair of ‘‘bulbs’’ on the penis that represent modifications of the primitive sacs, apparently through reduction of the lateral walls. In addition, the male is unique among North American *Leiobunum* in having a labrum greatly inflated at the tip. McGhee (1975) interpreted the transitional region between the laterally compressed and dorsoventrally compressed parts of the penile shaft of *L. holtae* as a ‘‘bulb’’ and placed it with *L. politum* and *L. bracchiolum* in a ‘‘bulbate’’ species group. We find no morphological or phylogenetic evidence to support this hypothesis. Our results indicate that the widespread *L. politum* is paraphyletic with respect to *L. bracchiolum*, which is limited to the eastern Appalachian Region, Piedmont, and portions of the Atlantic coastal plain (McGhee, 1975; JWS, orig. obs.). The two species are morphologically distinct where their ranges overlap (McGhee, 1975). In Maryland, for example, *L. politum* is found in woodlands with or without understory and *L. bracchiolum* occurs in herbaceous vegetation usually associated with trees. They can occur together but are readily distinguished by body size (McGhee, 1975) and coloration.

2.5. *Leiobunum calcar* group

The group is united by several morphological features and is recovered here as monophyletic with strong support (Fig. 2.1). Two species have been recognized historically, the morphologically uniform *L. nigropalpi* and the morphologically diverse *L. calcar*. Ingianni et al. (2011) described two additional species, *L. euserratipalpe* and *L. hoffmani*. The *calcar* group is united by a suite of reproductive features: the penis lacks subterminal sacs, although a pair of variably developed alae are often present (Fig. 2.1), and the proximal region of the male palpal tibia is inflated and denticulate for use in clasping trochanter I of the female during mating (Bishop, 1949b). The internal phylogenetic structure of the *calcar* group is not well resolved and is inconsistent with morphology, with the latter supporting *Leiobunum nigropalpi* as the plesiomorphic sister group to the remaining species (Table 2.1). In male *L. nigropalpi*, the palpal femur retains a retrolateral row of denticles rather than a distal cluster, the palps are gracile rather than robust, and the penis is relatively unspecialized (e.g., it retains a demarcation between glans and shaft) (Fig. 2.1). The inference derived from morphology is supported by analyses of the nuclear sequences, and it is possible that the conflicting mitochondrial signal results from deep coalescence and/or genetic introgression.

2.6. ***Hadrobunus*** **group**

Our analysis strongly recovers two *Leiobunum* species, *L. aurugineum* and *L. formosum*, as the monophyletic sister group to *Hadrobunus.* Like *Hadrobunus*, *L. aurugineum* has relatively short, robust legs and the opisthosomal dorsum is armed with retrorse spinulate tubercles. Our placement of *L. aurugineum* is therefore not surprising and, indeed, many museum specimens of *L. aurugineum* are already labeled ‘‘*Hadrobunus grandis*’’ (JWS, orig. obs.). In contrast, *L. formosum* is typical of *Leiobunum* in having long, thin legs and a weakly armed or unarmed scutum, although some populations also have retrorse armature (JWS, orig. obs.). An on-going revision of *Hadrobunus* has revealed additional morphological similarities between *Hadrobunus*, *L. aurugineum* and *L. formosum* that support the eventual transfer of the two *Leiobunum* species to *Hadrobunus*.

3. Future directions

Our results indicate that the leiobunine fauna of the eastern North America contains two major clades. The early-season *Leiobunum* clade encompasses mostly species that retain the plesiomorphic sacculate penis and the second clade contains mainly species that lack sacs (Fig. 2.1). A strong connection between eastern US and eastern Mesoamerican leiobunines has already been established (Hedin et al., 2012) and the current evidence suggests that the major lineage diversified in Mesoamerica before entering the US region and then diversified further. Future work will continue to explore cryptic diversity, especially in the *Hadrobunus* and *L. vittatum* groups. We will also focus on the evolution of penile traits in North American leiobunines, utilizing comparative methods to describe the evolution of reproductive morphology in male and female harvestmen and the corresponding mating systems across the phylogeny.

Tables

Table 2.1. Diagnostic features and general distribution of Leiobuninae included in analysis.

Group	Diagnostic features	Distribution [a]
Leiobuninae of Eastern North America (ingroup)		
Early-season *Leiobunum* group	Overwinters as juvenile, not egg	
L. verrucosum (Wood 1868)	Penis sacculate, dark trochanters	*c-e* USA, *se* Canada
L. flavum Banks 1894	Penis sacculate, light trochanters, large	*c-e* USA
L. new species	Penis sacculate, light trochanters, small	USA: *e* NE
L. ventricosum (Wood 1868)	Penis sacculate, elongate	*c-e* USA, *se* Canada
L. holtae McGhee 1977	Penis lanceolate, elongate, very thin	USA: *se* TN, *n* AL, *ne* GA
***Leiobunum vittatum* group**	Penis lanceolate; shaft thin, base broad	
L. vittatum (Say 1821)	Male palpal femur elongate	*c-e* USA, *sc-se* Canada
L. uxorium Crosby & Bishop 1924	Male palpal femur slightly elongate	*se* USA
L. relictum Davis 1934	Male palps not elongate	USA: *w* OK: Wichita Mtns
L. crassipalpe Banks 1900	Male palpal femur elongate, robust	USA: *e* OK, *n* AR, *s* MO

***Leiobunum politum* group**	Penis sacculate, sac reduced laterally	
L. politum (Wood 1868)	Larger body	*c-e* USA, *se* Canada
L. bracchiolum (McGhee 1977)	Smaller body	USA: *e* PA to *n* GA
***Leiobunum calcar* group**	Penis lanceolate, tapered; male palpal tibia modified proximally for clasping	
L. nigropalpi (Wood 1868)	Male palpal femur thin, no distal spine cluster	*e* USA
L. euserratipalpe Ingianni e*t al.* 2011	Male palpal femur thin, distal spine cluster	*e* USA
L. calcar (Wood 1868)	Male palpal femur robust, distal spine cluster	*c-e* USA, *sc-se* Canada
L. hoffmani Ingianni *et al.* 2011	Male palpal femur massive, distal spine cluster	USA: *nw* NC, *sw* VA
***Hadrobunus* group**	Retrorse scutal armature	
H. maculosus (Wood 1868)	Penis chisel-like, massive; short legs	USA: ME to *c* NC
H. new species 1	Penis chisel-like, massive; short legs	USA: *e* TN, KY, WV, *sw* PA
H. new species 2	Penis sacculate, small, sacs large	USA: *e* KS, MO, *s* WI, *w* IL
H. new species 3	Penis sacculate, small, sacs small	USA: *s* IL, *w* TN
L. aurugineum Crosby &	Penis sacculate, sacs	extreme *se* USA

Bishop 1924	posterior, short legs	
L. formosum (Wood 1868)	Penis lanceolate, weak armature, long legs	*c-e* USA

Other taxa

Eumesosoma roeweri (Goodnight & Goodnight 1943)	Penis sacculate, scutum tuberculate, short legs	*c* USA
Leiobunum aldrichi (Weed 1893)	Penis sacculate, white band on tibia II	*c-e* USA, *se* Canada
L. bimaculatum Banks 1893	Penis sacculate, large, light spots on carapace	extreme *se* USA, *se* VA
L. royali Goodnight & Goodnight 1946	Penis sacculate	Mexico: HG, SL, VZ

Leiobuninae of Western North America (outgroup)

Leiobunum townsendi Weed 1893	Penis sacculate	*sw* USA – *nc* Mexico
L. potosum Goodnight & Goodnight 1942	Penis sacculate	Mexico: DF, SL, PU, TL
Leuronychus pacificus (Banks 1894)	Penis sacculate	West Coast: *s* AK to BJ
Togwoteeus biceps (Thorell 1877)	Penis sacculate	*nw* Mexico – *sw* Canada

---

[a] Abbreviations: *c*, central; *e*, eastern; *n*, northern, *s*, southern; *w*, western. States: AK, Alaska; AL, Alabama; AR, Arkansas; BJ, Baja California; DF, Distrito Federal; GA, Georgia; HG, Hidalgo; IL, Illinois; KS, Kansas; KY, Kentucky; ME, Maine; MO, Missouri; NC, North Carolina; NE, Nebraska; OK, Oklahoma; PA, Pennsylvania; PU, Puebla; SL, San Luis Potosi; TL, Tlaxcala; TN, Tennessee; WI, Wisconsin; WV, West Virginia; VA, Virginia; VZ, Veracruz

Table 2.2. Taxon sampling for phylogeny.

Species	Locality	Voucher no.	Collector	Date
Leiobunum calcar	USA: NC: Clay Co.	OP 1394	M. Hedin	16-August-2007
L. calcar	USA: MD: Frederick Co.	OP 1234	J.W. Shultz	06-July-2007
L. calcar	USA: MS: Tishomingo Co.	OP 830	M. Hedin	12-August-2005
L. calcar	USA: TN: Cocke Co.	OP 814	M. Hedin	27-August-2005
L. calcar	USA: OH: Summit Co.	OP 1091	J.W. Shultz	01-June-2005
L. n. sp*. “hoffmani”* (Ingianni et al., 2011)	USA: VA: Grayson Co.	OP 1383	M. Hedin	11-August-2007
L. n. sp. *“euserratipalpe“* (Ingianni et al., 2011)	USA: MS: Lafayette Co.	OP 1235	P. Miller, G. Stratton	10-June-2007
L. n. sp. *“euserratipalpe”* (Ingianni et al., 2011)	USA: MD: Montgomery Co.	OP 1080	J.W. Shultz	01-July-2004
L. nigropalpi	USA: OH: Summit Co.	OP 1087	J.W. Shultz	01-June-2005
L. nigropalpi	USA: MD: Frederick Co.	OP 1075	J.W. Shultz	01-August-2004
L. nigropalpi	USA: AL: Cleburne Co.	OP 846	M. Hedin	13-August-2005

L. politum	USA: WI: Dodge Co.	OP 1414	M. McCormack	24-August-2007
L. politum	USA: MI: Calhoun Co.	OP 1076	J.W. Shultz	17-August-2002
L. politum	USA: NC: Haywood Co.	OP 819	M. Hedin	25-August-2005
L. politum	USA: AR: Lawrence Co.	Lpo-AR-A1	M. Hedin et al.	21-June-2009
L. bracchiolum	USA: NC: Guilford Co.	OP 1932	P. Nunez	19-September-2007
L. crassipalpe	USA: MO: Butler Co.	Lcr-MO-A1	J.W. Shultz	25-June-2009
L. crassipalpe	USA: MO: Ozark Co.	Lcr-MO-A2	M. Hedin et al.	22-June-2009
L. vittatum	CANADA: ON: Osawa Island	OP 1242	P. Miller et al.	02-July-2007
L. vittatum	USA: TN: Cumberland Co.	OP 835	M. Hedin	27-August-2005
L. vittatum	USA: OK: Cleveland Co.	Lvi-OK-A1	J.W. Shultz	25-June-2004
L. vittatum	USA: GA: White Co.	OP 1411	M. Hedin	16-August-2007
L. vittatum	USA: TN: Davidson Co.	OP 1405	M. Hedin	13-August-2007
L. uxorium	USA: VA: Smythe Co.	OP 1423	M. Hedin	13-August-2007
L. uxorium	USA: NC: Guilford Co.	OP 1934	P. Nunez	19-September-

				2007
L. relictum	USA: OK: Comanche Co.	OP 1078	J.W. Shultz	27-June-2004
L. relictum	USA: OK: Comanche Co.	Lre-OK-A1	J.W. Shultz	27-June-2004
L. aldrichi	USA: MI: Calhoun Co.	OP 1069	J.W. Shultz	17-August-2002
L. aldrichi	USA: MS: Tishomingo Co.	OP 829	M. Hedin	12-August-2002
L. aldrichi	USA: AL: Marshall Co.	OP 821	M. Hedin	17-August-2005
L. holtae	USA: GA: Dade Co.	OP 1382	M. Hedin	15-August-2007
L. holtae	USA: TN: Cumberland Co.	OP 1379	M. Hedin	10-August-2007
L. ventricosum	USA: SC: Oconee Co.	OP 1440	M. Hedin	20-August-2007
L. ventricosum	USA: AL: Winston Co.	OP 840	M. Hedin	13-August-2005
L. ventricosum	USA: TN: Blount Co.	OP 815	M. Hedin	27-August-2005
L. verrucosum	USA: NC: Buncombe Co.	OP 817	M. Hedin	25-August-2007
L. verrucosum	USA: TN: Cumberland Co.	OP 1412	M. Hedin	10-August-2007

L. n. sp. *1*	USA: NE: Lancaster Co.	Lne-NE-A1	S. Schwartz et al.	30-October-2006
L. flavum	USA: AR: Garland Co.	OP 833	M. Hedin	10-August-2005
L. formosum	USA:GA: Dade Co.	OP 1476	M. Hedin	14-August-2007
L. formosum	USA: FL: Jackson Co.	OP 841	M. Hedin	15-August-2005
L. formosum	USA: FL: Jackson Co.	OP 842	M. Hedin	15-August-2005
L. formosum	USA: AL: Jefferson Co.	OP 827	M. Hedin	13-August-2005
L. aurugineum	USA: FL: Alachua Co.	Lau-FL-A1	K. Prestwich	Summer 2009
L. royali	MEXICO: Veracruz, Xalapa	OP 1162	R. Macías Ordóñez	?
L. bimaculatum	USA: FL: Jackson Co.	Lbi-FL-A1	P. Miller	27-November-2009
L. townsendi	USA: AZ: Cochise Co.	OP 1081	B. Tomberlin	August-2004
L. potosum	MEXICO: Tlaxcala, Ixtacuixtla	OP 1161	R. Macías Ordóñez	?
H. maculosus	USA: NC: Pitt Co.	Hgr-NC-A1	A. Bailey et al.	07-August-2007
H. maculosus	USA: MD: Howard Co.	Hgr-MD-A1	J.W. Shultz	12-June-2004
H. maculosus	USA: MD: Howard Co.	Hgr-MD-A2	J.W. Shultz	12-June-2004

H. n. sp. *1*	USA: TN: Sevier Co.	OP 1060	M. Hedin, J. Cokendolpher	31-July-2000
H. n. sp. *2*	USA: MO: Ozark Co.	Hmi-MO-A1	M. Hedin et al.	22-June-2009
H. n. sp. *3*	USA: IL: Johnson Co.	Hhe-IL-A1	M. Hedin et al.	20-June-2009
Eumesosoma roeweri	USA: TX: Wichita Co.	OP 1058	J. Cokendolpher	2000
Togwoteeus biceps	USA: NM: Taos Co.	OP 1068	M. Hedin	03-July-2007
Leuronychus pacificus	USA: AZ: Cochise Co.	Leuropac-AZ-A1	J. Cowles	February-2009
Phalangium opilio	USA: MD: Montgomery Co.		J.W. Shultz	10-September-2003

Table 2.3: Gene and primer information for amplified target DNA. Standard ambiguity codes apply.

Gene	**Fragment**	**Primer (5'-3')**
ND1	mtDNA 1 (F)	CCTWATAAACTAATCATTTAGC
ND1	mtDNA 1 (R)	GAGTCTGARCTTGTYTCYGG
ND1	mtDNA 2 (F)	CCRGARACAAGYTCAGACTC
ND1	mtDNA 2 (R)	GGGTATATTCAAATTCGAAAAGG
tRNA Leu + 16S	mtDNA 3 (F)	TAGATAGAAACCAACCTGGC
tRNA Leu + 16S	mtDNA 3 (R)	GTGCWAAGGTAGCATAATCA
16S	mtDNA 4 (F)	CCTTTTCGAATTTGAATATACCC
16S	mtDNA 4 (R)	TGACCTCGATGTTGAATTAA
16S + tRNA Val	mtDNA 5 (F)	TGATTATGCTACCTTWGCAC
16S + tRNA Val	mtDNA 5 (R)	ACAAATCGCCCGTCACTCTG
12S	mtDNA 6 (F)	TGTAAATAAATGGCTTAAAGCTTCA
12S	mtDNA 6 (R)	GGCGGTATCTTATCCTYATAGAGG
28S	28S 1 (F)	ACCCGCTGAATTTAAGCATAT
28S	28S 1 (R)	GCTATCCTGAGGGAAACTTCGG
EF-1 α intron II	EF-1 α 1 (F)	GATTTCATCAARAACATGATYAC
EF-1 α intron II	EF-1 α 1 (R)	CTTTGTTCCAACATGTTATCTCC
EF-1 α intron III	EF-1 α 2 (F)	TACATYAAGAAGATTGGTTA
EF-1 α intron III	EF-1 α 2 (R)	GAACTTGCAAGCAATGTGAGC

Table 2.4: GenBank accession numbers for taxa listed in Table 2.2. Accession numbers GQ870643–GQ870668; GQ872152–GQ872185 are derived from Hedin et al. (2010).

Sample	Voucher no.	ND1, tRNA-Leu, 16S rDNA, tRNA-Val, partial 12S rDNA; mitochondrial DNA	28S cytoplasmic ribosomal DNA	Elongation factor 1-α introns I and II
Leiobunum calcar	OP 1394	GQ870653, JQ432316	JQ432258	GQ872157
L. calcar	OP 1234	JQ432317	JQ432259	JQ432223
L. calcar	OP 830	JQ432319	JQ432261	
L. calcar	OP 814	GQ870655, JQ432320	JQ432262	GQ872158
L. calcar	OP 1091	JQ432318	JQ432260	
L. n. sp. *“hoffmani”*	OP 1383	GQ870654, JQ432315	JQ432257	GQ872159
L. n. sp. *“euserratipalpe”*	OP 1235	JQ432321	JQ432263	
L. n. sp. *“euserratipalpe”*	OP 1080	GQ870656, JQ432322	JQ432264	GQ872160
L. nigropalpi	OP 1087	JQ432323	JQ432265	JQ432224
L. nigropalpi	OP 1075	JQ432324	JQ432266	JQ432225
L. nigropalpi	OP 846	JQ432325	JQ432267	JQ432226
L. politum	OP 1414	JQ432326	JQ432268	JQ432227
L. politum	OP 1076	JQ432327	JQ432269	JQ432228
L. politum	OP 819	JQ432328	JQ432270	JQ432229

L. politum	Lpo-AR-A1	JQ432329	JQ432271	
L. bracchiolum	OP 1932	JQ432330	JQ432272	JQ432230
L. crassipalpe	Lcr-MO-A1	JQ432331	JQ432273	
L. crassipalpe	Lcr-MO-A2	JQ432332	JQ432274	JQ432231
L. vittatum	OP 1242	JQ432333	JQ432275	JQ432232
L. vittatum	OP 835	GQ870651, JQ432334	JQ432276	GQ872155
L. vittatum	Lvi-OK-A1	JQ432335	JQ432277	JQ432233
L. vittatum	OP 1411	JQ432336	JQ432278	JQ432234
L. vittatum	OP 1405	GQ870652, JQ432337	JQ432279	GQ872156
L. uxorium	OP 1423	JQ432339	JQ432281	JQ432235
L. uxorium	OP 1934	JQ432338	JQ432280	JQ432236
L. relictum	OP 1078	JQ432340	JQ432282	JQ432237
L. relictum	Lre-OK-A1	JQ432341	JQ432283	
L. aldrichi	OP 1069	GQ870650, JQ432342	JQ432284	GQ872154
L. aldrichi	OP 829	GQ870649, JQ432343	JQ432285	GQ872153
L. aldrichi	OP 821	JQ432344	JQ432286	JQ432238
L. holtae	OP 1382	JQ432345	JQ432287	JQ432239
L. holtae	OP 1379	JQ432346	JQ432288	JQ432240
L. ventricosum	OP 1440	JQ432348	JQ432290	
L. ventricosum	OP 840	JQ432349	JQ432291	JQ432242
L. ventricosum	OP 815	JQ432350	JQ432292	JQ432243

L. verrucosum	OP 817	JQ432351	JQ432293	JQ432244
L. verrucosum	OP 1412	JQ432347	JQ432289	JQ432241
L. n. sp. *1*	Lne-NE-A1	JQ432352	JQ432294	
L. flavum	OP 833	JQ432353	JQ432295	JQ432245
L. formosum	OP 1476	JQ432354	JQ432296	
L. formosum	OP 841	JQ432356	JQ432298	JQ432247
L. formosum	OP 842	JQ432355	JQ432297	JQ432246
L. formosum	OP 827	JQ432357	JQ432399	JQ432248
L. aurugineum	Lau-FL-A1	JQ432358	JQ432300	JQ432249
L. royali	OP 1162	JQ432367	JQ432309	JQ432254
L. bimaculatum	Lbi-FL-A1	JQ432366	JQ432308	
L. townsendi	OP 1081	JQ432369	JQ432311	
L. potosum	OP 1161	JQ432370	JQ432312	
Hadrobunus sp.	Hgr-NC-A1	JQ432360	JQ432302	
H. maculosus	Hgr-MD-A1	JQ432361	JQ432303	JQ432251
H. maculosus	Hgr-MD-A2	JQ432362	JQ432304	
H. n. sp. *1*	OP 1060	JQ432359	JQ432301	JQ432250
H. n. sp. *2*	Hmi-MO-A1	JQ432364	JQ432306	JQ432252
H. n. sp. *3*	Hhe-IL-A1	JQ432363	JQ432305	
Eumesosoma roeweri	OP 1058	JQ432365	JQ432307	JQ432253
Togwoteeus biceps	OP 1068	JQ432371	JQ432313	
Leuronychus	Leuropac-	JQ432368	JQ432310	JQ432255

pacificus	AZ-A1			
Phalangium opilio		NC010766	JQ432314	JQ432256

Figures

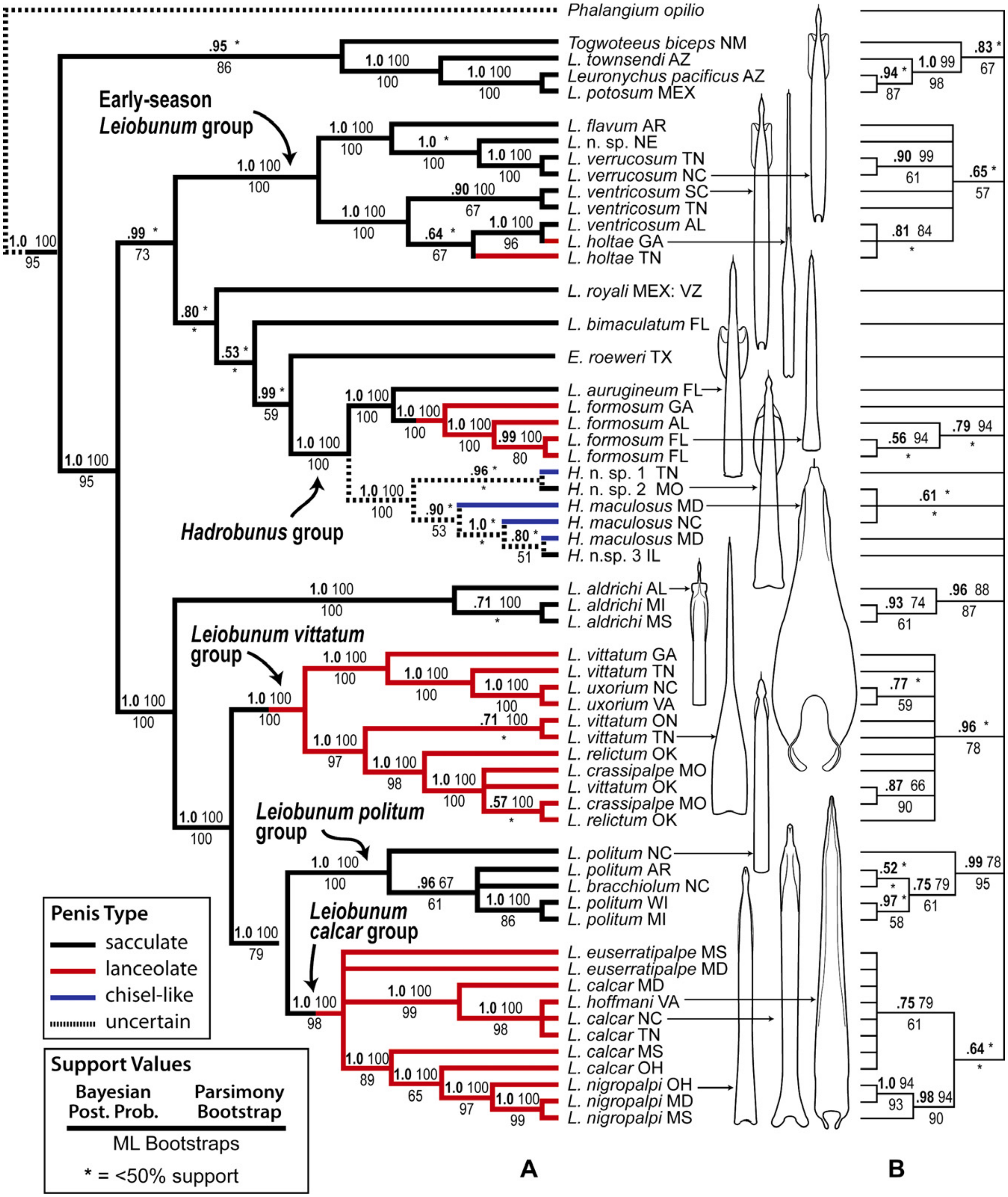

Figure 2.1: Bayesian likelihood phylogeny obtained with MrBayes 3.1.2 for (A) the combined data set of nuclear and mitochondrial characters with seven model-

tested partitions (jModelTest; Posada, 2008) and (B) the Bayesian likelihood phylogeny constructed with only nuclear genes 28S and EF1alpha. Values above nodes correspond to the Bayesian posterior probabilities and parsimony bootstrap percentages (left to right, respectively). Values below nodes indicate maximum likelihood bootstrap values. Support numbers for topologies derived from analyses of alternatively-partitioned data are given in supplementary information (see Fig. S2.1, Table S2.2). Figure center depicts dorsal perspective of penes for a selection of species to highlight genitalic diagnostic features (see also Table 2.1). Not to scale.

CHAPTER 3: Comparative Analyses of Reproductive Structures in Harvestmen (Opiliones) Reveal Multiple Transitions from Female Choice to Precopulatory Antagonism

Mercedes M. Burns, Marshal Hedin, Jeffrey W. Shultz

See Appendix 2 for supplementary table (Table S3.1) referenced in this chapter.

Abstract

Explaining the rapid, species-specific diversification of reproductive structures and behaviors is a long-standing goal of evolutionary biology, with recent research tending to attribute reproductive phenotypes to the evolutionary mechanisms of female mate choice or intersexual conflict. Progress in understanding these and other possible mechanisms depends, in part, on reconstructing the direction, frequency and relative timing of phenotypic evolution of male and female structures in species-rich clades. Here we examine evolution of reproductive structures in the leiobunine harvestmen or ‘‘daddy longlegs’’ of eastern North America, a monophyletic group that includes species in which males court females using nuptial gifts and other species that are equipped for apparent precopulatory antagonism (i.e., males with long, hardened penes and females with sclerotized pregenital barriers). We used parsimony- and Bayesian likelihood-based analyses to reconstruct character evolution in categorical reproductive traits and found that losses of ancestral gift-bearing penile sacs are strongly associated with gains of female pregenital barriers. In most cases, both events occur on the same internal branch of the phylogeny. These coevolutionary changes occurred at least four times, resulting in clade specific designs in the penis and pregenital barrier. The discovery of convergent origins

and/or enhancements of apparent precopulatory antagonism among closely related species offers an unusual opportunity to investigate how major changes in reproductive morphology have occurred. We propose new hypotheses that attribute these enhancements to changes in ecology or life history that reduce the duration of breeding seasons, an association that is consistent with female choice, sexual conflict, and/or an alternative evolutionary mechanism.

Introduction

Structures and behaviors associated with animal reproduction typically differ even among closely related species, although stability within a species tends to be maintained (Hosken and Stockley, 2004; Emlen, 2001). However, the mechanisms responsible for producing this widespread pattern remain uncertain even after 150 years of dedicated research by evolutionary biologists. Some workers have proposed a role for natural selection in reproductive diversification, either directly via lock-and key mechanisms (Masly, 2012; Shapiro and Porter, 1989) or indirectly via pleiotropy (Mayr, 1963), but there is little evidence for these processes in most systems that have been studied (Hosken and Stockley, 2004). A number of sexual selection mechanisms have also gained purchase in functional and evolutionary reproductive diversification paradigms. These include the perennial female choice—both obvious and cryptic (Bailey and Moore, 2012; Jagadeeshan and Singh, 2006; Eberhard, 2004a; Boughman, 2002; Pomiankowski and Iwasa, 1998; Eberhard, 1996), and the more-recent intersexual conflict (Vahed, 2007; Chapman, 2006; Arnqvist and Rowe, 2005;

Friberg et al., 2005; Gavrilets and Hayashi, 2005; Alonzo and Warner, 2000; Arnqvist et al., 2000) and sperm competition mechanisms (Gage, 2012; Snook, 2005; Simmons, 2001).

Which evolutionary processes lead to the diversification of reproductive structures? An evolutionary question of this magnitude requires diverse perspectives and approaches that include theory, experimentation and development of model organisms, all of which are fairly well represented in the recent literature. However, the phylogenetic comparative approach—wherein the direction, frequency and evolutionary context of specific evolutionary transformations are explored within species-rich clades—has been used less frequently to understand mating system diversity. This is despite the demonstrated value of this approach for understanding evolutionary patterns in other aspects of organismal biology, such as feeding and geographic distribution (Cooper et al., 2010; Losos and Glor, 2003). The recent paucity of such studies as applied to reproductive structures probably reflects the difficulty in targeting large clades that have undergone relevant evolutionary changes and for which a well-resolved phylogeny is available. In addition, these approaches can suffer from uncertainties inherent in all historical reconstructions (Boettiger et al., 2012; Huelsenbeck et al., 2000). Still, the phylogeny-based historical approach aids in the description and explanation of diversification that has occurred in natural systems at different evolutionary time scales. These perspectives are not available with single species studies or in comparative analyses that use phylogeny solely for the removal of statistical non-independence due to species relatedness.

Here we examine evolutionary patterns in the reproductive morphology of the leiobunine harvestmen or "daddy longlegs" of eastern North America. The group encompasses three genera—Leiobunum, Eumesosoma and Hadrobunus—with about 35 described species and 12 known-but-undescribed species. The taxonomic nomenclature of the group is currently in flux but recent molecular systematic analyses have revealed the monophyly of the group and its basic phylogenetic structure (Burns et al., 2012; Hedin et al., 2012). The reproductive morphology of the clade is diverse, but much of this diversity can be captured by three binary, categorical variables, that is, a penis with or without nuptial gift sacs, a female pregenital apparatus with or without a sclerotized barrier, and male pedipalps similar in size and shape to those of females or mechanically enhanced for clasping (Figs. 3.1–3.3). There is an apparent tendency for these traits to occur in two morphology based syndromes, one that is consistent with a mating system in which females choose males based on a precopulatory nuptial gift (courtship) and one in which precopulatory contact involves large or prolonged mechanical forces with more limited exchange of nuptial gifts (precopulatory antagonism). The goals for this study are thus 1) to reconstruct the direction and frequency of trait evolution, 2) to determine whether the two syndromes are real and reflected in correlated evolution of traits and 3) to determine if morphological change in a focal trait tends to precede or follow change in another trait.

Background: Mating and Reproductive Morphology in Leiobunine Harvestmen

In general, mating behavior in the leiobunine harvestmen is broadly divided into precopulatory and copulatory phases (Fig. 3.1). During the precopulatory phase the male uses his pedipalps to grasp the female behind the base of her second leg pair (coxa II); the male and female are positioned face-to-face with the long axes of their bodies in rough alignment (Machado and Macías-Ordóñez, 2007). The penis is usually everted during this phase and its tip may contact the female pregenital opening, but it does not penetrate the pregenital chamber (Fig. 3.2). The male offers a nuptial gift from accessory glands positioned near the opening to his pregenital chamber. The copulatory phase is characterized by penetration of the penis into the pregenital chamber and a change in body position in which the male assumes a more "face up" orientation. Insemination occurs within the pregenital chamber. These features of mating appear to be universal among the leiobunines of eastern North American, but details of reproductive morphology and mating behavior differ among species.

Species can be broadly divided into two categories: sacculate and non-sacculate (Fig. 3.3). In sacculate species, the penis has a bilateral pair of subterminal cuticular sacs that contain a secretion derived from accessory glands (Burns et al., 2012). When a male encounters a receptive female, he clasps her with his pedipalps and inserts the penis into the female’s mouth. The penis is rapidly withdrawn and its distal end is placed at the opening to the female’s pregenital chamber. The primary nuptial gift is followed by a secondary gift issued directly from the accessory glands. The female spends a variable amount of time (a few seconds to a few minutes) appearing to feed on the secretion. Although the chemical profile of the secretion and its potential effects on female fecundity are unknown, the female's active reception of the material and the apparent ubiquity of its transmission indicate that the label of nuptial gift is warranted (Gwynne, 2008). The copulatory phase of mating begins when the female opens the genital operculum and the male re-orients into the copulatory posture (Fig. 3.1). Females reject males by running away or adopting a face - down orientation (Machado and Macías-Ordóñez, 2007).

Many non-sacculate species begin mating in a similar way, but little, if any, primary nuptial gift is transferred. In some species, the male pedipalps are modified for strongly clasping the female (Fig. 3.3). The sterno-opercular mechanisms of females are usually sclerotized and appear to serve as reinforced pregenital barriers (Figs. 3.2C, 3.2D). The duration of the precopulatory phase varies considerably and can last for up to an hour. In some species, the pair maintains their precopulatory posture for long periods with brief intervals of struggling in which the male makes attempts at forcefully penetrating the female's pregenital chamber. We have not observed enough interactions to determine how often these encounters end in copulation.

Materials and Methods

Taxon Sample

Analyses were conducted using 25 species from the eastern North American clade of leiobunine harvestmen, and four outgroup species from a closely related clade occurring in Mexico and the western United States (Hedin et al., 2012). The sample included all genera and all but six described species from the eastern clade plus four undescribed species. Because discrete genital morphology does not vary within species and monophyly of species groups is well supported (Burns et al., 2012) (Fig. 3.4), we conducted our analyses using one population (i.e., one tip) from each multiply represented species examined by Burns et al. (2012) in both the phylogenetic and morphological analyses (Fig. 3.4). Table S3.1 in the supplementary materials includes additional details regarding taxon sampling for molecular and morphological assignment.

Phylogenetic Trees

All analyses were conducted using as a template the phylogenetic tree recovered by Bayesian analysis of mitochondrial and nuclear genes in (Burns et al., 2012). However, because the branch lengths of the original topology reflect rates of molecular rather than morphological evolution, we used the same molecular data (see Table S3.1 for GenBank accession numbers) to generate a set of ultrametric trees in which internodal lengths reflect time and lengths of all root-to-tip pathways were equal (Armbruster et al., 2009). Ultrametric trees were constructed using BEAST v1.7.1 (Drummond et al., 2012) assuming a Yule speciation process prior. The data matrix was divided into three partitions—mitochondrial DNA, 28S rDNA, and elongation factor 1-a—analyzed simultaneously using separate GTR+I+Γ models. Ultrametric branch lengths were calculated using unlinked and uncorrelated log-normal relaxed clocks separated by partition (Drummond et al., 2006). Two independent tree-searching analyses each ran for 100 million iterations, where one configuration was sampled per 1000 generations with the default 10% burn-in (Data deposited in the Dryad on-line repository: (http://dx.doi.org/10.5061/dryad.79d15).

The program TRACER v1.5 (Rambaut and Drummond, 2007) was used to ensure that effective sample sizes of the posterior distribution were greater than 1000 for each independent analysis. To achieve a more conservative burn-in of 30%, we discarded an additional 20% of sampled trees using LogCombiner v1.7.1 (Drummond et al., 2012). The posterior distributions of the two analyses were pooled to yield 1000 trees. Multiply represented taxa were pruned to one population per species (see Table S3.1 for localities) by list-applying (command 'lapply') the ''drop.tip'' function to the entire set of trees in the ape package (Paradis et al., 2004) available through the R statistical computing language (R Development Core Team, 2013). To ensure consistency with the branching pattern of the original Bayesian tree (Burns et al., 2012), the posterior distribution was filtered using a rooted backbone constraint tree (Fig. 3.4) in PAUP* v4.0b (Swofford, 2002) which preserved well-supported clades (i.e., posterior probabilities >0.95) while allowing for variation in the placement of poorly supported clades and species. This resulted in a distribution of 431 trees that was used in all analyses of character evolution.

Evolution of the Penis and Male Pedipalps

Males of each species were assigned one of three combinations of penile-sac (S) and pedipalpal (P) features. Species with bilateral penile cuticular sacs that convey a nuptial gift (Macías-Ordóñez et al., 2010) and simple "female-like" pedipalps were coded as S^+P^-; species that lack penile sacs and have simple pedipalps were coded as S^-P^-; and species that lack sacs but have pedipalps heavily modified for clasping (Fig. 3.3) were coded as S^-P^+ (Figs. 3.5A, 3.5B). States were determined for all species by original observations of anatomy. No species is known to have both penile sacs and modified pedipalps, so this combination of traits was not coded. That this combination is unobserved gives strength to our alternative model of male reproductive evolution, so we chose to ignore it, although alternative approaches might include the combination (Felsenstein, 2012).

The ancestral male morphology was determined using parsimony reconstructions with Mesquite v. 2.75 (Maddison and Maddison, 2011) and with BayesTraits Multistate (Pagel and Meade, 2006; Pagel et al., 2004). The latter was accomplished by comparing marginal likelihoods of two models: a 6-rate model in which all transitions between character states were possible, and a model that differs only in that state 0 (i.e., no penile sacs, simple pedipalps) was assigned to the root. As these models are not nested, they were compared using Bayes factors (Jeffreys, 1961).

To assess the direction of change in male morphology, two potential models of male character evolution were compared: the 6-rate model representing the possibility for transitions between all three character states (Fig. 3.5A), and a 2-rate model restricting transitions to the loss of penile sacs ($S^{+}P^{-} \rightarrow S^{-}P^{-}$) followed by the gain of modified pedipalps ($S^{-}P^{-} \rightarrow S^{-}P^{+}$) (Fig. 3.5B). The 2-rate model is an evolutionary trajectory wherein each transition is consistent with escalation in intersexual antagonism during mating. Changes from $S^{-}P^{+} \rightarrow S^{-}P^{-} \rightarrow S^{+}P^{-}$, possible in the 6-rate model, suggest decreasing precopulatory antagonism and/or an increase in reliance on courtship (i.e., female appeasement by the male).

Evolution of the Penis and Female Genital Operculum

Each species was assigned one of two discrete states for each character. The penis was coded as having either a bilateral pair of cuticular sacs that convey a nuptial gift (S+) or as lacking sacs (S^{-}); the female genital operculum was coded as either unarmed (B^{-}) (Fig. 3.2B) or as elaborated to form a pregenital barrier (B^{+}) (Figs. 3.2C, 3.2D). States were determined for all species by original observations of anatomy. We interpreted the evolutionary changes $S^{+} \rightarrow S^{-}$ and/or $B^{-} \rightarrow B^{+}$ as evidence for an increase in precopulatory antagonism and/or a decrease in female appeasement by the male and change in the opposite direction as a decrease in precopulatory antagonism and/or an increase in female appeasement by the male. Ancestral states were determined for each character using parsimony (Maddison and Maddison, 2011) and a hierarchical Bayesian method (Huelsenbeck and Bollback, 2001) implemented in SIMMAP v. 1.5 (Bollback, 2006). In the Bayesian approach, each character was modeled separately in accordance with standards outlined in Schultz and Churchill (1999); we used either an empirical character- bias prior derived from the frequency of terminal states or a β distribution prior where the best-fit α-shape value was derived from Markov chain Monte Carlo (MCMC) sampling (Bollback, 2006). The overall evolutionary rate for each character set was modeled using a Γ-tree prior obtained via MCMC sampling for the α-shape parameter and β-rate parameter (Bollback, 2006). Analyses were replicated with and without outgroup taxa to assess outgroup effects on the relative rates of character change. Root states were inferred from the marginal posterior probabilities for each state across all subsampled, outgroup-rooted trees (n= 431) with fixed branch lengths for each character.

We determined whether state changes in the penis and female genital operculum were correlated using the Discrete module in BayesTraits (Pagel and Meade, 2006). This was done by comparing the marginal likelihoods of two models: an independent 4-rate model in which state changes in the penis and female genital operculum were estimated separately (Fig. 3.5C) and a dependent 8 rate model (Fig. 3.5D) in which single-step changes between the four penis-operculum combinations (S^+B^-, S^+B^+, S^-B^+, S^-B^-) were estimated. Thus a comparison of log-likelihoods that favors the 4-rate model indicates no association between state changes, and a comparison that favors the dependent model indicates correlated change between the penis and female genital operculum.

SIMMAP was also used to test for correlations between male and female genital morphology across the posterior tree distribution using predictive sampling and stochastic character mapping via a continuous-time Markov chain (Huelsenbeck et al., 2003). The overall evolutionary rate for each character set was modeled with the Γ-distribution prior used in the ancestral state reconstructions, and bias priors for male and female characters were modeled either as β-distributions or empirical priors as in the ancestral state reconstruction analyses. Bayesian parametric bootstrapping was conducted by sampling each tree 10 times with 10 prior draws for a total of 43,100 samples for all model parameters. Results were summarized as M-values (i.e., the correlation between the histories of two characters across the phylogeny) and p-values (i.e., the probability that an association between penis state and female barrier presence/absence as extreme as observed could arise simply by chance).

In contrast to parsimony, likelihood- or Bayesian-based trait evolution methods can potentially assess whether change in one state is more likely to precede change in another—even along the same branch—by assigning different rates to these changes. Those states with higher rates are more likely to occur before changes in states with lower rates (Pagel, 1994). Assuming character dependence, it is therefore possible to test whether one character state change (e.g., penis loses sacs) promotes a different character state change (e.g., female gains pregenital barrier). We tested whether nuptial sac loss or pregenital barrier gains were significantly different by using the Discrete module in BayesTraits by comparing a dependent, ‘‘precedence-possible’’ 8-rate model in which transitions between the four penis-operculum combinations were estimated simultaneously (Fig. 3.5F) to a dependent 7-rate model (Fig. 3.5E) wherein gain of the pregenital barrier ($S^+B^- \rightarrow S^+B^+$) and loss of penile sacs ($S^+B^- \rightarrow S^-B^-$) were assumed to occur at the same rate. A comparison of log-likelihoods that favors the dependent, ‘‘no precedence’’ 7-rate model would indicate that the rates of increased antagonism from the ancestral condition are equivalent between the sexes, whereas a comparison favoring the 8-rate model indicates a difference between the rates of escalation between the sexes. In the event the 8-rate model is favored, the mean and variance of rates of escalation can be further compared between the sexes. The sex that was most likely to have initiated the escalation can then be determined by its significantly higher mean rate of morphological change.

General Procedures for BayesTraits Model Testing

All model comparisons in BayesTraits (Fig. 3.5) were made after analyzing trait evolution using a Markov-chain Monte Carlo algorithm with standard uniform rate priors, 2.1×10^8 to 6.0×10^9 iterations, 30% burn-in, and a rate deviation of 0.001–2.0 in order to reach a target acceptance rate of 20–40% per run. At least four independent analyses were performed for each model (see Table 3.1). Log files were uploaded to TRACER to determine stabilization of log-likelihoods (standard error of no more than 0.03 and a visual inspection of the harmonic mean traces). Although model harmonic means should theoretically approach model marginal model likelihoods (Xie et al., 2011; Pagel and Meade, 2006; Pagel et al., 2004), this use of harmonic means has been criticized (Xie et al., 2011; Raftery et al., 2007). Therefore we chose to approximate marginal likelihoods using the "Analysis → Calculate Bayes Factors" function of TRACER (Rambaut and Drummond, 2007) summarized in Newton and Raftery (1994) with modifications by Suchard et al. (2001), calculating 1000 bootstrap replicates of the log-likelihood traces. The mean Bayes factor for each model was calculated and used in model log-likelihood comparisons (Table 3.1). Where model pairs of interest were nested, marginal likelihood approximations were compared using log-likelihood ratio tests. Except where noted, significance was determined where the test statistic value surpassed the χ^2 distribution critical value at an α value of 0.05. Degrees of freedom were calculated by solving for the difference in estimated parameters.

Results

Evolution of the Penis and Male Pedipalps

The ancestral male reproductive morphology was inferred by considering the likelihood of the evolutionary trajectory of male traits when root state was fixed or not fixed. A comparison of Bayes factors from the 6-rate, fixed-root model (Fig. 3.5A), where a root state of S^+P^- was constrained, to those from a similar model where no constraint was imposed, showed no appreciable difference in marginal likelihoods of the models (K = 0.538). This result indicates that the co-occurrence of penile sacs and simple male pedipalps is the primitive state for the eastern North American clade of leiobunine harvestmen, which is consistent with the conclusion based on parsimony (Fig. 3.4). Comparison of the marginal likelihood approximations of the 6- rate ‘‘no precedence’’ model, where change between any of the three discrete male reproductive characters is possible, to a 2-rate ‘‘penis-precedence’’ model, where only two transitions are allowed, indicated no significant difference between the two models (log-likelihood ratio test: χ^2 = 2.996, D.F. =4, $p<0.1$). Given this result, the simpler 2-rate ‘‘penis-precedence’’ model is preferred, and we conclude that there may have been a tendency for penile sacs to be lost before the male pedipalps were enhanced for clasping the female. The likelihood of this model is further supported by the lack of species with both enhanced pedipalps and penile sacs.

Evolution of the Penis and Female Genital Operculum

In order to assess the ancestral states of male and female reproductive morphology with hierarchical Bayesian analysis, the probability distribution priors were estimated for each character set using an MCMC-sampling method (Huelsenbeck and Bollback, 2001). In all SIMMAP analyses, Γ-tree priors for the overall evolutionary rate of each trait were applied. The overall evolutionary rate best-fit shape (α) and rate (β) parameters for penis morphology were α = 3.515, β = 0.038, and for barrier presence, α = 3.108, α= 0.036. Character-bias priors were modeled with either an empirical approach based on the frequency of tip states, or with a β distribution prior. The best-fit α values for each character-bias distribution were $\alpha = 5.888$ for penis morphology and $\alpha = 5.906$ for morphology of the female genital operculum.

Character mapping under parsimony (Fig. 3.4) supported the parallel loss of penile sacs from a sacculate ancestor ($S^+ \rightarrow S^-$) and gain of female pregenital barricade from ancestors with an unarmed genital operculum ($B^- \rightarrow B^+$). At least four such transitions are necessary for each character (Fig. 3.4), although this number is dependent on topology, which we varied in our analyses due to species paraphyly (Burns et al., 2012). These results were consistent with those obtained from the Bayesian approach implemented in SIMMAP. The presence of penile sacs (S^+) was recovered as the ancestral male character state with marginal posterior probabilities ranging from 78% to 80% (with probability being dependent on use of either the two-state empirical or β-bias prior and inclusion/exclusion of the outgroup). Absence of a pregenital barrier (B^-) was the most likely ancestral female character state, with marginal posterior probabilities of 77% to 96% (with the probability being dependent solely on inclusion or exclusion of outgroup character states in the analysis). Results from two methods thus support an ancestral taxon wherein males had sacculate penes and females lacked a pregenital barrier.

To assess the hypothesis that there are two syndromes of coevolved morphological features, we first needed to determine whether state changes in the penis and female barrier were correlated. We used the BayesTraits Discrete module to compare marginal likelihoods of two alternative hypotheses modeling either independent or dependent change in traits (Figs. 3.5C vs. 3.5D). Log-likelihood ratio tests of the marginal likelihood approximations of these models favored the dependent, 8-rate model (χ^2 =9.672, D.F. = 4, $p<0.05$). We conclude that the evolution of male and female reproductive structures is correlated across the phylogeny.

Using SIMMAP we also demonstrated a correlation between male and female reproductive morphology. Bayesian predictive distributions were generated using stochastic mapping of male and female reproductive traits to the filtered posterior tree distribution. When compared to the actual trait states by species, a mean correlation between penis morphology and female pregenital barrier presence of 0.147 ($p<0.01$) was found under the empirical prior, and a correlation of 0.151 ($p<0.05$) was derived using the β-bias prior. Individual state covariation between sacculate penis type and absent pregenital barrier (Empirical: m_{00} = 0.063, $p<0.01$, β: m_{00} =0.065, $p<0.01$) and non-sacculate penis type and present pregenital barrier (Empirical: m_{11} = 0.068, $p<0.01$, β: m_{11} = 0.07, $p<0.05$) was found to be positive and significantly distinct from the predictive distribution. The relationships of sacculate penis type with presence of pregenital barrier (Empirical: m_{01} =20.054, $p<0.01$, β: m_{01} =20.055, $p<0.01$) and nonsacculate penis type with a lack of female pregenital barrier (Empirical: m_{10} =20.052, $p<0.01$, β: m_{10} =20.053, $p<0.01$)—both trait combinations seen in a small but non-zero number of species in the phylogeny—co-varied negatively, yet remained significantly different from the predictive distribution.

As male and female morphology was demonstrated to covary across the phylogeny, we additionally tested whether the evolutionary rate at which penile sacs were lost was equal or unequal to the rate at which females acquired the pregenital barrier, all relative to the sacculate, barrier-free ancestor. We compared the likelihood of a 7-rate ‘‘No Precedence’’ model where the rates of pregenital barrier acquisition and loss of penile sacs were forced to be equal, to an 8-rate "Precedence-Possible" model (Fig. 3.5E). Comparisons of marginal likelihoods revealed a significant difference between models and favored the 8-rate scheme (Fig. 3.5F) (χ^2 =9.936, D.F. = 1, p<0.01). Thus, the rates of change of the penis and female genital operculum cannot be assumed to be equal, and the precedence of one sex’s trait change over the other is supported. However when comparing rates of character change and accounting for rate variance, the ‘‘Precedence-Possible’’ model does not appear, on average, to estimate a higher rate for either transition (μ_{q12} vs. $_{q13}$ = 10.94±18.27, D.F. = 3, t= 1.905, p = 0.0765). An increased number of simulations or alternative priors on m might change the significance of this difference. Ultimately, there is evidence that changes in the penis and female genital operculum are correlated and that rates of state changes are unequal, which suggests that change in one may precede change in the other. Parsimony on the backbone constraint tree (Fig. 3.4) suggests pregenital barrier development may have preceded the loss of sacs, but this result is subject to tree topology. As uncertainty in topology was included in the model testing procedure, no conclusion regarding character evolution precedence may be made by parsimony alone, although improved sampling and resolution of the *Hadrobunus* species group might alter this. We found no evidence that change in one sex strongly tended to precede change in the other.

Discussion

Patterns in the Evolution of Reproductive Structures in Leiobunine Harvestmen

The results from our analysis indicate that the leiobunine harvestmen of eastern North America are descended from an ancestor with reproductive structures that are consistent with a mating system dominated by courtship where males entice or appease females to obtain copulation. Results from both Bayesian and parsimony-based methods of character reconstruction showed that ancestral males had a subterminal pair of penile cuticular sacs used in conveying a nuptial secretion to the female during the precopulatory phase of mating (Figs. 3.1B, 3.3). The male pedipalps were used to clasp the female at the base of her second leg pair but were morphologically similar to those of females. The pregenital openings of females lacked sclerites that might serve as a barrier to forced intromission by the male. This syndrome of reproductive features has persisted in several diverse lineages, and these offer opportunities to explore further the details of the ancestral system. It is reasonable to suppose that the evolutionary mechanism of female mate choice has played a predominant role in shaping the ancestral reproductive syndrome. There have also been at least four phylogenetically independent transitions from the ancestral system toward morphologies and behaviors consistent with precopulatory antagonistic behavior.

This assumes no parallel gains of the nuptial gift sacs, a reasonable assumption given the complexity of the structure and its function in mating (Felsenstein, 2004). We suspect that the number of independent transitions from sacculate to non-sacculate conditions will increase as phylogenetic relationships within the Hadrobunus group are clarified. In each case, penile sacs have been lost and females have evolved sclerotized pregenital barriers. In addition, the male pedipalps of species within the calcar and vittatum species-groups are enhanced for clasping the female. Each transition has resulted in a different construction of the penis, the female pregenital barrier (Fig. 3.2) and male pedipalps (compare Figs. 3.1A, 3.3).

Our results indicate that loss of penile sacs and elaboration of male pedipalps are correlated. In fact, modified pedipalps always co-occur with non-sacculate penes, although not all non-sacculate species have enhanced male pedipalps. This evolutionary trajectory supports the hypothesis that precopulatory antagonism has originated or increased several times in leiobunine phylogeny, a hypothesis further supported by the correlation found between male and female morphological states. There is some additional evidence from our Bayesian modeling of the evolution of the penis and male pedipalps that the loss of penile sacs tends to precede the elaboration of the male pedipalps (Fig. 3.4). Interestingly, there are few morphological specializations in females that appear to be dedicated to resisting clasping by males. The only possible exception occurs in the Hadrobunus group, where females in all species (both sacculate and non-sacculate) have a spike-like process or ‘‘coxal spur’’ on the posterior margin of the basal segment of the second leg, where the base of the male pedipalpal tarsus likely contacts the female (Shultz, 2012).

The timing of the loss of penile sacs and gain of pregenital barriers are strongly correlated. The Bayesian analysis of character evolution showed that a difference likely exists in the rates of the two transformations, which may indicate a tendency for one kind of evolutionary change to precede the other (Pagel, 1994). However, additional tests aimed at resolving these rates failed to find significant differences, and it was not possible to determine whether evolution in the structures of one sex tends to lead the coevolutionary change.

The distribution of morphological characters made parsimony-based character mapping similarly uninformative for reconstructing the sequence of change in the penis and pregenital barrier. The ancestral condition (penile sacs present, pregenital barrier absent) and one derived condition (penile sacs absent, pregenital barrier present) were by far the most common, but unambiguous losses of penile sacs and gains of female pregenital barriers mapped to the same branches and were necessarily interpreted as effectively simultaneous events. However, two species, *Hadrobunus grandis* and an undescribed *Hadrobunus* (*H*. n. sp. 3 IL) have both sacs and barriers, and one species, *Leiobunum relictum*, lacks both sacs and barriers. Depending on their exact phylogenetic positions, these species could represent either an intermediate stage in the transition from courtship to antagonism or a reversal from antagonism back to courtship. Although we regard a reversal to the sacculate condition *per se* as unlikely (Felsenstein, 2004), the secondary loss of a pregenital barrier is more plausible.

In fact, both *L. relictum* and the undescribed *Hadrobunus* n. sp. 2 MO show evidence of incipient or vestigial pregenital barrier structures that are fully developed in closely related taxa. The phylogenetic placement of these species requires corroboration by additional molecular data and analyses.

Explaining Evolutionary Change in Reproductive Structures

Our present work on the natural history and morphology of leiobunine harvestmen suggests an association between the type of precopulatory mechanism within a species and the duration of its breeding season. Specifically, species with potentially longer breeding seasons tend to have sacculate penes and other features consistent with female enticement by males, while species with shorter breeding seasons tend to have non-sacculate penes and traits associated with precopulatory antagonism. Tropical leiobunines have potentially long breeding seasons and virtually all species retain the ancestral conditions of sacculate penes, simple male pedipalps and unfortified female pregenital openings (J.W. Shultz, pers. obs.). Furthermore, males of these species are typically much smaller than females and tend to have short, poorly sclerotized penes with relatively large gift-bearing sacs. In contrast, species with features consistent with precopulatory antagonism (non-sacculate penes, enlarged male pedipalps, female pregenital barriers) are limited almost exclusively to north temperate regions (J.W. Shultz, pers. obs.), where breeding seasons are presumably limited by the onset of cold winters. Non-sacculate species overwinter as eggs and reach the final instar in midsummer or later. Significantly, those populations with the most well-developed male palps and female pregenital barriers tend to occur on mountains (e.g., *Leiobunum hoffmani* and *L. calcar*) (Ingianni et al., 2011), where breeding seasons are likely to be short. There are also sacculate species in the north temperate region but most overwinter as immatures, attain adulthood in late spring and have potentially long breeding seasons (Fig. 3.4: "early-season" clade). There are exceptions to these patterns (e.g., *L. aldrichi* and *L. politum* are sacculate but mature in summer), and the precise onset of sexual maturity and duration of breeding seasons are unknown for all species. Additional research will be required to define the precise reproductive phenology for all eastern leiobunines, but these differences may be key to identifying the mechanism(s) by which reproductive structures have diversified. In light of these life history traits, multiple coevolutionary scenarios may be invoked to identify the origin and/or maintenance of reproductive morphology in the leiobunine harvestmen. We offer three hypotheses that may explain the association between male and female armaments observed across the phylogeny.

1. Natural Selection and the Resource-limitation Hypothesis. In primitively sacculate leiobunines, males make a material contribution to females in the form of an apparently all-or- nothing primary nuptial gift delivered by penile sacs as well as a secondary gift offered directly from the male accessory glands. The environment could impact male genitalic structure indirectly via fitness costs associated with the time and energy used in producing nuptial gifts. Long breeding seasons may provide ample time to replenish gifts, and the cost of losing a gift to an unreceptive female may be relatively low. However, short breeding seasons offer less time for males to acquire the raw materials to produce new gifts (Lewis et al., 2004), and wasting gifts on unreceptive females may result in high fitness costs (Boggs, 1995). The effect could be exacerbated if resource limitations also result in females placing greater demands on males for nutritional gifts prior to copulation. In populations where breeding seasons are short, natural selection could favor changes that reduce male costs, such as the reduction or loss of the all-ornothing primary gift and the penile sacs that them. Predictions of this hypothesis could be tested in sacculate species by comparing mechanisms of gift delivery in populations with breeding seasons of different durations. These tests would require the use of continuously varying features rather than the presence/absence characters examined here.

Reduction or loss of the primary nuptial gift would presumably entail an evolutionary response in mechanisms that govern female receptivity (Boggs, 1995), but it seems unlikely to result directly in the evolution of female pregenital barriers; that is, the reduction of nuptial gifts is not in itself a coercive or antagonistic change warranting the evolution of resistance structures in females. However, it may be that a behavioral form of precopulatory antagonism was present as a facultative strategy in the ancestral mating system or was regularly adopted near the end of the breeding season when males no longer had sufficient time to replenish nuptial gifts. Thus, shorter breeding seasons may shift the relative duration and/or intensity of ancestrally coexisting strategies, as seen experimentally in seed beetles (Cayetano et al., 2011), and this could explain the coevolutionary loss of penile sacs and gain of female pregenital barriers found in our study system. Whether or not behavioral precopulatory antagonism existed in the ancestral mating system or evolved later—perhaps in response to environmental effects on males—two additional alternative hypotheses may account for antagonistic morphologies observed in leiobunine harvestmen.

2. Female Choice and the Shifting-signal Hypothesis. The ancestral presence of gift-bearing penile sacs is consistent with a mating system dominated by female mate choice; females may have chosen males based on the quality of their material ‘‘display.’’ If the loss of penile sacs reflects excessive male fitness costs imposed by short breeding seasons, the ancestral material signal would need to be replaced by a different signal if female choice is to persist. The correlated loss of penile sacs and origin of female pregenital barriers may reflect a shift from a nutritional/chemical signal of male quality to a mechanical/stimulatory signal. Coevolution of reproductive ‘‘armaments’’ between the sexes could reflect competition among males to enhance the mechanical signal offered to females (i.e., force produced by the penis or pedipalps) and enhancements to the female that allow her to safely assess forceful mechanical signals (i.e., the female pregenital ‘‘barrier’’). This evolutionary process might outwardly resemble sexually antagonistic coevolution, but would be maintained as a form of female choice for superior mates by using female "resistance" as a screen (Codero and Eberhard 2003; Eberhard, 1996).

However, persistent control of mating outcomes by females in this system would require the female to be mechanically superior to males, unless forced copulation itself represents a kind of female choice (Brennan and Prum, 2012). One implication of the shifting-signal hypothesis is that the ancestral nutritional/chemical signals appear to be a direct fitness benefit to the female while the mechanical signal represents indirect benefits through increased offspring viability via good genes (Reinhold, 2004) or the product of a Fisherian sexy sons process (Huk and Winkel, 2008; Tallamy et al., 2003).

Evidence from other systems indicates that offspring resulting from coercive encounters may have lower fitness (Gasparini et al., 2011; Maklakov and Arnqvist, 2009), but the question of whether the indirect benefits derived from female preferences for coercive males are significant enough to drive changes in female resistance has yet to be answered to the satisfaction of the field (Brennan and Prum, 2012; Cameron et al., 2003).

3. Intersexual Conflict and the Male-male Competition Hypothesis.

Shortened breeding seasons should increase competition among males for access to females, especially within polygynadrous species like harvestmen. Mechanisms of male-male competition can themselves be detrimental to female fitness, whether by overriding female preferences and preventing females from mating with preferred suitors (Wong and Candolin, 2005) or by producing structures and behaviors in the context of intrasexual conflict that lead to female loss of fitness during mating (Eberhard and Cordero, 2003). Males may monopolize females via prolonged pedipalpal clasping or mate guarding (Zatz et al., 2011), thereby limiting the time available to the female for feeding, oviposition or mating with preferred males (Mullter et al., 2007), while also exposing the female to predators (Cothran, 2004). While superficially appearing to be beneficial or at least not harmful to females by reducing mating rate (Maklakov et al., 2005), these male behaviors may have a net detrimental effect on female fitness. Also, by-products of sperm competition, a form of post-copulatory male-male competition, may lower female long-term fertility (Maklakov et al., 2005) or longevity (Alonzo and Pizzari, 2013).

The hypotheses proposed here invoke an overarching role for the environment in precipitating evolutionary change in reproductive structure and behavior and thereby offer an alternative to the near-exclusive focus on female choice and sexual conflict that have tended to dominate recent discussions. Our proposals anticipate a positive relationship between the duration of breeding season and the intensity of material-based courtship and/or an inverse relationship with the intensity of forceful interactions between the sexes. The focus on duration of breeding season does not deny significant roles to either female choice or sexual conflict in shaping reproductive evolution but offers a testable explanation of reproductive diversity by assessing the strength of associations between ecological, morphological, and behavioral variables. In contrast, the predictions of female choice and sexual conflict tend to differ mainly in the difficult-to-measure fitness outcomes for the two sexes (Chapman et al., 2003). Indeed, when considering fitness in the broad sense, antagonistic precopulatory behavior appears to be explained as readily by female choice for male mechanical abilities as by intersexual conflict (Brennan and Prum, 2012). Progress towards integrating these heretofore competing mechanisms may require an alternative perspective, like the one initiated in this paper.

Tables

Model	Run 1	Run 2	Run 3	Run 4	Mean
No Precedence (Fig. 3.5A)	-29.497±0.06	-29.66±0.062	-29.54±0.047	-29.72±0.056	-29.61±0.056
Penis Precedence (Fig. 3.5B)	-30.97±0.048	-31±0.044	-30.95±0.037	-31.493±0.04	-31.10±0.042
Fixed Sacculate Root (Fig. 3.5A)	-30.17±0.047	-30.145±0.05	-30.09±0.047	-30.17±0.051	-30.14±0.049
Independent Change (Fig. 3.5C)	-38.492±0.06	-38.404±0.05	-38.47±0.059	-38.39±0.047	-38.44±0.054
Dependent Change (Fig. 3.5D)	-35.23±0.037	-32.85±0.047	-33.15±0.062	-33.18±0.058	-33.6±0.051
No Precedence (Fig. 3.5E)	-38.99±0.019	-38.55±0.018	-38.59±0.018	-38.16±0.019	-38.57±0.019

Table 3.1: Model Bayes factors. Bayes factors from four independent runs per model in BayesTraits (Pagel and Meade, 2006; Pagel et al., 2004) and means used in log-likelihood ratio tests. Bayes factors were calculated using TRACER 1.5 (Rambaut and Drummond, 2007) with 1000 replicates of the log-likelihood traces. See Figure 3.5 for model design details.

Figures

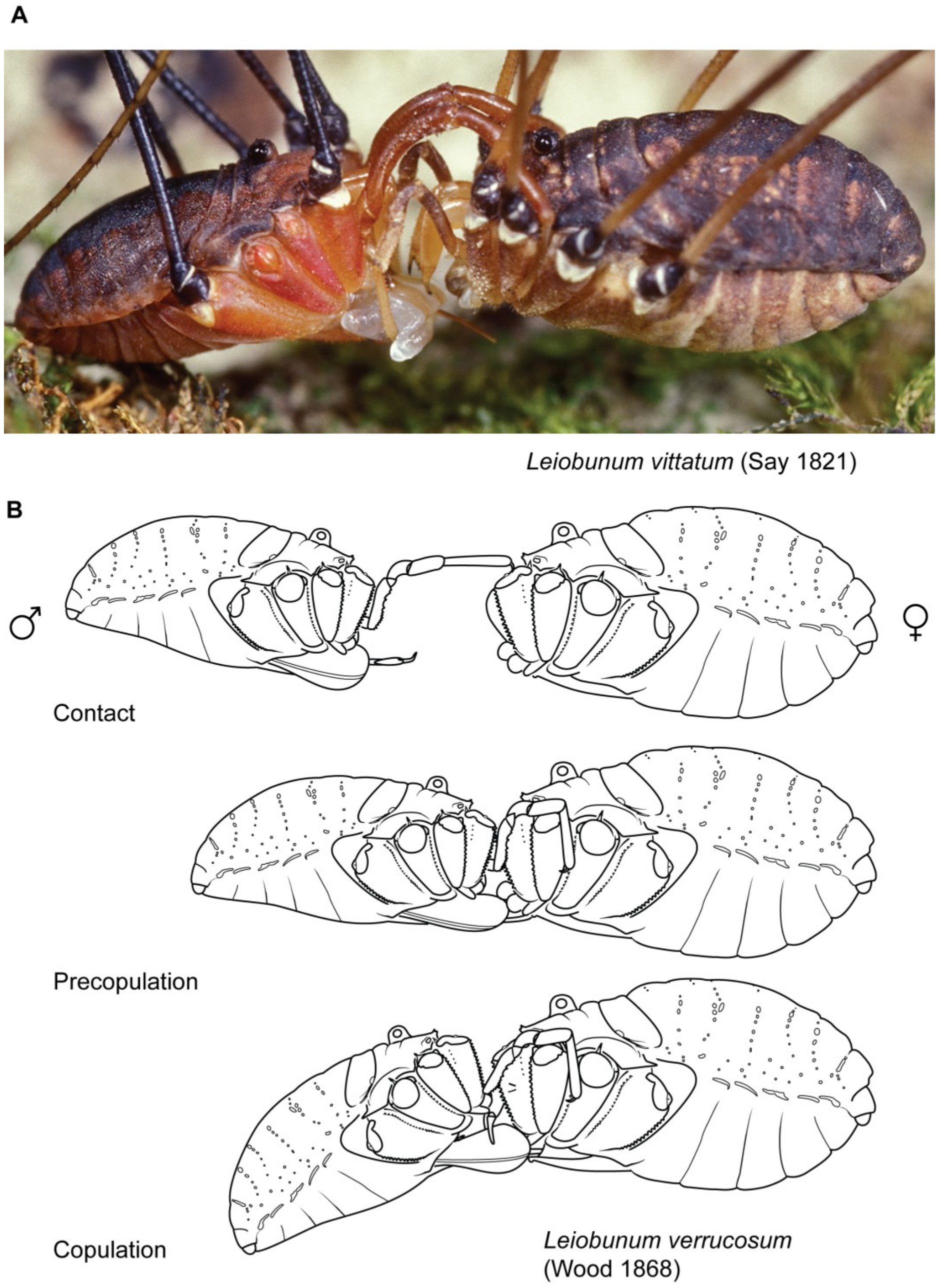

Figure 3.1: Mating behavior and morphology in leiobunine harvestmen.

(A) Precopulatory behavior in *Leiobunum vittatum*. Male on left, female on right. Photograph courtesy of Joe Warfel (Eighth-Eye Photography). (B) Major phases in mating in *Leiobunum verrucosum* (semi-diagrammatic, legs not included for clarity).

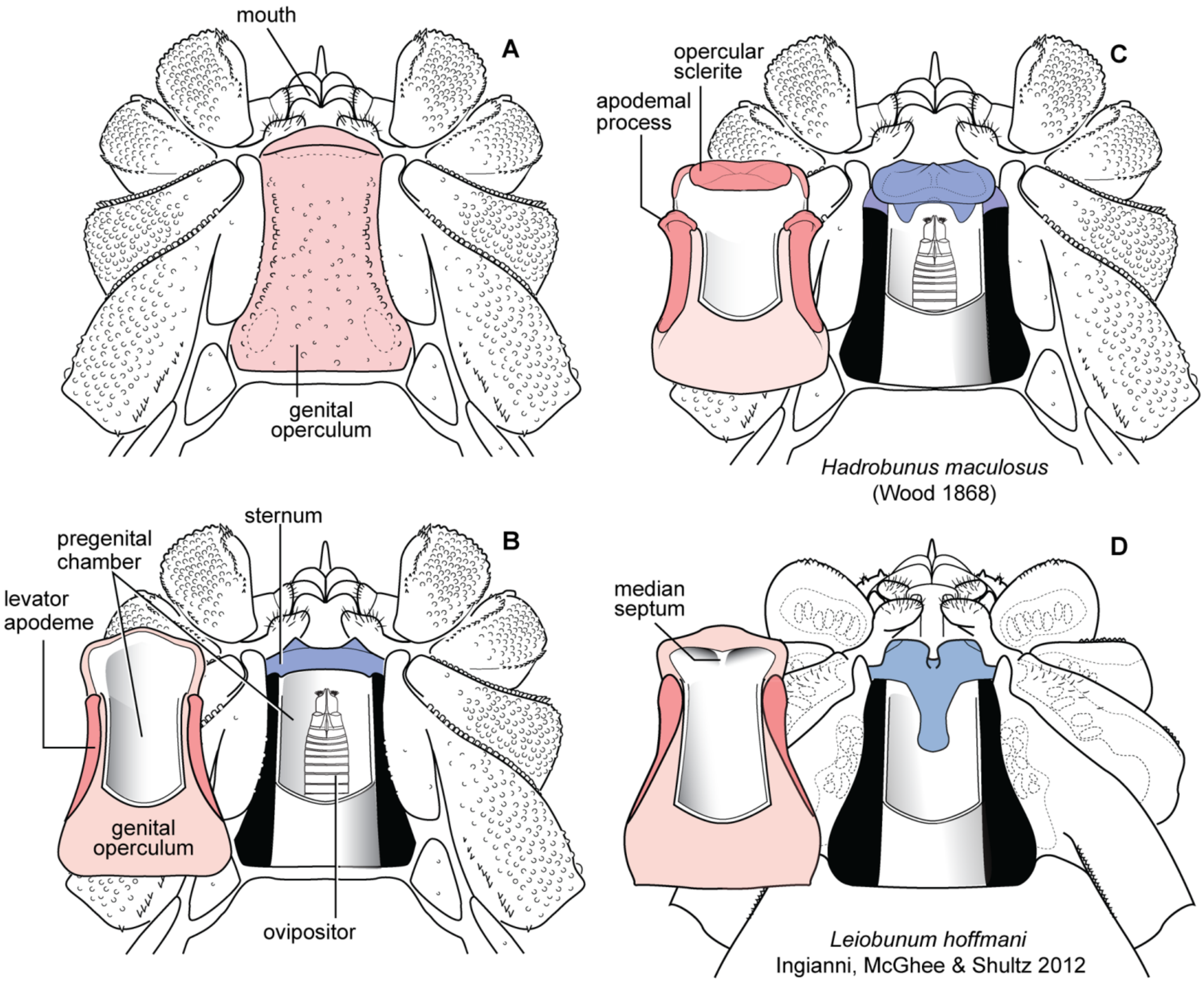

Figure 3.2: Female genital morphology in leiobunine harvestmen.

(A) Ventral surface of generalized female showing relative positions of the feeding apparatus and pregenital opening. (B) As in A, but with genital operculum removed and flipped to show the inner structures of a simple (primitive) operculum and sternum, not modified into a pregenital barrier. (C) Ventral surface of *Hadrobunus maculosus* from same perspective as B, showing pregenital barrier (see also Fig. 3). The large sclerotized sternum engages the opercular sclerite anteriorly and apodemal processes posteriorly. (D) Ventral surface of *Leiobunum hoffmani* from same perspective as B and C, showing pregenital barrier (see also Fig. 3.3). The anterior median notch in the sclerotized sternum engages a sclerotized median septum on the genital operculum; the posterior margin of the sternum abuts the anterior margin of the levator apodeme (based on Ingianni et al. (2011)). In both C and D, a barrier is formed by a sclerotized sternum wedged between anterior and posterior elements of the genital operculum.

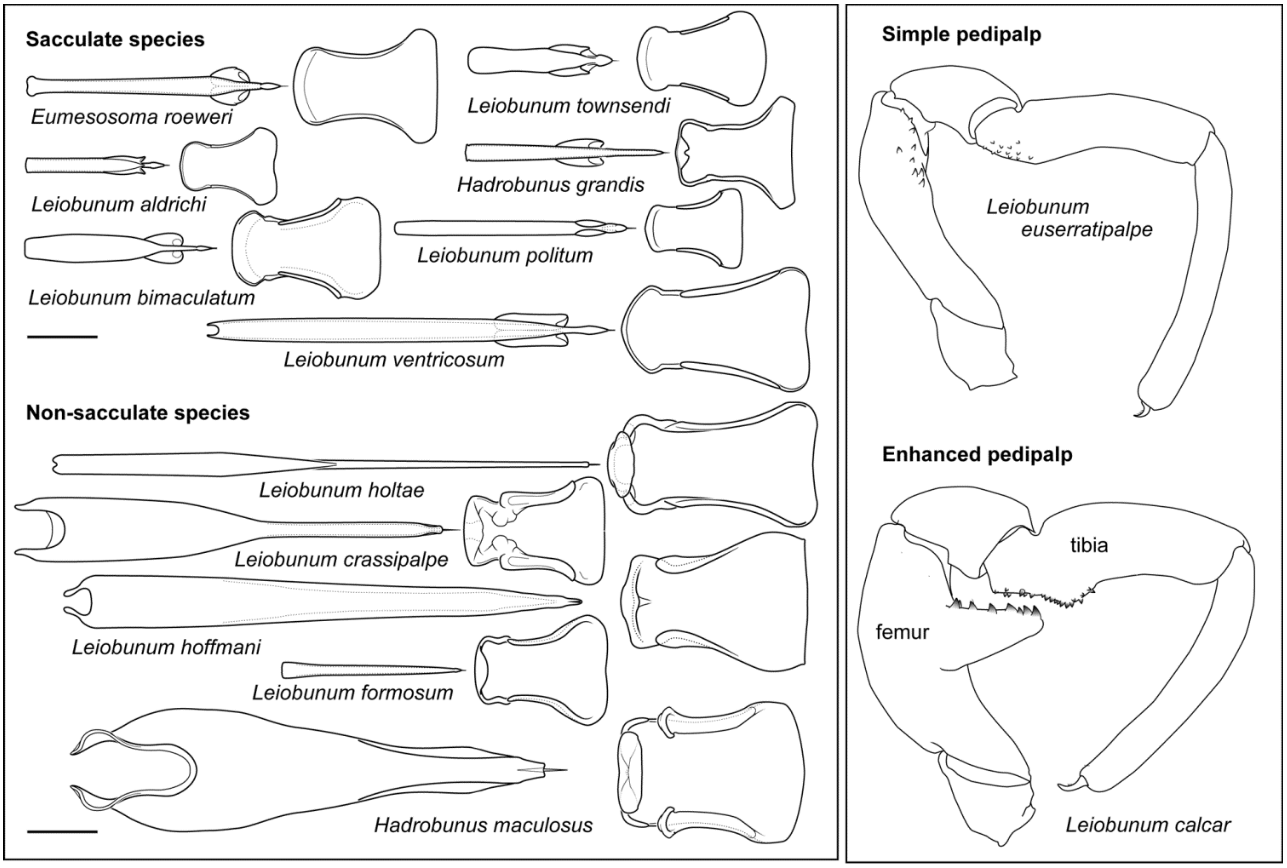

Figure 3.3. Structures from representative sacculate and non-sacculate species of leiobunine harvestmen.

Penes are depicted from a dorsal view. The genital opercula are shown from the inner (dorsal) perspective (compare with Fig. 3.2 B-D). All penes and opercula (right box) are drawn to the same scale; bar = 1 mm. The pedipalps are from male *Leiobunum euserratipalpe* and *L.calcar* (Ingianni et al., 2011). Simple male pedipalps are roughly similar in shape and relative size to those of females. The enhanced male pedipalps (left box) depicted have femoral apophyses which are used in concert with the base of the tibia to clamp the trochanter of the female's first pair of legs during mating. See Figure 3.1A for a different form of enhanced male pedipalp, in which the overall length of the pedipalps is sexually dimorphic (longer in males relative to females).

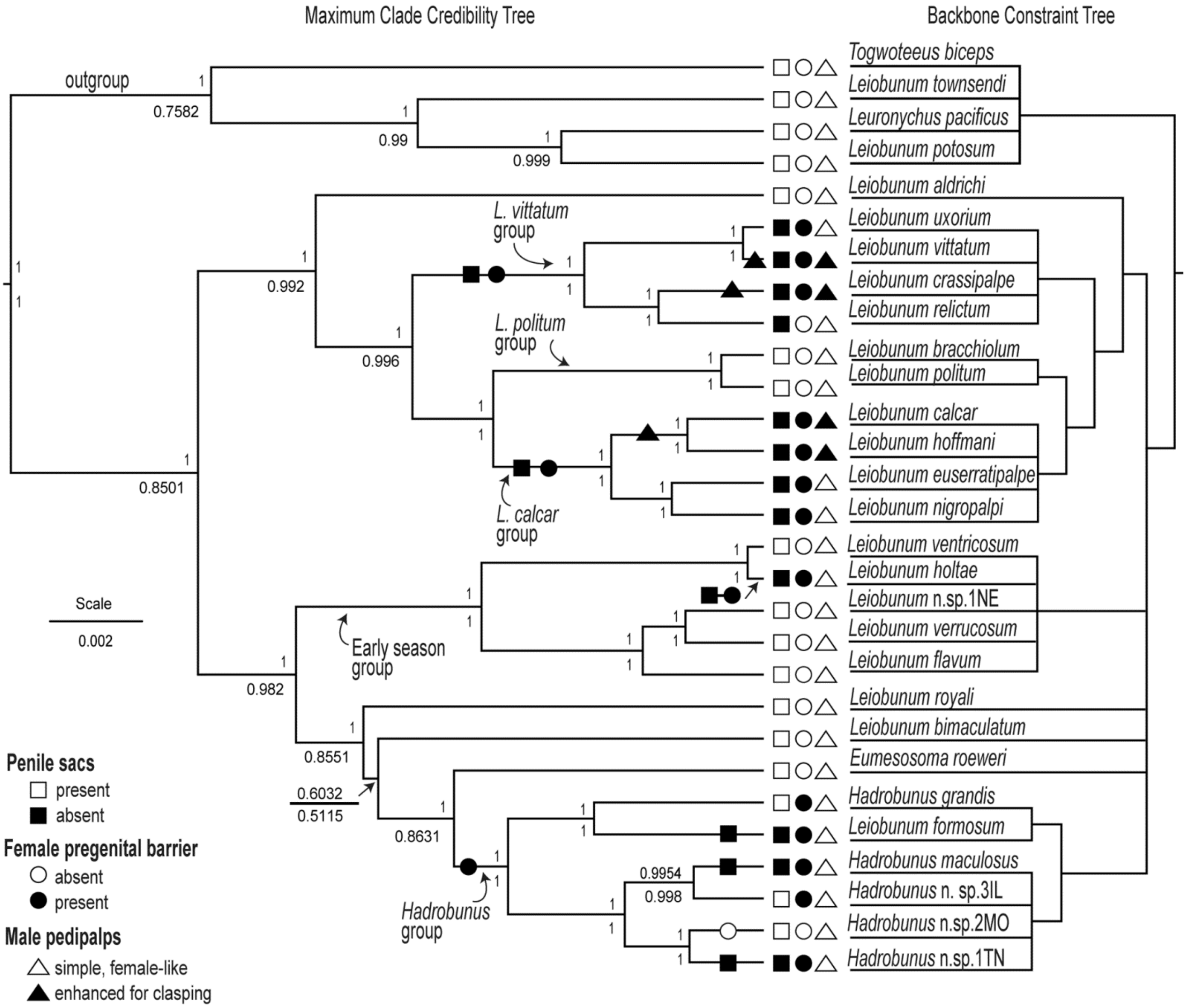

Figure 3.4. Phylogenetic hypotheses and distribution of reproductive characters.

The maximum clade credibility Bayesian tree (left) was assembled using the TreeAnnotator program (Drummond et al., 2012), visualized with FigTree v1.3.1 (Rambaut, 2009), and depicts relationships recovered in BEAST v1.7.1 (Drummond et al., 2012) for trees that passed the backbone constraint tree (right). Values above branches indicate the posterior probabilities per node for filtered trees (n=431). Values below braches are the posterior probabilities of the maximum clade credibility tree for a subset of 1000 random trees resampled from the original posterior probability distribution. Scale is in substitutions per site for the filtered subset maximum clade credibility tree. The most parsimonious distribution of reproductive characters (assuming no parallel gains in penile sacs) are mapped to the maximum clade credibility tree. Geographic codes are given for undescribed species: IL=Illinois, MO=Missouri, NE=Nebraska, TN=Tennessee. The backbone constraint tree (right) depicts relationships that were well supported (>95% posterior probability) in the (Burns et al., 2012) tree and that were used to generate sets of trees for the present study.

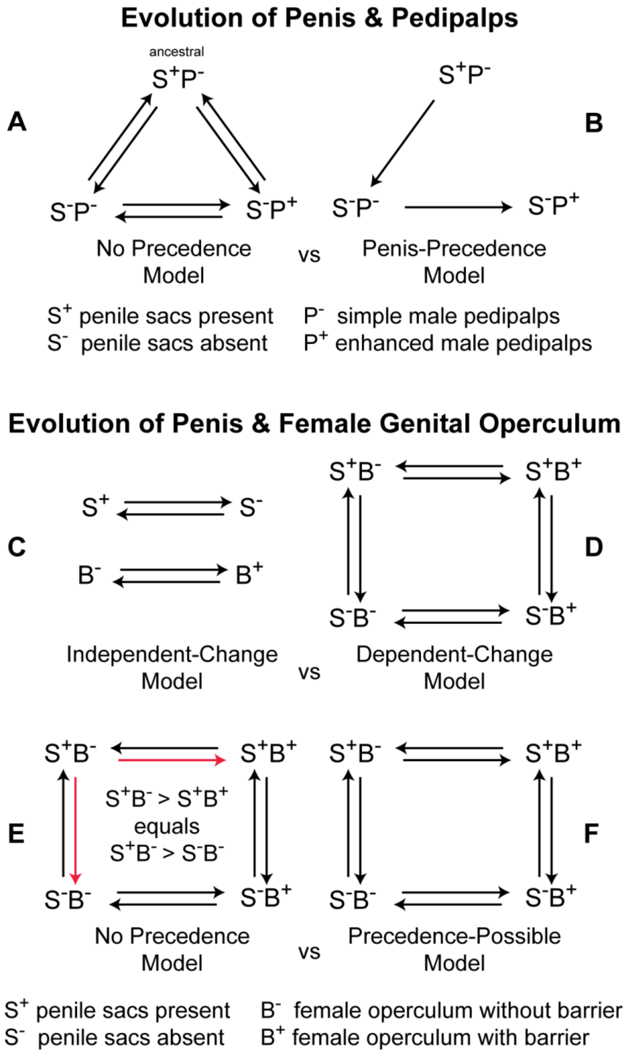

Figure 3.5. Transition models used to test hypotheses for the evolution of reproductive characters with Bayesian analysis.

(A) No-precedence model of male morphological evolution versus (B) Penis precedence model, where male morphological transitions are limited to sacculate (S^+) to nonsacculate (S^-) penis and simple pedipalps (P^-) to enhanced pedipalps (P^+). The root of A was treated as fixed to S^+P^- (Table 3.1, row 3) or determined empirically (Table 3.1, row 1). (C) Independent and (D) dependent models of discrete male and female reproductive morphology. Here, the female pregenital barrier is coded as present (B^+) or absent (B^-). Both models allow for all possible character transitions. (E) No precedence model was compared to dependent model (F), where character precedence is possible. In this model, penile sac loss ($S^+B^- \rightarrow S^-B^-$) and barrier acquisition ($S^+B^- \rightarrow S^+B^+$) are constrained to have equal rates of evolution.

CHAPTER 4: Comparative analyses of biomechanical reproductive traits in harvestmen (Arachnida, Opiliones) support intersexual coevolution via simultaneous sexual selection mechanisms

See Appendix 3 for supplementary tables (Table S4.1) and figures (Figure S4.1, S4.2) referenced in this chapter.

Abstract

Reproductive traits have a long history as taxonomic characters, but their precise functions and the combination of evolutionary processes underlying their diversification are not well understood. Most researchers attribute diversity in reproductive structures to either sexual selection by female choice, intersexual conflict or to some poorly-defined synthesis of the two. In order to assess the presence or absence of simultaneous effects of choice and conflict, we analyzed biomechanical variables from both sexes of 29 harvestman species using phylogeny-based comparative approaches. Our results corroborated the hypothesis that female choice and intersexual conflict can operate simultaneously at differing intensities to generate a continuous spectrum of forms. Canonical correlation analysis of male and female traits revealed a strong relationship consistent with sexual coevolution in precopulatory structures. Species with pregenital barriers specialized for intersexual conflict dominated one end of the spectrum, those lacking such specializations (including those with gift-bearing penile sacs) dominated the other, and there was a significant region of overlap. Similar results were obtained with principal components analysis. Furthermore, linear discriminant analysis could not reliably distinguish groups defined by the presence or absence of gift-bearing penile sacs or groups defined

by the presence or absence of female pregenital barriers, results that are inconsistent with the hypothesis that female choice and intersexual conflict act in a mutually exclusive manner. Our results suggest that the relative intensities of female choice and intersexual conflict that have shaped the reproductive mechanisms of individual species can be quantified. This ability will allow statistical comparisons with quantifiable ecological, life-history or social variables and may ultimately reveal the arrangement of evolutionary factors that shape diversity in reproductive structures.

Introduction

Recent attempts to explain the rapidly evolving, species-specific diversity of reproductive structures have tended to focus on the relative impacts of two evolutionary mechanisms—sexual selection by female choice (Eberhard, 1996) and intersexual conflict (Arnqvist and Rowe, 2005; Chapman et al., 2003). In mating systems dominated by female choice, females prefer males with features that either benefit the female directly (e.g. nuptial gifts, access to resources) or indirectly by indicating positive genetic contributions to offspring (Tazzyman et al., 2012; Head et al., 2005; Calsbeek and Sinervo, 2002). Intersexual conflict occurs when the fitness of one sex is enhanced by a mating event while the fitness of the opposite sex is reduced, as when multiple matings enhance fitness in males but decrease fitness in females (Hosken and Stockley, 2005). In such cases, reproductive structures in males may evolve to increase the probability of mating successfully by coercion and those of females may evolve to resist coercive matings, perhaps leading to a series of reciprocal, escalating adaptations called a sexual arms race (Gage, 2004; Arnqvist and Rowe, 2002).

Both female choice and intersexual conflict are widely acknowledged as having a significant influence on the observed diversity of reproductive behavior and morphology, but the manner and extent of their co-functionality in a single mating system is an on-going subject of discussion (Brennan and Prum, 2012). There has been a tendency for researchers to describe mating systems and reproductive structures as having been shaped largely or entirely by either sexual conflict or female choice (Pizzari and Snook, 2003). For example, Eberhard (2004a, 2004b) reviewed the taxonomic literature on terrestrial arthropods and, based on interpretations of published illustrations and descriptions of genitalia, categorized species into those shaped by female choice and those shaped by conflict. He concluded that conflict plays a comparatively minor role in shaping diversity. Such skepticism about the importance of intersexual conflict has spurred researchers to highlight examples of conflict-based mating systems, as in bedbugs (Siva-Jothy, 2006), seed beetles (Gay et al., 2010), waterstriders (Eldakar et al., 2010; Arnqvist and Rowe, 2002), flies (Nandy et al., 2014), diving beetles (Bergsten and Miller, 2007), and many others. It is possible that the choice versus conflict dichotomy is a normal polemical stage in the emergence of a new research topic. However, there is an implicit assumption that the two mechanisms are mutually exclusive (Parker, 2006). On the other hand, many workers assume that female choice and intersexual conflict probably act simultaneously with differing intensities and that different species may be placed along a hypothetical spectrum, with conflict-dominated species at one end and female choice-dominated species at the other (Simmons, 2014), although it appears that no rigorous empirical examples of this concept have been published. The principal goal of the present study is to determine whether reproductive structure diversity within a group of species is better accommodated by two categories representing female choice and intersexual conflict, or a continuous spectrum of intermediates with extreme examples of choice and conflict occupying opposite ends of parameter space.

Results from our previous study of reproductive structures in the leiobunine harvestmen of eastern North America (Burns et al., 2013) appeared to corroborate the view that female choice and intersexual conflict are mutually exclusive processes. In that study, we examined the phylogenetic distribution of two binary traits, one in each sex, that are involved in precopulatory interactions: males have either a pair of gift-bearing sacs near the end of the penis or not (Fig. 4.1A); females have either a pregenital barrier or not. Of the four possible male/female trait combinations, two were widespread among the 29 species examined; one was consistent with female choice (males with gift-bearing sacs, females without pregenital barriers) and the other with intersexual conflict (males without sacs, females with pregenital barriers). The two ambiguous or intermediate trait combinations—male with sacs, female with barrier and males without sacs, female without barrier—were found in two and one species, respectively. Parsimony and phylogenetic comparative analyses showed that the “female-choice” combination is primitive for the clade and was replaced by the “intersexual-conflict” combination at least four times, with the loss of penile sacs and gain of female pregenital barriers evolving effectively at the same rate within each derived lineage. Together, the paucity of species with intermediate trait combinations and the seemingly rapid switch from choice-based to conflict-based traits suggests that intermediate stages were short-lived or unstable, although maintained in a few, unusual circumstances. These observations and interpretations are consistent with the proposal that female choice and intersexual conflict act as essentially as mutually exclusive processes, at least within the precopulatory mechanisms of leiobunine harvestmen.

Still, the ability of our previous analysis to determine whether female choice and sexual conflict act in a mutually exclusive or simultaneous fashion was limited by several factors, particularly the low number and qualitative nature of the traits examined. In fact, our use of binary traits may have biased the outcome in favor of a conclusion that choice and conflict are incompatible evolutionary processes (Berglund et al., 1996). Further, it is not clear that the male and female traits we used have a direct functional relationship. Specifically, while the presence of gift-bearing penile sacs in a species strongly suggests the presence of female choice, their absence does not necessarily indicate the adoption of a coercive mating strategy in the male; that is, the female need not evolve pregenital barriers to defend against the absence of nuptial gifts from the male. Thus, a more rigorous assessment would require the use of multiple continuously distributed traits from both sexes that can in principle span a spectrum of values consistent with different intensities of female choice and/or intersexual conflict. In addition, such traits should ideally reflect functional interactions between the sexes, such that male and female traits can be expected to covary with the intensity of female choice and/or intersexual conflict and to coevolve with each other (Wedell et al., 2006). Under these conditions, the hypothesis that choice and conflict act simultaneously could be corroborated if species fall along a continuous multivariate spectrum representing the relative impacts of the two mechanisms (McGill and Brown, 2007). The hypothesis of mutual exclusivity would be corroborated by finding two distinct clusters of species, one characterized by variables that indicate intersexual conflict, and the other characterized by variables that indicate female choice, or the lack of conflict-related variables.

In the present study, we measured several continuously distributed morphological traits in leiobunine harvestmen which are associated with precopulatory behavior and that are expected to vary in proportion to the relative effects of female choice and sexual conflict. These are largely biomechanical variables that indicate the relative magnitude of forces that structures can generate, transmit or resist and include body size, cuticular investment in male palps, penes and female genital opercula, relative force production by muscles and associated lever systems, and estimates of penile strength. These variables should be impacted most strongly by intersexual conflict (especially forced copulation) rather than female choice. Thus, their covariation and discrimination power should be greater for species with female pregenital barriers, as theory predicts barriers (physical or functional) should best indicate the presence, but not magnitude, of intersexual conflict (Gavrilets, 2000). Species with gift-bearing penile sacs, an indicator that female choice is operating at some level within the species, should be distinguished by their low values of conflict-based features. Reference to these heuristic categorical grouping variables allowed us to assess the polarity of continuous distributions of species along a multivariate choice-to-conflict axis and to categorize clusters of species as being united by female choice or intersexual conflict.

Our results demonstrate the covariation of reproductive biomechanical traits within males and between males and females, a finding that is consistent with long coevolution in reproductive structures with precopulatory functions (Fig. 4.1). However, continuous traits were not sufficient to distinguish categorical groups based on discrete morphology. Taken together, these findings suggest sexual selection mechanisms operate simultaneously to effect mating system change, and that via evaluation of reproductive morphologies, the intensity of these mechanisms may be quantified.

Methods

Taxon sample and phylogeny

In total, we collected measurements from 2-10 specimens each per 29 species (*Hadrobunus hedini* traits were incompletely sampled, and thus this species was dropped from some analyses) for all variables except the force produced by the penile retractor muscle. All morphological data came from samples with geographic ranges contiguous with those of the molecular samples used to build the phylogeny (Table S1). All traits were log-transformed to limit variable heteroscedasticity and linearize relationships between traits. Specimens were preserved in 70-100% ethanol.

To provide an evolutionary framework and correct for variance due to shared evolutionary history, we employed comparative methods using the maximum clade credibility tree (Fig. 4.2) developed from a posterior distribution of trees reconstructed from nuclear and mitochondrial sequences (Burns et al., 2013; BEAST, Drummond et al., 2012). The posterior distribution was filtered (Fig. 4.2) using an unresolved topology based on Burns et al., 2012. Thus the filtered posterior distribution preserves well-supported deep phylogenetic relationships among the leiobunine harvestmen while allowing for topological variation in species groups.

Morphological and biomechanical variables

Our goal was to determine whether female choice and intersexual conflict could act simultaneously to different degrees on a set of reproductive features, or whether these two mechanisms are incompatible and only act in a mutually exclusive manner. Our approach requires quantitiative reproductive features with values that vary continuously in direct or inverse proportion with expectations from female choice, sexual conficit or both. We measured 13 reproductive variables that should increase in magnitude with sexual conflict (i.e. coercive mating) and decrease with female choice. Three variables were obtained from females (body size, relative closing force of genital operculum, cuticular investment in genital operculum) and 10 from males (body size, penis length, width of penile fulturae (stiffening rods), relative force of intrinsic penile, penile protractor, and penile retractor muscles; cuticular investment in pedipalps and penis, penile section modulus across the X and Y axes).

Digital photos of reproductive features were obtained with a PaxCam digital camera mounted on either a Leica MZ APO dissecting microscope (0.63× or 1.0× objective lens, 8–80× zoom) or Wild Heerbrugg Makrozoom 1:5 with 6.2-32× zoom. Measurements in millimeters were obtained from digital photos imported into ImageJ v.1.44p (Rasband, 2012). Measurements were size-corrected and log-transformed and the mean from three to 10 specimens per species were used to calculate a species mean that was used for analysis. A summary of the traits sampled and the direction of change predicted by intensification of sexual conflict is provided in Table 4.1.

Body size and correction for size effects. Male harvestmen are typically smaller than conspecific females. However, we expected that the female: male body-size ratio should decrease and that absolute sizes of males and females should increase in proportion to the intensity of physical contests between the sexes. Size was measured as the transverse width of the carapace, measured at the point where coxa I and II (Fig. 4.1) meet, as a measure of body size. The carapace is a single large sclerite that is unlikely to fluctuate in size or shape due to preservation or to nutritional or reproductive status. The relative values of many physical variables change predictably in systems that scale isometrically.

For instance, a variable that changes in proportion to cross-sectional area (e.g., muscle force) would be divided by the square of carapace width to correct for changes in size.

Relative closing force of the female genital operculum. The genital operculum covers the pregenital chamber and operates like a trapdoor, hinged at its posterior margin and opening at its anterior margin. Closing force is produced by a bilateral pair of muscles (opercular levators) that attach at distinct muscle scars along the lateral margins of the operculum (Fig. 4.1B). The muscles extend dorsally into the body, where their fibers attach to an internal skeleton, the endosternite (Shultz, 2000). The anterior fibers of a closer muscle attach to the surface of the muscle scar at about 90° and essentially all contractile force contributes to opercular closing. However, attachment angles become increasingly acute in more-posterior fibers, and a diminishing portion of their contractile force contributes to closing. All together, the function of the levator is critical to the formation of the female pregenital barrier, when present.

The relative closing force of each muscle was estimated by determining muscle scar width (w) in mm and fiber attachment angle (θ) in degrees at six evenly spaced points (w_1-w_6) along the lateral muscle scar. Using GraphPad Prism, v. 5.04 (GraphPad Software, San Diego, Calif., USA), the values of ($w_n \times \cos \theta_n$) were plotted against scar length to w_n for each specimen. These data were fitted using a least-squares polynomial regression. The resulting equation was integrated over the interval 0 to total scar length to obtain the total relative closing force produced by the muscle (F_{in}). Because the genital operculum is a lever system, the relative closing force at the anterior margin (F_{out}) equals F_{in} multiplied by the muscle's mechanical advantage (L_{in}/L_{out}) (Davidovits, 2008), where L_{in} is the distance from the hinge to the point where F_{in} is applied, and L_{out} is the distance from the hinge to the anterior margin (Fig. 4.1). L_{out} was measured directly and L_{in} was the longitudinal position of the centroid of F_{in} (Fig. 4.1): that is, the point along the muscle scar where the area under the regression curve anterior and posterior equaled $F_{in}/2$. Because the maximum contractile force of a muscle is proportional to its effective cross-sectional area (Krivickas et al., 2011), we corrected F_{out} for body size by dividing by the square of carapace width.

Relative force of penile muscles. We estimated the relative forces generated by three muscles associated with movement of the penis. The fibers of the intrinsic penile muscle (Fig. 4.1) arise from the inner surfaces of the penis and insert on a tendon that attaches subterminally at the glans-shaft joint. The muscle flexes the glans towards the shaft and potentially stiffens or bends the shaft. The penile protractor muscle arises on the ventrolateral surface of the genital operculum and an adjacent sternite and inserts at the base of the penis. Contraction of the protractor pushes the penis forward, an action that would be particularly important in attempting forced copulation, and may also be used in changing penis orientation. The penis retractor arises at the posterior end of the body and attaches at the base of the penis. It pulls the penis posteriorly into the pregenital chamber and, like the protractor, may change the angular position of the penis.

We randomly selected 3-6 fibers in each muscle and measured their cross-sectional area and angle with respect to the long axis of the penis. The average cross-sectional area was multiplied by the total number of muscle fibers to obtain the relative maximum force of the muscle. This value was then multiplied by the cosine of the average angle to yield the relative effective force that each muscle could exert along the midsagittal axis of the penis (intrinsic muscle) or body (protractor and retractor), The mechanical advantage of the intrinsic muscle was determined by measuring the input and output levers in ImageJ and multiplying this value by the muscle’s relative effective force to yield the total intrinsic penile force.

Penis length. Based on our unpublished anatomical and behavioral observations, it appears unlikely that longer penes offer an advantage for reaching the female’s primary genital opening once the penis has accessed her pregenital chamber. Rather, penis length appears to be related to the mechanics of penile eversion. Short penes are pushed forward largely by hemolymph pressure that everts the entire pregenital chamber of the male, resulting in the exposed penis being mounted on a flexible, fluid-filled “balloon” (haematodocha). In contrast, long penises can be pushed forward by contraction of protractor muscles with forces greater than those provided by haematodochal expansion. Penis length was corrected for body size by dividing by carapace width.

Penile fulturae (stiffening rods). The flexible walls of the male pregenital chamber contain a bilateral, ventrolateral pair of longitudinal sclerites that articulate posteriorly with the base of the penis and anteriorly with the anterior margin of the genital operculum (Fig. 4.1). These rods deform during penile movement and appear to act as springs that may assist protraction and/or retraction of the penis depending on its position. We predicted that wider fulturae store and return more mechanical energy than narrower fulturae and thus that wider fulturae are more likely to be associated with coercive mating. We took the mean width of two to three measured fulturae for each male specimen and corrected for size by dividing by carapace width.

Cuticular investment. We predicted that the maximum mechanical force that a sclerite can transmit or resist varies in proportion to the amount of its constituent cuticle. We measured cuticular investment in three structures—the penis, male pedipalps and female genital operculum (Fig. 4.1). Each structure was removed from each individual. The body (minus legs removed at the coxa-trochanter joint) and the isolated reproductive structures were macerated in a 5% KOH solution at 65-68° C for 24-48 hours, rinsed in 100% ethanol, and dried overnight at 65-68° C. The mass of the body and each part were determined with a Mettler Toledo MT5 microbalance (resolution to 0.001 μg), and the ratio of the mass of each part to total body mass was calculated. These mass ratios required no size correction.

Estimated flexural stiffness of penile shaft. Harvestman penes can be viewed as elongate hollow beams. When comparing a series of beams of similar composition, the relative magnitudes of several mechanical parameters can be estimated from cross-sectional profiles (Fig. 4.3). For example, a beam's flexural stiffness increases with both the amount of material that resists bending and its distance (d^4) from the beam’s flexural axis, where dorsal or ventral bending has a horizontal (X) axis and lateral bending has a vertical (Y) axis (Fig. 4.3). Flexural stiffness is estimated by the second moment of area (I_x, I_y). Here we compared penes using the elastic section modulus (Z_x, Z_y), which is calculated as $I_x/d_{y\ \mathrm{max}}$ or $I_y/d_{x\ \mathrm{max}}$, respectively, and estimates a beam’s elastic strength (i.e., the smallest flexural force that will permanently damage the beam). Because the highest tensile and compressive forces experienced in bending occur farthest from the flexural axis, the material located at the maximum radius (d max) will be the first to fail. Elastic section modulus scales in proportion to the cube of linear distance to the flexural axis and should thus vary in proportion to body volume and body mass.

Penes were isolated and embedded in JB-4 plastic medium (Electron Microscopy Sciences) following the manufacturer’s specifications for tissue infiltration. Samples were oriented longitudinally in the block during polymerization following guidelines in Consentino et al. (2010) and maintained overnight at 4°C under vacuum. Two to three 5-µm sections were obtained from the mid-shaft of each penis using a Microm HM 325 microtome. Outlines of the cuticle and lumen of each section were traced from digitized photographs using a

Wacom Pen Tablet in Adobe Photoshop CS4 to create high-contrast images (Fig. 4.3). Images were imported into ImageJ and values for Z_X and Z_Y were obtained using the MomentMacroJ module, v.1.4 (Christopher B. Ruff, Johns Hopkins University, www.hopkinsmedicine.org/fae/mmacro.htm). Each Z_X and Z_Y value was corrected for size by dividing it by the cube of carapace width. Species means of log-transformed, size-corrected section moduli were used in statistical analyses.

Data analysis

Log-transformed species trait means were compiled and imported into R (R Development Core Team, 2013). To avoid predefining the evolutionary process for the variety of traits measured, we opted to use lambda (Pagel, 1999; Boettiger et al., 2012), a scalar that is multiplied along all internal edges of the phylogeny. The resultant maximum likelihood estimate of lambda indicates the degree to which a trait evolves according to a Brownian motion model—a lambda of 1 indicates high phylogenetic signal, whereas 0 indicates that variation in the trait cannot be explained by shared ancestry (Boettiger et al. 2012).

Topological uncertainty. Recent papers dealing with the application of comparative methods have highlighted the need to include phylogenetic uncertainty in models of character evolution (de Villemereuil et al., 2012; Huelsenbeck et al., 2000). Throughout this work we utilized the maximum clade credibility tree in phylogenetic comparative analyses, but these methods typically assume that the tree is known without error. We explored the distribution of maximum likelihood estimates of lambda (MLEL) recovered for each of the 13 traits that we measured. We used a Z-test to assess whether the MLEL of the maximum clade credibility tree was significantly lower than the mean MLEL of the filtered posterior distribution, and a Wilcoxon test to compare the MLEL of the maximum clade credibility tree to the distribution median. We explored the effects of topology and branch length on the maximum likelihood estimate of lambda by determining the maximum likelihood value of lambda for each trait and each tree of a filtered Bayesian posterior tree distribution (Burns et al., 2013) using the fitContinuous program available in the R package *geiger* (Harmon et al., 2008). We then assessed whether the maximum clade credibility lambda was significantly higher than the mean and median lambda values of the posterior distribution using a one-tailed Z-test and Wilcoxon test, respectively.

Testing for sexual coevolution in reproductive structures. A fundamental assumption of our approach is that biomechanical reproductive variables coevolve between the sexes in a manner consistent with our variable-specific functional interpretations summarized above. We tested this assumption using a phylogenetically-corrected canonical correlation analysis (Revell, 2012; Revell and Harrison, 2008) with variables categorized by sex. Our assumption predicts a significant positive correlation across the male and female axes. Furthermore, species showing evidence of female choice (i.e., having gift-bearing penile sacs and biomechanical variables with lower magnitudes) should predominate at one end of the distribution and those showing evidence of intersexual conflict (i.e., female pregenital barriers and biomechanical variables with higher magnitudes) should predominate at the other. Given the potentially important effect of body size, we conducted one analysis with male and female body size and another without.

We also used phylogenetic generalized least squares methods to test for correlations between pairs of variables that we expected to have significant functional interactions (e.g., maximum relative protraction force of the penis and closing force of the female genital operculum). In addition, we explored correlations among male traits that are expected to operate synergistically during precopulatory encounters, including section modulus, penile and pedipalpal cuticle investment, and maximum relative force produced by the intrinsic penile and protractor muscles. As in the multivariate analyses, we used the empirically determined maximum-likelihood value of lambda as the evolutionary model parameter. Regressions were computed for all species and for species separated by categorical morphological factors—nuptial gift sac presence or absence (male trait regressions) and female pregenital barrier presence or absence (male and female trait regressions).

Testing for continuous or clustered distributions of species. The hypothesis that female choice and intersexual conflict operate in a simultaneous but graded manner predicts that species should be distributed continuously along multivariate axes, ranging from strongly "conflict-adapted" species at one end to strongly “choice-adapted” at the other. The hypothesis that the two mechanisms are incompatible and operate in a mutually exclusive manner predicts that species should be distributed in two distinct clusters, one comprising “choice-adapted” species and the other with “conflict-adapted” species. These predicted patterns were assessed using three methods. First, we examined graphical representations of the canonical correlation described above to determine if species were distributed continuously or were clustered at the extremes. Second, we conducted phylogenetic principal components analyses (Revell, 2009a) on all data as well as data from each sex separately to assess whether variation was distributed continuously or discontinuously. Finally, we used phylogenetic (Schmitz and Motani’s classification method, 2009) and standard linear discriminant analysis (MASS package; Venables and Ripley, 2002) to determine whether species could be consistently clustered into one of two groups based on biomechanical reproductive variables. We performed two discriminant analyses, one using presence or absence of penile gift-bearing sacs as the grouping variable and one using presence or absence of female pregenital barriers as the grouping variable. Membership of species in each group is listed in Table S4.1 and summarized in Figure 4.2. We tested the discriminant model incorporating all continuous variables using the Wilk’s Lambda test statistic implemented in multivariate analysis of variance (MANOVA). We regarded a statistically significant discriminant model with 100% separation as evidence for the hypothesis that female choice and intersexual conflict are mutually exclusive mechanisms and imperfect classification as evidence favoring the hypothesis that the two mechanisms operate simultaneously.

Results and Discussion

Topological uncertainty

Four traits—female body size, intrinsic penile relative force, penile cuticular investment, and penile section modulus over the Y-axis (Z_y)—had maximum likelihood estimates of lambda (MLEL) derived from the maximum clade credibility tree that were significantly lower than the mean and median of the posterior distribution (Table 4.2). Figure S4.1 shows the frequency distributions across the reference trees for each of these four traits, with the mean, median, and maximum clade credibility tree lambda values indicated. Investigation of phylogenies yielding MLEL in the 99th percentiles of the distributions indicated there were no consistently appearing trees between the four traits with diverging maximum clade credibility tree MLEL, and indeed the topologies of these trees varied only in the positions of two taxa, *L. bimaculatum* and *L. royali*. This indicates the more extreme skewness of the MLEL values of the posterior distribution for these four traits appears to be created primarily due to the interaction of trait value distribution and branch lengths.

We additionally found that the MLEL for many traits approached 0 (Table 4.2), indicating the low phylogenetic signal in these traits. While for some analyses this might present a convincing case for choosing to avoid phylogenetic correction altogether, we utilized comparative methods both focusing and controlling for phylogenetic signal in this work, and opted to include the phylogenetic correction when appropriate. In keeping with our expectation of collaborative evolutionary processes at work in shaping reproductive traits, we avoided any assumption of evolutionary process in our analyses by using maximum likelihood-based estimates of lambda to standardize the correlation matrices and remove phylogenetic variances whenever possible. Using simple statistical approaches to compare the maximum clade credibility tree lambda, we addressed the growing concern felt by applied phylogeneticists that topological variation, ignored in most analyses, could affect our data analysis. We found that for most measured traits, the maximum clade credibility tree lambda estimate did not differ from either the mean or median of the reference distribution. For four traits, however, we found maximum clade credibility tree lambda was significantly lower than both the mean and median lambda reference values. In each of the cases, the values of the mean, median and maximum clade credibility lambda were very low, and differences between the maximum clade credibility tree and reference distribution trees with lambda in the 99th percentile appeared to be largely based on branch length, not topology. Thus, it is unlikely that our analyses would be affected were another tree from the same distribution employed instead of the maximum clade credibility tree.

Intersexual coevolution in reproductive structures

Intersexual multivariate correlations. We combined all variables into a phylogenetic canonical correlation analysis (pCCA) where the maximum likelihood value of lambda was estimated to rescale the phylogeny and apply the resultant branch corrections to the trait correlation matrix (λ = 6.75e-05, lnL λ = 175). Traits were organized by sex, yielding a total of three canonical factors. Scores and canonical factor coefficients for factor 1 are plotted in Figure 4.4A. We found significant major axis regression correlations between factor coefficients for male and female variables in the first (R^2=0.898, p<1e-13) and second canonical factors (R^2=0.647, p<1e-06). Likelihood ratio tests indicate the probability of zero correlation between CF1x and CF1y was very low (CF1: χ^2=72.7, p<1e-05) and for CF2, the probability of zero correlation increased to marginal significance (CF2: χ^2=26, p=0.054). Concerned about the strong effect of body size in the data set, we reanalyzed the canonical variates without female or male body size (Fig. 4.4B; λ = 6.75e-05, lnL λ = 43.55), and found that while the linear relationship between male and female reproductive trait combinations in CF1 remained strong (R^2=0.561, p<1e-05) the probability of zero correlation between male and female variables on CF1 rose slightly (CF1: χ^2=22.6, p=0.126).

Results from phylogenetic principal components analysis, using traits evaluated for each sex separately (Fig. 4.5A, B) and combined (Fig. 4.5C) are consistent with pCCA results. Female body width and relative levator muscle force were highly correlated (Fig. 4.5B), even after correcting force data by body width (PC1 and 2 account for 91.85%; λ = 6.75e-5, lnL λ = 45.62); both body size as well as muscle force load highly on principal component 1 (>0.92 for each), while cuticle investment in the operculum loads primarily on PC2 (>0.99). Male variables, by contrast, are less well explained by two axes (Fig. 4.5A; PC1 and 2 account for 61.02%; λ = 6.75e-5, lnL λ = 79.52). While principal component 1 for male traits encompassed the majority of reproductive characters with equivalent sign, indicating a general axis of antagonistic traits, cuticular investment-based traits (stiffening rod thickness, penile and pedipalpal cuticular investment) loaded more strongly on PC2 (loadings: -0.5, -0.68, -0.76 respectively), and shape-based traits (penile section modulus) were most strongly related to the third PC (16% of total data variance). In the pPCA including all traits (Fig. 4.5C; PC1 and 2 account for 57.52%; λ = 6.75e-05, lnL λ = 175), we again see presumptive "conflict" traits for both sexes, such as opercular levator and intrinsic penile muscle relative force, loading strongly on PC1 (loadings: -0.88, -0.72) with PC2 claiming more of the variance particularly in cuticular traits of the male, such as stiffening rod thickness (-0.55), and cuticular investment in pedipalps (-0.79) and penis (-0.66). Relative force produced by penile retractor muscle data was not included in the latter two analyses, as sampling for this character was incomplete.

These results are consistent with our analytical assumptions that 1) there should be a strong multivariate correlation between reproductive traits of males and females consistent with intersexual coevolution, as both x- and y-axis contribute to the linear relationship between traits, and 2) species with traits consistent with sexual conflict and coercive mating should occupy one end of the distribution and species with traits consistent with female appeasement, not coercive mating, should occupy the other. In Figure 4.4A, species with nuptial sacs, lacking female pregenital barriers, are concentrated in the upper right quadrant (I) of the graph and those without gift-bearing sacs and with female pregenital barriers are concentrated in the lower left (III). In Figure 4.4B we see the same result, although the dominate morphotype in each quandrant is exchanged. All pPCAs (see plots in Figure S4.2 for pPCA species scores without factor loadings for clarity) produced a similar pattern: low scores on the first principal component tended to belong to species with pregenital barriers and no sacs, while species with sacs and no barriers had higher scores, but here too there was a large degree of overlap. Thus, when coded by sac and barrier presence, species were partially discriminated by the multivariate trait axes, but there was a region across the origin where species of all categories scored.

Bivariate correlations between the sexes. Male and female cuticular structures were expected to have correlated mass values (controlling for total body mass with legs removed) because of the consistent dimensions and potential of these traits to interact during pre-copulatory interactions, thus driving a coevolution of phenotypes. However, we did not find significant correlations between cuticle investment of the female genital operculum, which functions as a part of the pregenital mechanism to exclude the penis, and the male clasping pedipalps ($R^2=0.018$, $p>0.1$) nor was there a correlation between opercular and penile investment ($R^2=0.012$, $p>0.5$). Similarly, there was no significant correlation between penile section modulus (Z_x)—a relative measure of penile flexural strength that would render the penis more capable of prying at the female operculum—and operculum investment (R^2=0.098, p>0.1). Limiting the analysis to species with or without female pregenital barriers did not change the significance or increase the R^2 of these data.

After accounting for phylogeny we found a strong positive relationship between log-transformed body size in male and female leiobunines (all data: R^2=0.84, p<0.0001), even when grouped by presence/absence of female pregenital barriers (no barrier: R^2=0.8634, p<0.0001; barrier: R^2=0.7688, p<0.001) (Fig. 4.6A). Typical for arthropods, females are always larger than males, but decreasing female: male body size ratios may indicate increasing precopulatory antagonism, as body size improves male coercive ability. However, a number of species fall outside of the 95% confidence interval of body size (m=1.542, least-squares regression, forced through origin). Above the interval, where males are even smaller than females than is typical for the clade, outliers are near equally sacculate species (*Eumesosoma roeweri, Togwoteeus biceps, Leiobunum bracchiolum, L. aldrichi, L. politum*) and non-sacculate species (*L. uxorium, L. nigropalpi, L. relictum, L. holtae*). Species with lower female: male ratios, found below the interval, lack penile sacs (*Hadrobunus maculosus, Leiobunum hoffmani, L. crassipalpe, L. formosum, L. calcar*). Only one sacculate species, the western North American outgroup, *Leuronychus pacificus,* has atypically large males.

Intersexual comparisons of maximum relative forces revealed several significant correlations. Closing force of the female genital operculum was positively correlated to penile protraction (R^2=0.2414, p<0.01), and intrinsic penile muscle force (R^2=0.2643, $p<0.01$) (Fig. 4.6B, C). This result indicates a significant coevolutionary pattern between functional components that should interact directly during coercive mating. Penile retraction force was estimated for a subset of species (N=19), but we also found a strong correlation (R^2=0.4527, $p<0.001$) between it and closing force of the female genital operculum (Fig. 4.6E). Separate analyses of penile protraction force versus opercular closing force by barrier-present grouping additionally increased R^2 values marginally, though at the cost of an increased p-value (Fig. 4.6D; Protractor-levator: R^2=0.3753, $p<0.05$). Relationships between the intrinsic penile muscle-levator and retractor muscle-levator relative force pairs became statistically marginal with this grouping variable, however (IPM-levator: R^2=0.2138, $p>0.05$; Retractor-levator: R^2=0.3015, $p>0.05$). Species without female barriers do not show significant relative muscle force correlations (IPM-levator: R^2=0.062, $p>0.1$; Protractor-levator: R^2=0.0007, $p>0.5$; Retractor-levator: R^2=0.085, $p>0.1$). A similar effect was seen when nuptial gift sac presence was used as the grouping variable: species without sacs had significant IPM-protractor and levator-protractor relative muscle force relationships (IPM-levator: R^2=0.4616, $p<0.01$; Protractor-levator: R^2=0.5751, $p<0.01$; Retractor-levator: R^2=0.3015, $p>0.05$) and species with sacs did not (IPM-levator: R^2=0.014, $p>0.5$; Protractor-levator: R^2=6.3e-05, $p>0.5$; Retractor-levator: R^2=0.085, $p>0.1$).

Bivariate correlations within males. We examined correlations between several pairs of male variables, testing the potential for synergistic effects between several presumptive conflict-based traits, including penile section modulus (Z_x), penile and pedipalpal cuticular mass, and maximum relative forces of penile protraction and the intrinsic penile muscle (Fig. 4.7A-D). Of these combinations, only penile versus pedipalpal cuticle mass (Fig. 4.7C; $R^2=0.3335$, $p<0.001$), and maximum relative penile protraction force versus intrinsic penile muscle force (Fig. 4.7B; $R^2=0.3143$, $p<0.01$) yielded statistically significant correlations after correcting for body size and phylogeny. However, the linear relationship between protraction and intrinsic penile muscle forces deteriorates when species with and without penile sacs are analyzed separately, and neither subgroup produces a statistically significant correlation. For penile and pedipalpal cuticular investment, sorting values by penile sac presence yielded a significant correlations among species with penile sacs (Fig. 4.7D; $R^2=0.324$, $p<0.05$) and without sacs (Fig. 4.7D; $R^2=0.8115$, $p<0.0001$). Penile section modulus (Z), a measure of flexural strength, did not covary significantly with other male traits, although we found a strong correlation between Z_x and Z_y when all species were included ($R^2=0.8079$, $p<1e-10$) (Fig. 4.7A). The regression shows that bending strength trends slightly greater across the dorsoventral (X) axis ($m=1.032$), but there was no tendency for species without penile sacs to have greater dorsoventral section moduli than species without sacs ($t=1.617$, D.F.=26, $p=0.1179$). This result is inconsistent with our predictions that greater strength in bending may offer an advantage to males of species with conflict-based mating.

Evidence for continuous or clustered distributions of species

We used canonical correlation and principal components to assess the covariation of reproductive structures within and between male and female harvestmen. These methods additionally produced species scores on the multivariate function that display meaningful patterns. A graphical depiction of male and female axes from the first canonical function (Fig. 4.6A) revealed a continuous distribution with conflict-dominated species (those with female pregenital barriers) dominating one end of the distribution, choice-dominated species (those with penile gift-bearing sacs) dominating the other end, and a broad region of overlap. Likewise, principal components analyses (Fig. 4.5 A-C) produce species score distributions that place conflict-and choice-dominated species along a rough gradient formed by PC1. These results suggest that species at the extremes of the distribution may be categorized as conflict- or choice-dominated, as in the case of our earlier study (Burns et al., 2013), but that this categorization is incomplete and oversimplified. Additionally, these tests are not optimized for group classification (McLachlan, 2004), and data reduction can bias influences on the multivariate function towards traits that best represent both groups.

Phylogenetic and standard linear discriminant analyses were performed to determine whether genitalic diversity in harvestmen represents a continuum that reflects simultaneous contributions of female choice and intersexual conflict or two distinct classes reflecting the mutually exclusive effects of these two mechanisms. Under the grouping variable of penile nuptial gift sac presence/absence, continuous variables measured in our study contributed to 85% species discrimination into morphological categories with standard statistics (Fig. 4.8A). There was a slight improvement to a 12.4% mean error rate when trait error structure incorporated the multivariate branch scalar estimate of lambda, which we obtained during phylogenetic principal components analysis (λ= 6.75e-05). Discrimination based on standard statistics increased to 89% when we used female pregenital barrier presence as the grouping variable, which was consistent with results derived from phylogenetic methods (mean error rate: 10%). However, likely due to the small sample size relative to the number of parameters incorporated into the discriminant axis, neither sacs (Fig. 4.8A; Wilk's λ=0.44, $F_{12,15}$=1.56, p=0.2054) nor barriers (Fig. 4.8B; Wilk's λ=0.46, $F_{12,15}$=1.47, p=0.2387) provided a significant discriminant model. When the same models were constructed with a subset of biomechanical traits with structure coefficients of -0.5 or less (max. relative forces of female genital operculum, penile protraction, and intrinsic penile muscle forces; mean penile fultura thickness, penis length and penis cuticular mass) the models became significant (sacs: Wilk's λ=0.55, $F_{6,21}$=2.81, p<0.5 ; barriers: Wilk's λ=0.54, $F_{6,21}$=2.98, p<0.5) but species discrimination was incomplete for both grouping variables (sacs: 82%; barriers: 85%). The inability of these models to discriminate species into distinct classes is inconsistent with the view that reproductive structures can be readily partitioned into female choice or intersexual-conflict categories, but supports that proposal for a continuum of intermediate forms.

Predictor variables that contributed significantly to the discriminant function were assessed for the full model using calculated structure coefficients. For both grouping variables, penis length (sacs, β= -0.72; barriers, β= -0.73) and maximum relative force of the penile protraction (sacs, β= -0.75; barriers, β= -0.81), were the most critical diagnostic traits in the discriminant function, specifically for identifying non-sacculate, barrier-present species. When barrier presence was the grouping variable, the structure coefficient for maximum relative opercular closing force decreased from -0.52 to -0.69, improving classification of barrier-present species. This change in contribution to classification signifies the importance of female variables to species classification, and may have resulted from the group change of *Hadrobunus grandis*, a species with both penile sacs and female pregenital barriers. When discriminant model cross-validation was performed using species jack-knifing to create a training data set for the remaining single taxon to be tested against, we found four species (*L. minutum, L. ventricosum, L. holtae,* and *L. vittatum*) were misclassified under the sac grouping variable (Fig. 4.8A). Three species (*L. flavum, L. holtae,* and *L. nigropalpi*) were misclassified when data were trained on the barrier grouping variable (Fig. 4.8B).

Conclusions

Simultaneity of sexual conflict and female choice

Our attempt to integrate biomechanics, sexual selection, and macroevolution has yielded several interesting findings regarding the evolution of morphological specialization into courtship and conflict-based systems in the leiobunine harvestmen, and illuminated new avenues for sexual selection research. The primary goal of this work was test the veracity of the mutually exclusive hypothesis, in which mechanisms of sexual selection, female choice and sexual conflict, operate separately to place species into choice or conflict-based categories. The alternative to the mutually exclusive hypothesis would be the simultaneous hypothesis, wherein existing species diversity would create a continuum ranging from mating systems dominated by female choice to mating systems dominated by sexual conflict, with a broad range of intermediates. At the multivariate level, our data do not make an ironclad discrimination between species with a particular discrete morphological classification, as multivariate tests of the discriminatory power of biomechanical variables were not found to be significant for either female or male character groupings. However, even when we limited parameters to the most discriminating variables with structure coefficients of 0.5 or higher, the discriminant functions prepared for these group variables were unsuccessful at perfectly classifying species with present or absent penile nuptial gift sacs or female pregenital barriers, particularly for the former. The lack of success of these functions shows that continuous traits identify a broad range of overlap between the features of species from antagonistic and enticement-based mating systems. Thus, these results support the simultaneous hypothesis for the generation of reproductive diversity.

In previous analyses (Burns et al., 2013), few leiobunine species could be described as “intermediate” in discrete reproductive phenotype. These included

Hadrobunus grandis, a sacculate species in which females have pregenital barriers similar to those seen in other members of genus *Hadrobunus,* and *Leiobunum relictum,* a species of contentious but more likely derived phylogenetic position with non-sacculate males and females lacking pregenital barriers. Using continuously-varying biomechanical characters, these species were surprisingly well classified in discriminant analyses, but many more support the hypothesis of simultaneous mechanistic action to generate a spectrum of functional forms. However, we found six species were misclassified in our discriminant analyses, potentially indicating intermediacy in their biomechanical attributes. These included three antagonistic-group species (*L. holtae, L. vittatum,* and *L. nigropalpi*) misclassified as enticement-group species, and three with the opposite issue (*L. ventricosum, L. minutum,* and *L. flavum).* Based on structural coefficients calculated for each predictor trait, it appears non-sacculate, barrier-present taxa were primarily misclassified due to their small protractor relative forces, thin stiffening rods and low penis weights. It is interesting that all misclassified sacculate, barrier absent species are closely related members of the “early-season” *Leiobunum* clade (Fig. 4.2); these species are among the largest sacculates, with long, heavy penes that must be supported by thick stiffening rods. Overall, phylogeny did not exert a strong effect in discriminant analyses; the shared related reproductive features of the “early-season” group may have contributed to morphological misclassification or measurement error could have played a role in imperfectly translating trait function to species classification. We found discriminatory power improved when barrier presence was used as the classification criteria, although the most critical predictors for proper classification were largely penile measures. This speaks to the heightened utility of female characters as signals for mating system change; the presence of a pregenital barrier better identifies the correlated presence and fitness consequences of precopulatory antagonism.

Canonical factor and principal components analyses indicated strong correlations between standardized variable combinations that encapsulate the intensity of sexual conflict within the species, both with and without body size included in the analysis. Thus, we are confident that our trait selection, biased towards features expected to vary with the intensity of precopulatory antagonism, has captured the range of sexual conflict in this clade. Removal of body size changed the sign of most species scores and produced the greatest discrimination between sacculate and non-sacculate groups, with species from high conflict mating systems, such as *Hadrobunus maculosus* and *Leiobunum crassipalpe,* showing the highest scores. Sacculate species had the lowest scores on this factor axis, but several non-sacculate, barrier present species, such as the smallest members of the *vittatum* and *calcar* groups, *L. uxorium* and *L. nigropalpi,* have similar scores. If the mutually exclusive hypothesis were supported, these groups would occupy separate regions of the canonical function plot. As this is not the case, we hypothesize that there may be at least as many non-sacculate mating strategies at work as there are non-sacculate species groups, and, though far fewer, there appear to be sacculate taxa that share at least some features of the conflict-based systems in common with non-sacculate species. While canonical correlation and regression analyses found non-sacculate taxa had the highest values for antagonistic traits such as male body size and male and female relative genital muscle force, the distribution of antagonistic trait values varied based on clade. Non-sacculate *Hadrobunus* (including *Leiobunum formosum*) had great consistency in conflict based traits, regularly presenting the most extreme conflict trait values, but non-sacculate clades from the genus *Leiobunum* show wide variation in their trait values, with diminutive members of these clades appearing alongside more distantly related sacculate species in nearly every phylogenetic regression. This apparent structuring of the non-sacculate clades is reflected in low bivariate and multivariate phylogenetic signal values (Table 2), supporting our view that selection mechanisms are not exclusive processes, but instead combine to favor the development of extreme conflict traits in some species.

Utility of continuous mating system functions

As we have discussed previously (Burns et al., 2013), several lines of evidence support environmental and phenological mediation of conflict and choice sexual selection mechanisms. Species with potentially longer breeding seasons tend to have sacculate penes and other features consistent with female enticement by males, while species with shorter breeding seasons tend to have non-sacculate penes and often, as our data show, traits associated with precopulatory antagonism. Additionally, species with non-sacculate phenotype are limited almost exclusively to north temperate regions, where they overwinter as eggs and do not appear to reach sexual maturity until summer or early fall. Populations with the most extreme antagonistic specializations tend to occur on mountains (i.e., *Leiobunum hoffmani* and some Appalachian populations of *L. calcar*) where breeding seasons are likely to be especially short. Taken together, the results of our work suggest morphological specializations in non-sacculate species with quantitative traits adaptive for mating antagonism may be maintained as part of a feedback loop, in which long periods are required for males and females to achieve the size, muscle mass, and cuticle investment necessary for mating success in a rapidly dwindling season. Time and energy spent in growth minimizes time available for reproduction, presenting a selection pressure on males to mate quickly and, perhaps, more coercively. This would elicit compensatory response in females to develop mechanisms for controlling mating rate. Outwardly this feedback loop could present as a sexual arms race (Gage, 2004), but the loop would presumably be dampened by the absolute constraints of the surrounding environment. However, temporal variation in mating system and alternative mating strategies employed by either sex are poorly understood for this and other burgeoning model systems of sexually antagonistic coevolution and our knowledge of the precise onset of sexual maturity and duration of breeding seasons for leiobunine harvestmen is sorely incomplete. With precise information regarding environmental or phenological constraints encountered by a species, we could employ multivariate methods as described in this paper to generate a vector of sexual conflict intensity, which could subsequently be regressed against quantitative data for any particular external condition (i.e.

breeding onset, latitude) to test hypotheses linking sexual conflict to ecological conditions. This approach would also be helpful for testing alternative hypotheses for the formation of the continuum of morphological specialization. If conflict orginates via an environmental gradient, and our analyses capture a snapshot of the movement of species along a mechanistic range, sampling populations along the environmental gradient should reveal intraspecific variance in specialization that may show corresponding degrees of overlap with sympatric species. Regarding these approaches, we expect that future macroevolutionary work in this system will require additional attention paid to trait model design and complexity, for example by adopting an Ornstein-Uhlenbeck evolutionary model of biomechanical reproductive traits based given the potential in this system for environmental constraints placed on antagonistic traits (Beaulieu et al., 2012; Weir et al., 2012).

Co-variance of intersexual conflict-based traits

After accounting for shared history and environmental effects via sampling, body size correction, log-transformation, and use of phylogenetic comparative methods, the results of our analyses indicate the sex-specific reproductive biomechanical traits we measured co-vary. We found significant correlations between male reproductive traits for which increasing values would increase potential mating antagonism, and phylogenetic principal components analyses of the size-corrected and log-transformed traits indicate most of these traits load highly on the first component. An exception to this observation is seen in cuticular investment traits, which tended to load on principal component 2 (PC 2). Considering species scores in our principal components analyses, it appears PC 2 may be a better descriptor of skeletal traits. Only one of these traits, penile cuticular mass, appears to have a female choice-based function. This is because penile cuticular mass is affected by presence of nuptial gift sacs, and species with these sacs as a whole are distributed almost equally on PC 1 and 2 (Fig. 4.5A, C), while species without sacs are found largely along PC 1. Female operculum mass loaded strongly with PC 2 in female-only analysis, but both the sign and strength of this trait loading shifted when male and female traits were combined. The position of the pedipalpal investment vector also presents a bit of a puzzle, as we expected the modified pedipalps in some non-sacculate species would result in higher investment values and a higher loading on PC 1. We did find a correlation between pedipalpal and penile cuticle that was attributable only to sacculate species which may explain the results of the principal components analysis of male and all data.

Bivariate regressions were employed to examine the relationships of variables for which we had a specific, functional prediction. We found a strong correlation between male and female body size. This alone might not indicate a sexual arms race—body size increases over evolutionary time are commonly seen in other clades (Hendry et al., 2014; Allen et al., 2011; Hunt and Roy, 2006), and the dynamics controlling these evolutionary increases are as easily attributed to natural selection as to sexual selection (Hone and Benton, 2005; Blanckenhorn, 2000). However, most species with lower than normal female-to-male body size ratios, established by the 95% confidence interval for the regression, were non-sacculate, barrier present species. This supports the view that size evolution is responsive to some mechanism of sexual selection as at least a dominate force. Significantly, similar, though less extreme examples of correlated evolutionary states were seen between relative force production by genital muscles in males and females. We found that maximum relative closing force was significantly correlated to all three of the male genital muscle forces we estimated, but the highest correlation was between muscles of the male that project the penis forward and the muscles of the female that close the genital operculum, presumably against intrusion by the male penis. This relationships was expected, as these variables all displayed similar patterns of loading in principal components analyses, but finding such a result between two functional antagonistic traits suggests that subsequent attempts to verify these forces experimentally could prove valuable for an improved characterization of precopulatory mating interactions.

One of our bivariate analyses proved to be reflective of correlations between traits only in putatively conflict-based groups—species with female pregenital barriers or lacking penile sacs—when regressing female levator by male protractor relative muscle forces (Fig. 4.6D). This trend was not found for species with nuptial sacs or lacking pregenital barriers. This result suggests that the mechanisms of female choice and sexual conflict may in fact be mutually exclusive, and thus producing significant correlations between functionally-linked reproductive traits at a finer scale of character resolution than is resolvable under the two broadly-based mating systems explored here. Each genital feature, or responsible reproductive gene, may be separately affected by female choice and sexual conflict, but in species where features are similarly influenced by sexual selection, trait correlations or gene linkages would be found. Intermediacy, such as we have defined it in the simultaneous mechanism hypothesis, may thus be a function of the macroscale of systems we have attempted to describe, but to track correlated changes in genes or genital traits as a function of specific selection mechanisms, an experimental approach (as in Cayetano et al., 2011) would be required.

We have shown the utility of selecting functionally informative reproductive traits for phylogenetic comparative analysis. Still, defying some prior predictions, the strongest reproductive trait correlations in our analyses occurred between traits of the same category (i.e., size, estimated force or skeletal investment) of the same modality within males and females. Additionally, the magnitude of male and female trait correlations appeared to change with the type of trait, with body size showing the greatest positive linear correlation. It is unclear why this apparent structure resulted, but if all the traits are to contribute to the overall function and behavior of the individual, it is possible a hierarchy of evolutionary modularity dictates the modification of suites of traits over others (Klingenberg and Marugán-Lobón, 2013). That is, given the many adaptive strategies of increasing body mass, size traits may be the first to undergo rapid change given a background of mating system evolution, and size traits may be the first to contribute to an increase in precopulatory mating antagonism. Higher order traits reliant on changes in shape, muscle orientation, or lever length, such as the strength and functionality of genital mechanisms, may require a greater threshold of selective pressure to respond to changes in mating system. Investigation into the relative rate differences between body size and other conflict trait evolution will be necessary to evaluate the evolvability of different features associated with mating system change.

Tables

Table 4.1: Biomechanical characters measured in analysis and the direction of change predicted by intensification of sexual conflict.

Trait	Description	Prediction
Body size	Transverse width of the carapace	Decreasing female: male ratio, as increasing male size relative to female size improves male coercive ability
Penis length	Base to glans length	Increasing length allows for greater muscle attachment in protraction
Intrinsic penile muscle force	Glans-shaft articulation width * (# of fibers * mean cosine fiber angle) / Glans length	Increasing force to flex glans against female operculum
Penile protractor force	# of fibers * mean cosine fiber angle	Increasing force to protract large penes and change penile orientation
Penile retractor force	# of fibers * mean cosine fiber angle	Increasing force to retract large penes and change penile orientation
Opercular levator force	$\int_{0}^{apodeme\ length} (\text{cosine fiber angle} * \text{width of apodeme}) \sim \text{apodeme length to width waypoint})$	Increasing force to strengthen pregenital barrier
Operculum investment	Dry mass of female genital operculum	Increasing mass constitutes

		sclerotization, forming pregenital barrier
Penile investment	Dry mass of penile shaft	Increasing mass subsequently increases maximum mechanical force transmitted by penis in coercion (prying at the female genital operculum)
Pedipalp investment	Dry mass of pedipalps	Increasing mass subsequently increases maximum mechanical force transmitted by pedipalps in clasping
Fultura thickness	Mean width of 2-3 fultura	Wider fultura return greater energy to penes in protraction
Z_x	Second moment of area (I_x)/ cuticle thickness (d_y)	Increasing section modulus indicates increasing resistance to flexion
Z_y	Second moment of area (I_y)/ cuticle thickness (d_x)	Increasing section modulus indicates increasing resistance to flexion

Table 4.2: Results of one-tailed Z- and Wilcoxon tests of maximum clade credibility tree (Fig. 4.2) maximum likelihood estimates of lambda (MLEL) against means and medians of reference distribution (N=431; Burns et al. 2013) for 13 measured traits. A p-value greater than alpha=0.05 (noted with **) signifies the reference distribution statistic is significantly higher than that of the MLEL. Four traits, female size, intrinsic penile muscle force, penile cuticular investment, and section modulus (Z_x), had MLEL values that were significantly distinct from both the mean and median of the posterior distribution of trees (Fig. S4.1).

Trait	mean MLEL	median MLEL	MCCT MLEL	Z-test p-value	Wilcoxon p-value	MCCT significantly lower than:
Male size	0.00153	1.73E-15	2.67E-15	0.00049**	1	mean
Female size	1.64E-15	1.07E-15	1.11E-15	0.00016**	0.02621**	mean and median
Penis length	7.9E-5	4.75E-16	1.08E-15	0.1589	1	neither
Intrinsic penile muscle force	1.07E-15	8.06E-16	6.67E-16	<2.2E-16**	4.5E-14**	mean and median
Penile protractor force	0.0137	2.87E-15	5.53E-15	8.26E-10**	1	mean
Penile retractor force	0.692	0.735	0.79	1	1	neither
Opercular levator force	0.0198	3.46E-15	6.26E-15	<2.2E-16**	1	mean
Operculum investment	4.36E-16	3.24E-16	5.75E-16	1	1	neither
Penile investment	5.21E-16	3.87E-16	1.32E-16	<2.2E-16**	<2.2E-16**	mean and median
Pedipalp investment	0.214	0.248	0.31	1	1	neither
Fultura thickness	0.00029	5.69E-16	2.72E-16	0.1589	<2.2E-16**	median
Z_x	0.088	9.11E-16	1.40E-15	1.06E-14**	0.9974	mean
Z_y	0.0216	1.38E-15	2.95E-16	1.07E-5**	<2.2E-16**	mean and median

Figures

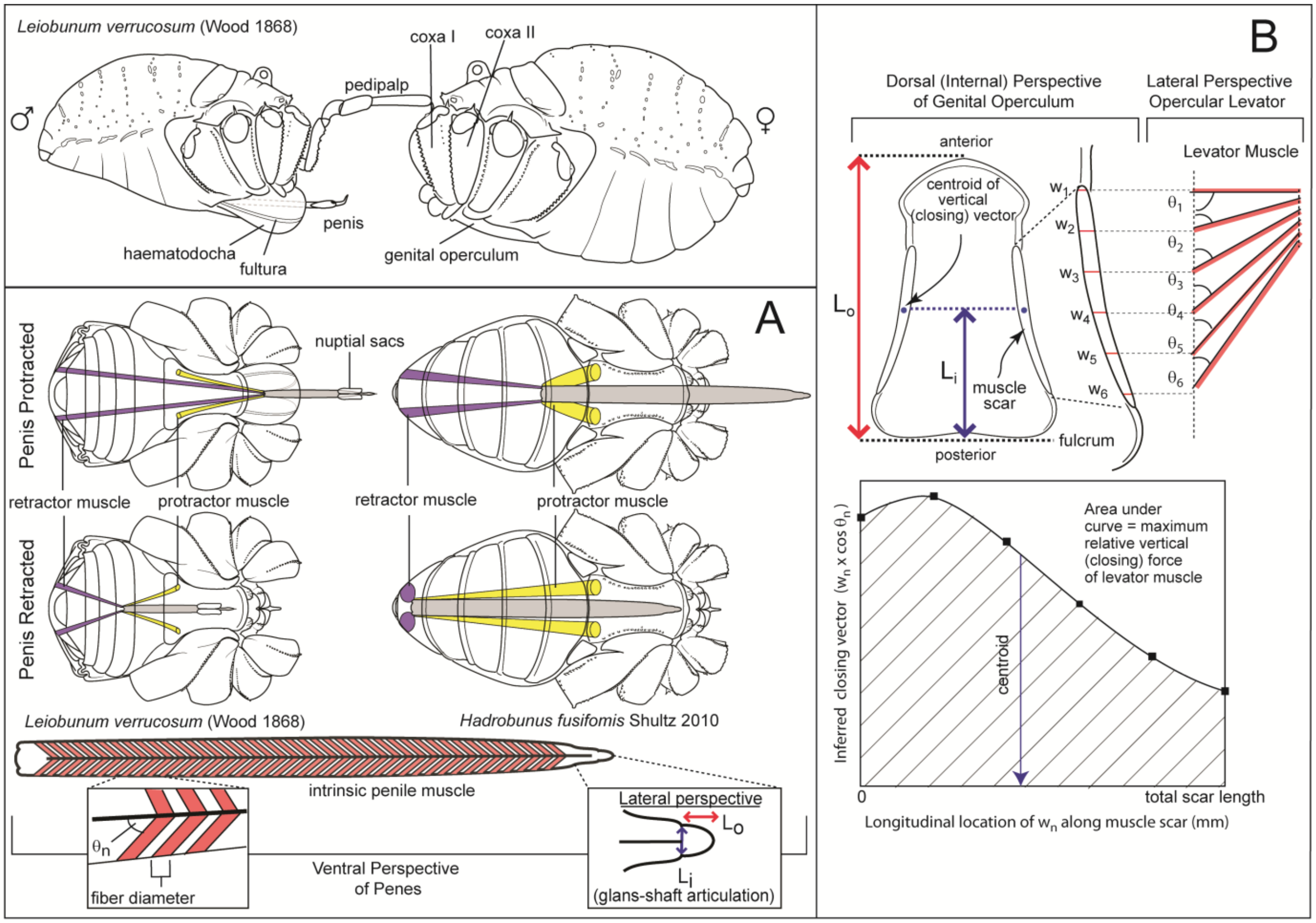

Figure 4.1: Summary of mating and reproductive muscle morphology in male and female leiobunine harvestmen. Precopulatory behavior in a leiobunine harvestman, *Leiobunum verrucosum*; male left, female right. Nuptial gift sacs on penis, when present, are paired distal cuticular sacs which deliver fluid nuptial gift. Box A shows ventral views of sacculate and non-sacculate penes; extruded and relaxed penile protractor (yellow) and penile retractor (purple) and penile intrinsic muscle (pink) are displayed in *Leiobunum verrucosum* and *Hadrobunus fusiformis* (this species not included in analysis). Intrinsic muscle lever-out (L_o; length of glans) and lever-in (L_i; glans-shaft articulation width), used to estimate relative muscle effort, are inset in lateral view. Method for measuring intrinsic penile relative effort shown: diameter of circular cross-section *d* yields the area of $\pi(0.5d)^2$ which is multiplied by average fiber angle θ and the number of fibers. Box B shows dorsal (internal) views of the female genital operculum, with lateral levator muscle and muscle scar indicated. Accompanying graph illustrates the method for calculating opercular lever centroid (and thus opercular L_o), and inferring relative levator effort: $(\int_0^{apodeme\ length}(\mathrm{wn} * \cos \theta\mathrm{n}) \sim \text{scar length to wn})$.

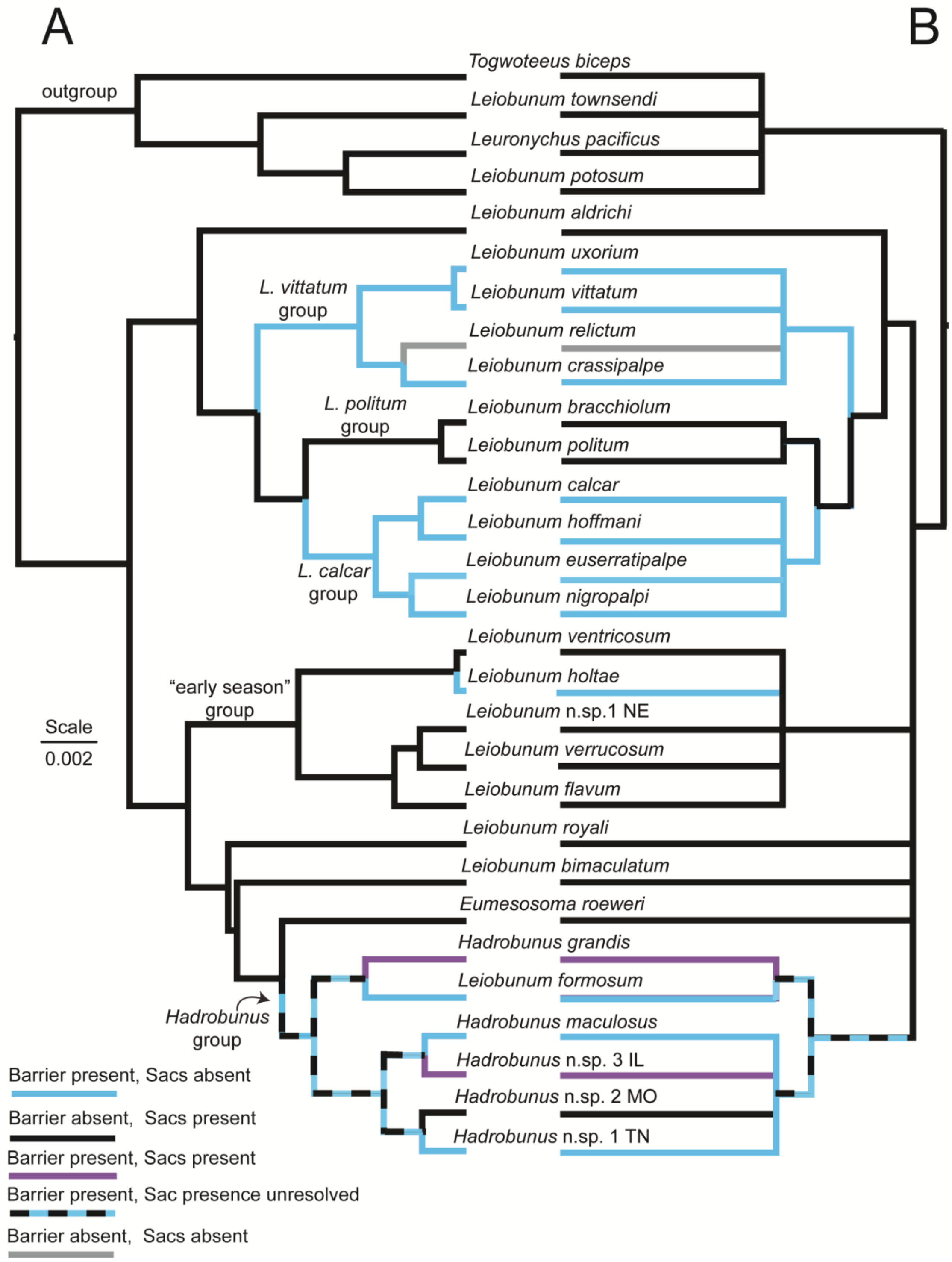

Figure 4.2: Maximum clade credibility and backbone constraint trees. The maximum clade credibility Bayesian tree (A) was assembled using the TreeAnnotator program (Drummond and Rambaut, 2007), visualized with FigTree v1.3.1 (Rambaut, 2009), and depicts relationships recovered from

mitochondrial and nuclear characters in BEAST v1.7.1 (Drummond et al., 2012) for trees that passed a backbone constraint tree (B) based on the Bayesian likelihood phylogeny from Burns et al., 2012. Scale is in substitutions per site for the filtered subset maximum clade credibility tree. The most parsimonious distribution of reproductive characters (assuming no parallel gains of nuptial sacs) is plotted on branches corresponding to nuptial gift sac presence and female pregenital barrier absence (black), and sac absence and barrier presence (blue). Barrier and sac presence is indicated with purple branches (taxa with this classification include *Hadrobunus grandis* and *Hadrobunus n. sp.* 3, *Leiobunum relictum*—non-sacculate, barrier absent—is indicated in light gray. The history of sac presence is unresolved via parsimony for *Hadrobunus,* thus these branches are coded as hashed blue and black. Discrete character groupings can additionally be found in Table S1. Geographic codes are given for undescribed species: IL=Illinois, MO=Missouri, NE=Nebraska, TN=Tennessee.

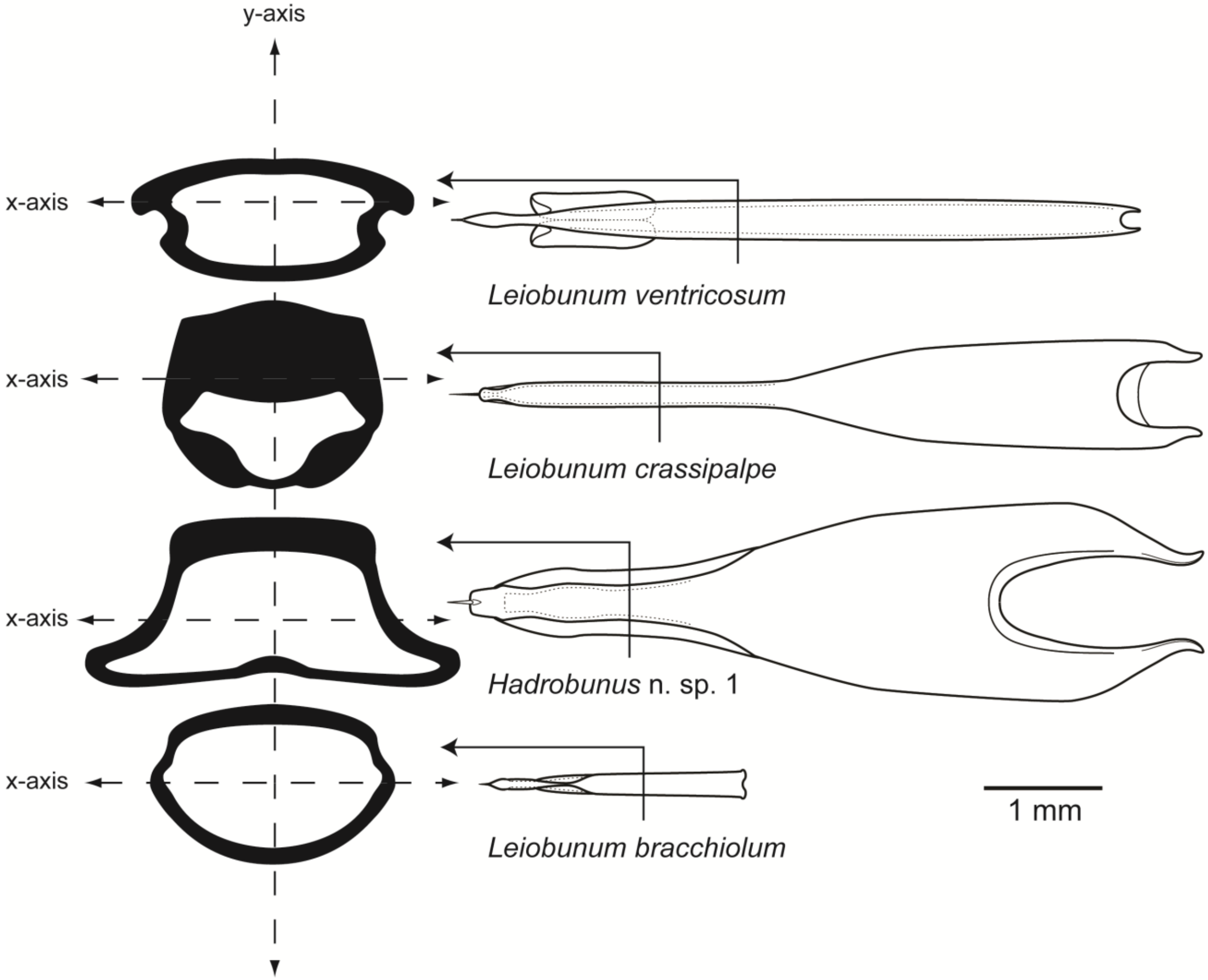

Figure 4.3: Penes and cross-sections from a sample of leiobunine species. Examples are displayed for males of four species: *Leiobunum ventricosum* (sacculate), *L. crassipalpe* (non-sacculate), *Hadrobunus* n. sp. 1 (non-sacculate), and *L. bracchiolum* (sacculate). High-contrast images of penile cross-sections (on left) were generated in order to estimate section modulus (Z_x, Z_y), which are estimates of flexural strength. X and Y axes of cross-section are indicated. Dorsal perspectives of penes are shown on the right. The scale applies to whole penes only.

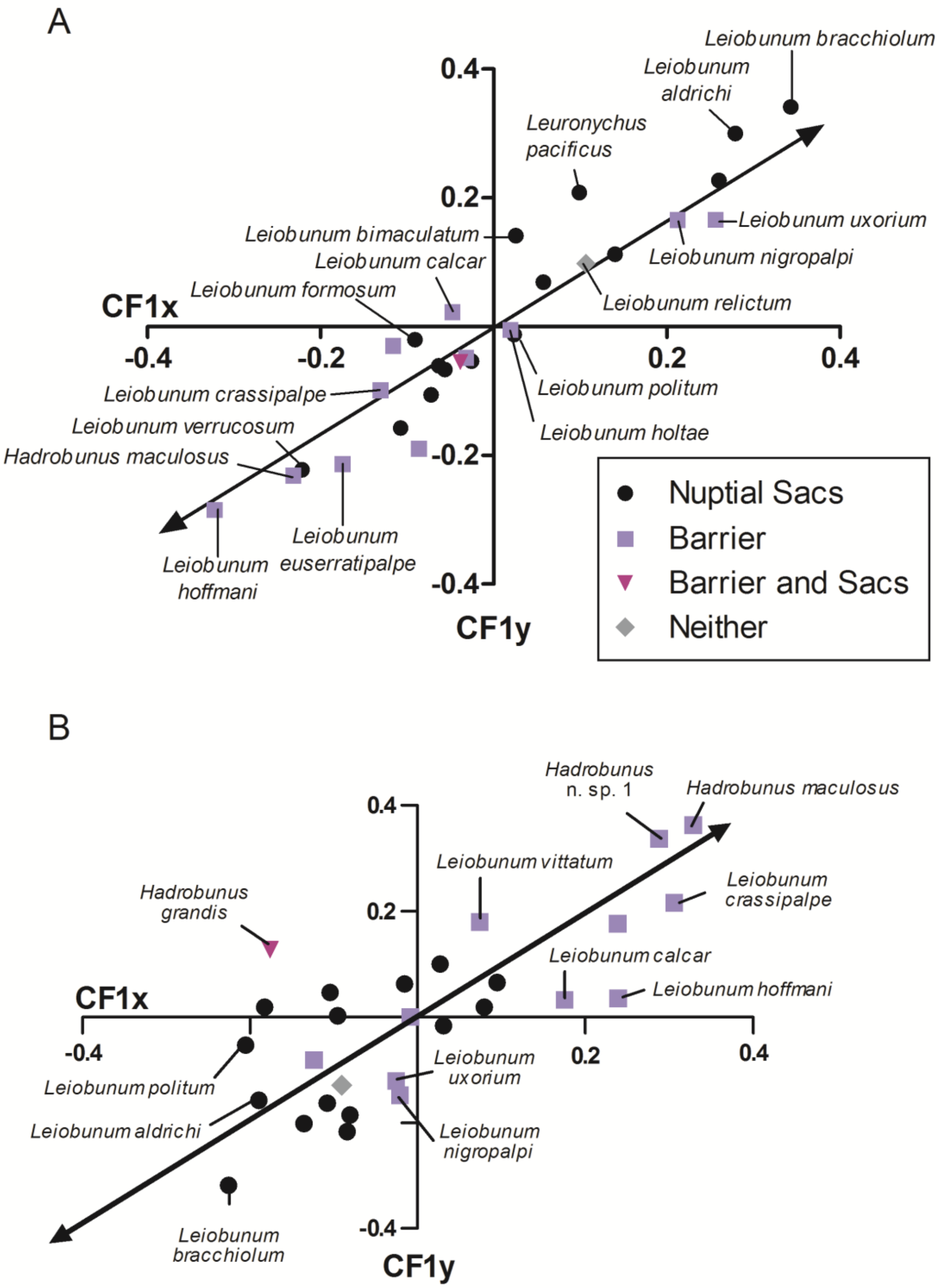

Figure 4.4: Phylogenetic canonical correlation graphs. A-B) Species scores on canonical function 1 from phylogenetic canonical correlation analyses including male and female size (A; major-axis regression of CF1: R^2=0.898, p<1e-13) or excluding size data (B; major-axis regression of CF1: R^2=0.561, p<0.00001).

Male traits comprise canonical function X-axis and female traits comprise canonical function Y-axis. In plotting the canonical factors, morphological distinction was applied to each species score: either antagonistic (female pre-genital barrier present) or female enticement-based (nuptial gift sac present), and was applied to each species score. *Hadrobunus grandis*—sacculate, barrier present—was indicated with violet triangles; *Leiobunum relictum*—non-sacculate, barrier absent—was indicated in light gray diamonds.

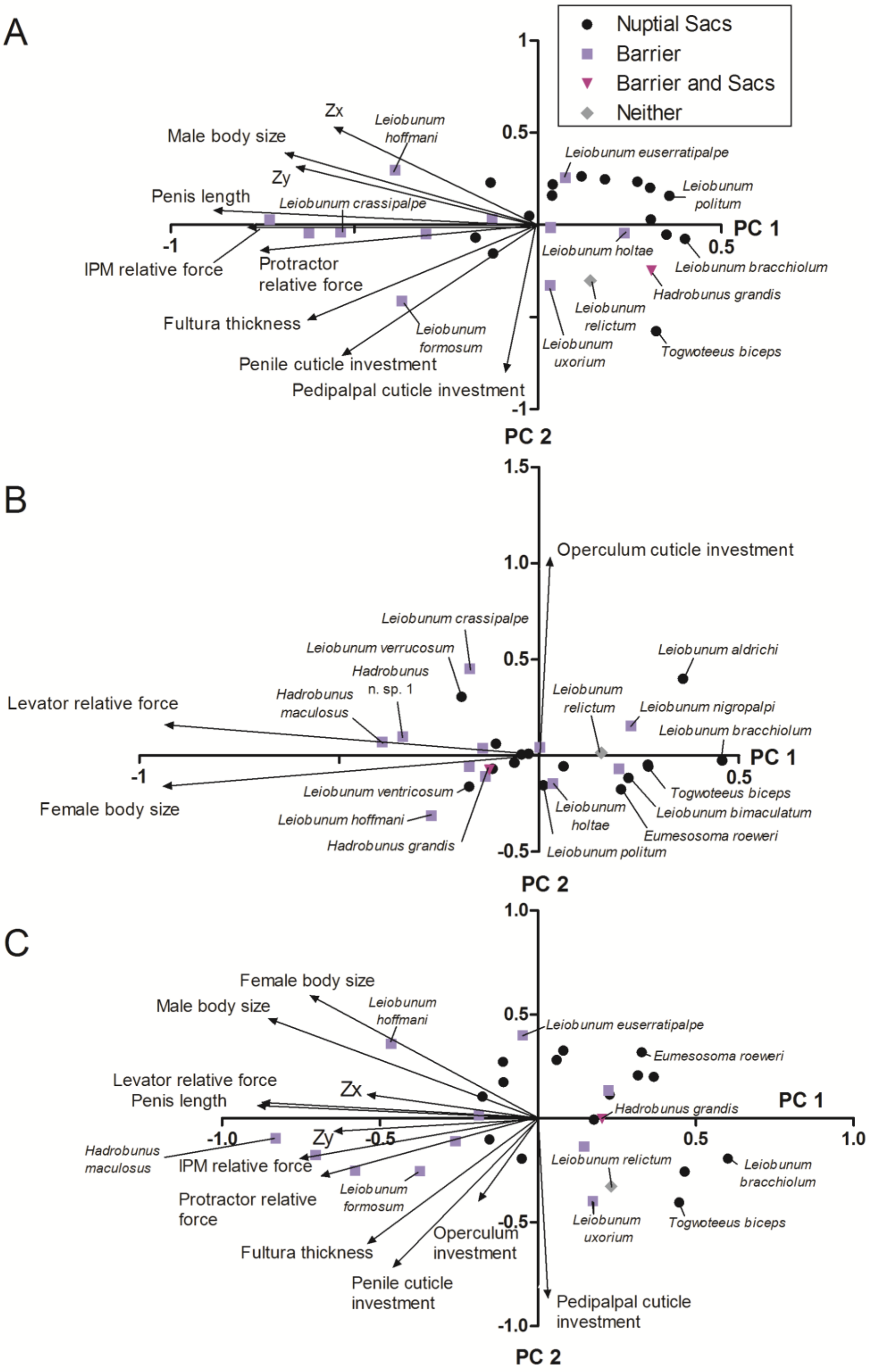

Figure 4.5: Phylogenetic principal components graphs. A-C) Phylogenetic principal components analyses of (A) male (PCs 1 and 2: 61.02% variance), (B)

female (PCs 1 and 2: 91.85% variance), and (C) all reproductive traits (PCs 1 and 2: 57.52% variance). Morphological distinction was applied to each species score: either antagonistic (female pre-genital barrier present) or female enticement-based (nuptial gift sac present), and was applied to each species score. *Hadrobunus grandis*—sacculate, barrier present—was indicated with violet triangles; *Leiobunum relictum*—non-sacculate, barrier absent—was indicated in light gray diamonds.

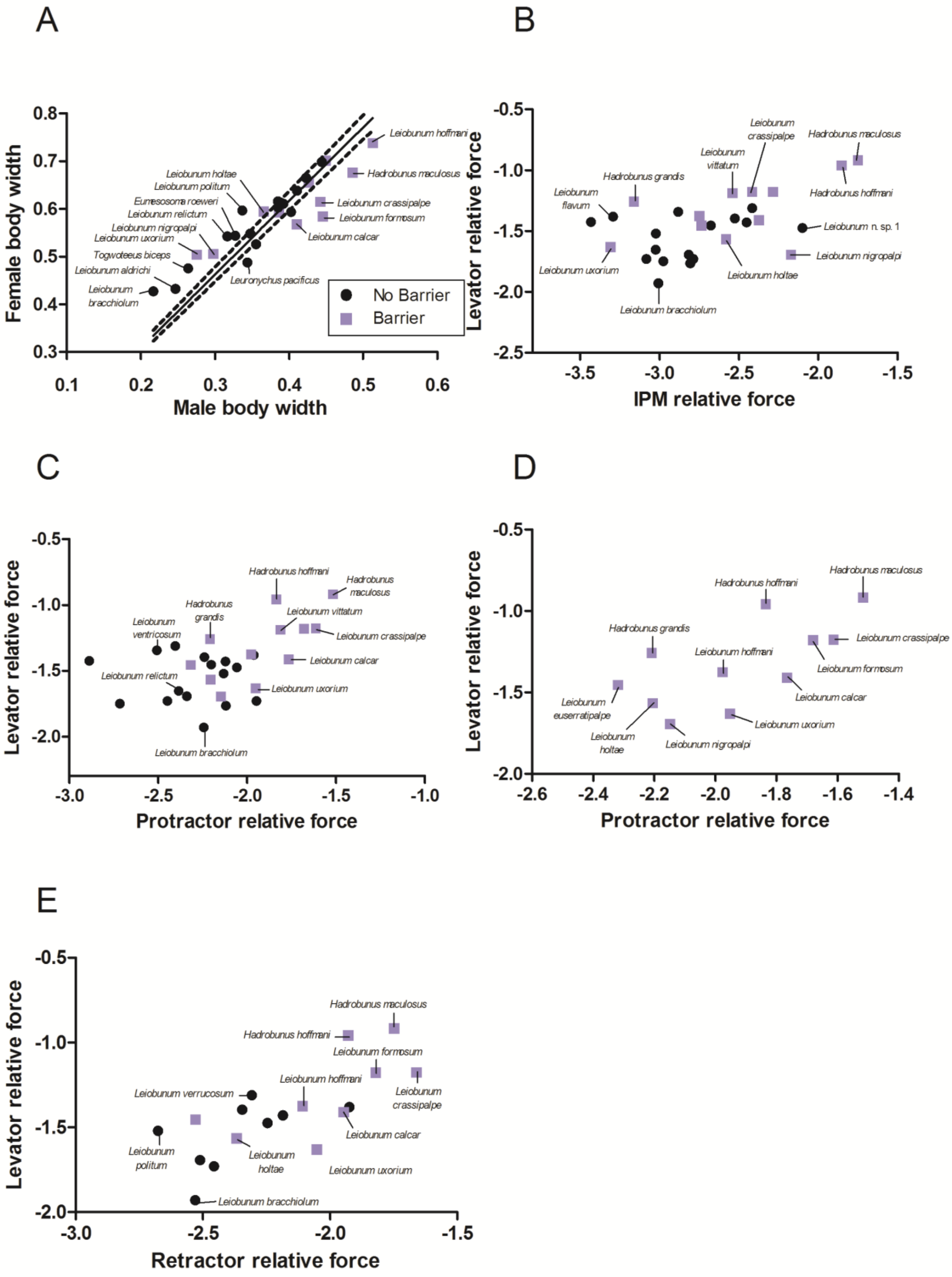

Figure 4.6: Phylogenetic regressions of male and female traits. A) least-squares regression results for log-transformed body size (solid line) with 95% confidence

intervals plotted (dotted lines) (phylogenetic generalized linear model: $R^2=0.8368$, $p<0.0001$) B-E) size-corrected, log-transformed plots of significant female by male reproductive traits for B) female levator muscle versus intrinsic penile muscle relative force for all species ($R^2=0.2643$, $p<0.01$), C) levator muscle versus penile protractor muscle relative force for all species ($R^2=0.2414$, $p<0.01$) and D) for barrier present species only ($R^2=0.5751$, $p<0.01$), and E) levator muscle versus retractor muscle relative force for all species ($R^2=0.4527$, $p<0.001$). In all figures, barrier absent species scores are identified with black circles, and barrier present species with blue squares.

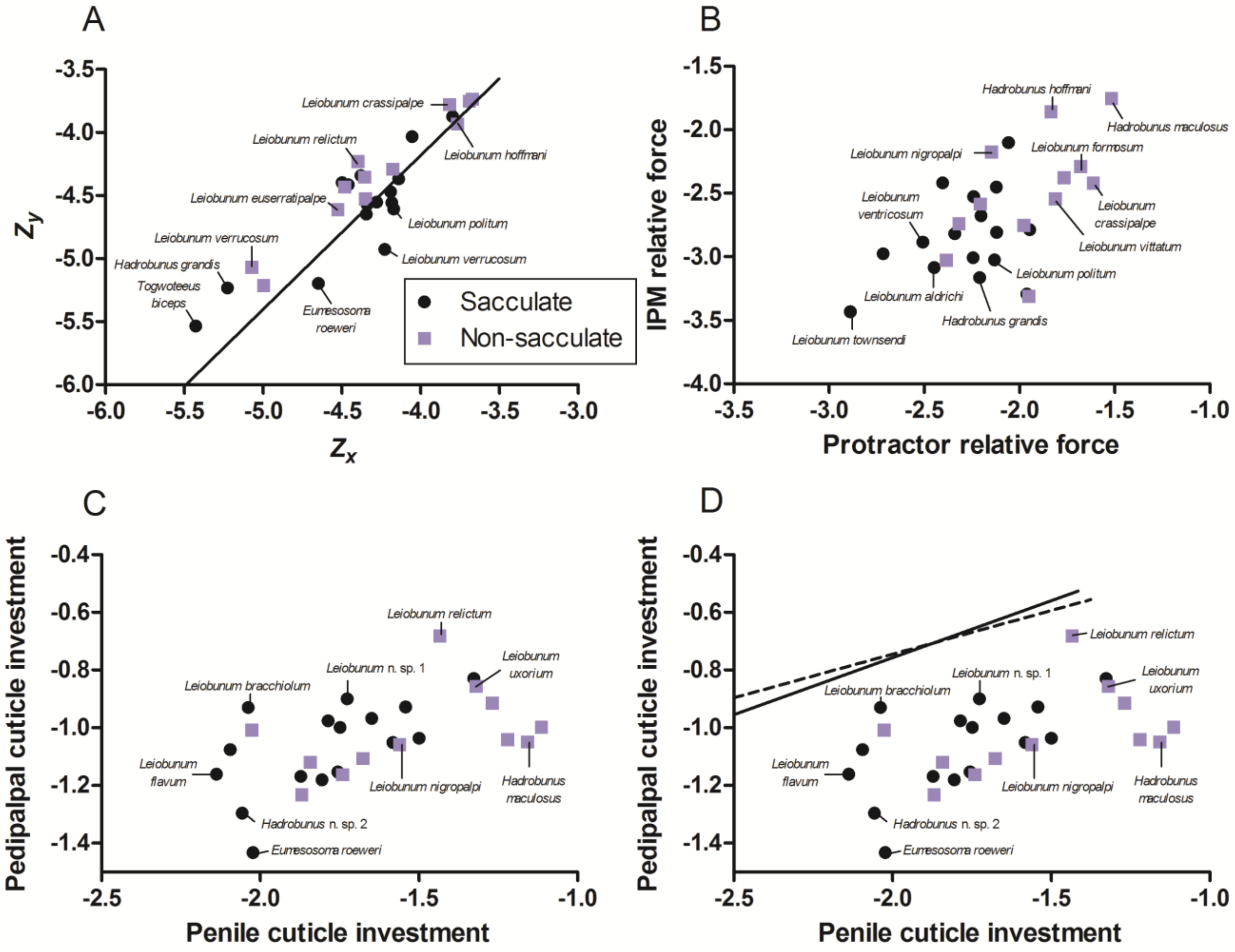

Figure 4.7: Phylogenetic regressions of male traits. A-D) Phylogenetic regression results for size-corrected, log-transformed male trait correlations, including A) least-squares regression of section modulus of the X- and Y-axes (phylogenetic generalized linear model: R^2=0.8079, p<1e-10), B) intrinsic penile by penile protractor relative force (R^2=0.3143, p<0.01), C) penile and pedipalpal cuticle investment (R^2=0.3819, p<0.001), and D) penile and pedipalpal cuticle investment analyzed separately by sac presence (dotted line, phylogenetic generalized linear model: R^2=0.324, p<0.05) or absence (solid line, phylogenetic generalized linear model: R^2=0.8115, p<0.0001). In all figures, sacculate species scores are identified with black circles, and non-sacculate species with blue squares.

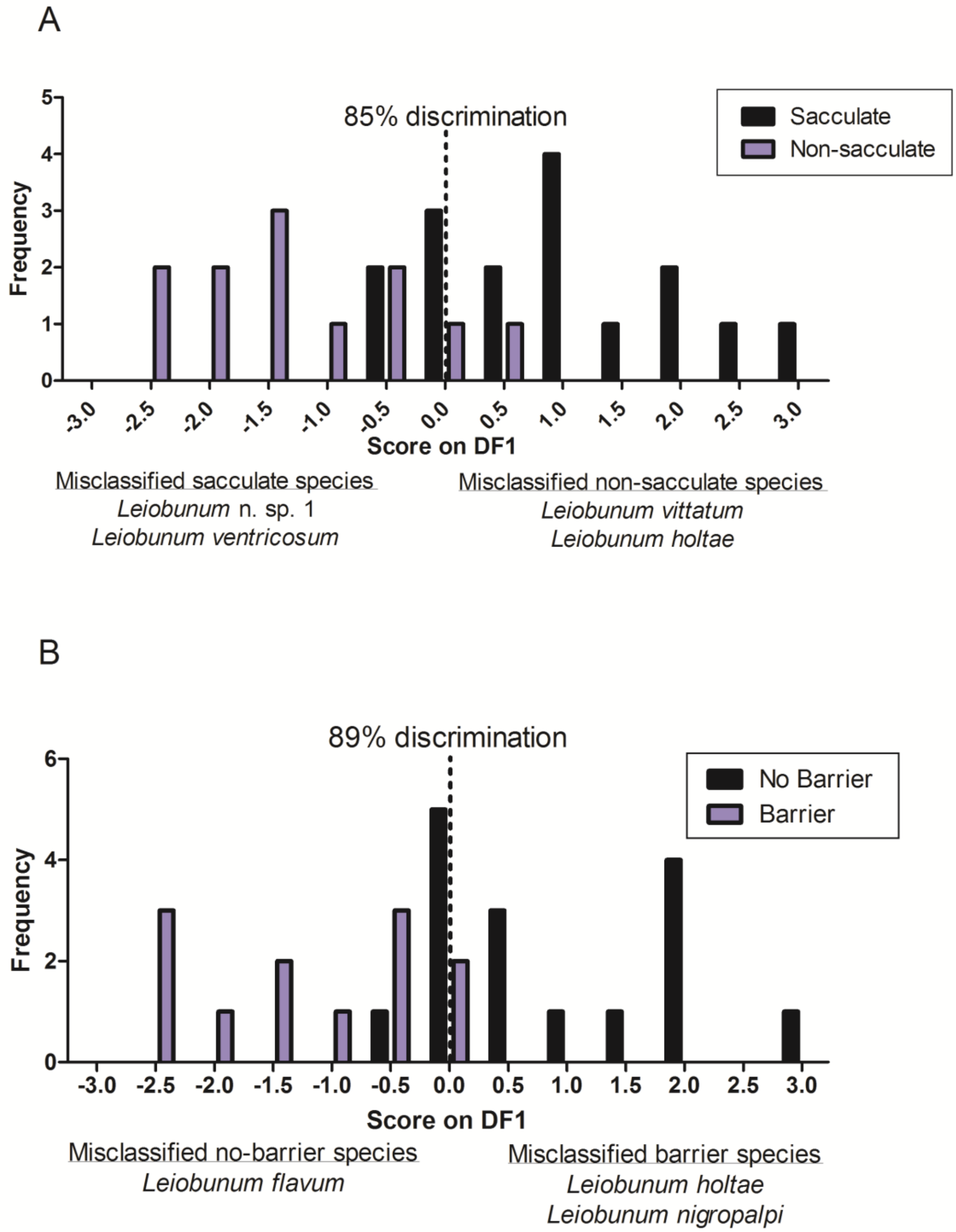

Figure 4.8: Histograms of discriminant classification. Species scores on linear discriminant function 1, based on all biomechanical data under (A) penile nuptial gift presence and (B) female pregenital barrier presence as grouping variables. While over-parameterization reduced the significance of the discriminant models (grouping variable: sacs, Wilk's $\lambda=0.44$, $F_{12,15}=1.56$, $p=0.2054$; barriers, Wilk's $\lambda=0.46$, $F_{12,15}=1.47$, $p=0.2387$), 85-89% discrimination was achieved. Bar color

distinguishes group assignment: black= sacculate/barrier absent, blue= non-sacculate/barrier present.

CHAPTER FIVE: Variation in the mechanical properties of male genitalia in harvestmen is consistent with variation in mating strategies

See Appendix 4 for supplementary table (Table S5.1) referenced in this chapter.

Abstract

Research on the evolution of reproductive traits often invokes "genital mechanics" without quantifying the mechanical forces that these structures can actually apply or resist. The present study takes an experimental mechanical force approach to describe mechanical properties in the diverse male genitalia of the eastern North American “daddy-longlegs” genus *Leiobunum.* In some species, males have cuticular penile sacs that provide a nuptial gift to females prior to mating. The sacs are absent in other species, but in these, females display complex genital barriers that appear to prevent males from accessing the pregenital chamber. We hypothesize that the evolutionary loss of gift sacs in males and gain of pregenital barriers in females reflects the increasing intensity of sexual conflict, and that this change should be reflected in differences in genital mechanics of sacculate and non-sacculate species. We determined the stiffness (spring constant), resilience ratio, rate of viscoelastic relaxation (time to 90% loss of applied force), and maximum experimental resistance in dorsal, ventral and lateral flexure for 10 species of *Leiobunum.* We then examined these mechanical force traits using phylogenetic comparative methods to assess the evolutionary mode, tempo, and covariation of mechanical force traits. Strong phylogenetic signal was present for many mechanical force traits and stochastic character mapping followed by evolutionary rate estimation indicated support for

divergent evolutionary rates in sacculate and non-sacculate lineages. When support for rate heterogeneity was found, non-sacculate species typically had higher evolutionary rates. However, only 90% relaxation time varied significantly between sacculate and non-sacculate species, and these results were not recapitulated in simulations of the character across the phylogeny. Phylogenetic principal components analysis demonstrates that the *calcar* non-sacculate lineage is strongly distinct from other species, exemplified by large increases in penile cuticular resilience ratio, initial test resistance, and 90% relaxation time, and we found these species displayed the highest values in significant regressions of dorsal by ventral traits. Together these results indicate that although non-sacculate lineages may represent a phylogenetic extreme characterized by increased propensity for precopulatory antagonism, specific lineages likely differ in their approaches to mating.

Introduction

Accounting for the extreme diversity in reproductive structures in the animal kingdom is a perennial goal for evolutionary biologists (Leonard and Cordoba-Aguilar, 2010; Day and Young, 2004). Traditionally, most workers have focused on the obvious, external, species-specific, and often-exaggerated or bizarre traits of the males (Hosken and Stockley, 2004). Although recent efforts to identify female genital variation have yielded some success (Tanabe and Sota, 2013; Sanchez et al, 2011; Brennan et al., 2007), the majority of studies have focused solely on males (Rowe and Arnqvist, 2012; Jagadeeshan and Singh, 2006;

Arnqvist, 1998). This approach has its merits, considering that species with male intromissive genitalia may have both pre- and post-copulatory functions (Eberhard, 2010) each may experience a different form of sexual selection, including female preferences (Kokko et al., 2003), sperm competition (Parker et al., 2013), and cryptic female choice (Albo et al., 2013; Eberhard, 1996). In a comparative context, male genital features can indicate the presence and direction of sexual selection mechanisms based on the distribution of traits on a phylogenetic historical framework and function of traits in mating (Burns et al., 2013; Arnqvist, 1998). However, despite the frequent use of the term "genital mechanics" in the literature (Blest and Pomeroy 1978; Huber 1993; Huber and Eberhard 1997; Eberhard 1993, 2004), reproductive function is often assumed in the absence biomechanical evidence, a situation which may lead to the misrepresentation of the evolutionary processes at work (Cayetano et al., 2011).

In the present study, we focus on the mechanical properties of male genitalia in order to assess sexual selection in ten eastern North American species of harvestmen from the genus *Leiobunum* (Fig. 5.1). Species in this group are annual and polygynandrous, allowing ample opportunity for female choice as well as inter-and intra-sexual conflict (Curtis and Machado, 2007). When retracted, the reproductive structures in both sexes are contained within a large pregenital chamber that occupies the ventral part of the abdomen and opens just posterior to the mouth. This chamber is guarded ventrally by a large ventral sclerite, the genital operculum, with a posterior transverse hinge that operates like a drawbridge. In males, the genital operculum opens to allow the penis to emerge anteriorly from the body, typically borne on a flexible balloon-like haematodocha that is inflated by fluid pressure and maintained, in part, by cuticular fulturae (stiffening rods; Fig. 5.1). The penis is a cuticular tube that ends in a short glans with a thin stylus that bears the primary genital opening. The glans and stylus are moved with respect to the penis shaft by the tendon of a pinnate muscle spanning the majority of the hollow penile cavity. Our behavioral and mechanical observations also indicate that the penis may also function to open the female genital operculum (Fig. 5.1) by force during precopulatory interactions. These coercive interactions may be common in a subset of leiobunine species that have lost the plesiomorphic penile sacs (Burns et al., 2012; Fig. 5.1). In fact, in nearly all species in which males that lack gift sacs, the female has pregenital barrier. These female and male morphological states have been shown to be derived, dependent, and correlated to each other and the direction of their evolution indicates a transition from mating systems characterized by female appeasement to precopulatory antagonism (Burns et al., 2013).

While the evolution of a physical reproductive barrier in females is consistent with the presence of sexual conflict (Gavrilets, 2000), there is no obligatory functional basis for the absence of nuptial gift sacs to indicate a transition to coercive mating. However, the demonstrated correlation between the loss of gift sacs in males and gain of reproductive barriers in females supports the hypothesis that nuptial sac loss is an indication of increasing intersexual antagonism. Given the limitations of presence/absence characters in inferring reproductive evolution, (Burns et al, 2013) we measured biomechanical variables that are likely to differ in different mating systems. We specifically evaluated penile responses to bending, hypothesizing increased bending resistance and/or persistent elastic response (i.e. resistance to bending does not change as a function of time) to indicate the increased influence of sexual conflict in species mating systems. Minimal resistance to bending and/or a rapid viscoelastic relaxation response would thus suggest lower coercive ability, greater accommodation to the female, and a decreased role for sexual conflict. In cross-section, penes of many *Leiobunum* species are dorsoventrally flat, a condition which would typically accommodate bending across the tranverse axis and inhibit lateral bending (Macdonald, 2001) and in Chapter 4 in which we found penile flexural stiffness (based on elastic section modulus) was only slightly greater for the dorsoventral flextural axis (x) relative to the lateral flexural axis (y). Therefore we further speculated that dorsal and ventral bending resistance should be increased in sexual conflict contexts, as stiffer genitalia may allow for improved coercive ability in males. To sum, the goals for this study were thus to determine the evolutionary direction and tempo, and potential covariation in male genital mechanical variables of male *Leiobunum*, in order to test the hypotheses that variables associated with penile bending as experienced by males in precopulatory encounters are positively correlated, indicating penile evolution towards improved function in a coercive context.

Materials and Methods

Species sampling

We collected and studied 60 male harvestmen from 10 species of the genus *Leiobunum,* including five sacculate species (*L. ventricosum, L. verrucosum, L. aldrichi, L. politum, L. bracchiolum*) and five non-sacculate species (*L. uxorium, L. vittatum, L. nigropalpi, L. euserratipalpe, L. calcar*) (see Table S5.1 for additional species information). All non-sacculate species examined are known to have females with sterno-opercular pregenital barriers, and likewise all sacculate species studied have females with no barrier. Specimens were maintained in laboratory terraria with food and water *ad libitum* until sacrifice.

Force transducer apparatus

To simultaneously evaluate displacement and force production of samples, we prepared an apparatus consisting of a force transducer system (Model 404A; Aurora Scientific Inc.) attached to a translation stage (OptoDC Servo Motor Driver #001; Thor Labs) and a displacement transducer (contact sensor: SG-DVRT-4; signal conditioner: DEMOD-DVRT; Microstrain, Inc.) with the contact sensor placed against the force transducer case (Fig. 5.2). The displacement transducer was calibrated by measuring the change in voltage from rest to a displacement of 1 mm (1150.7mV).Thor Labs software was used to control displacement of the sample at a constant velocity of 1 mm/s.

Experimental protocol

Specimens were sacrificed by placing them in a freezer at 0°C for 10 minutes, after which the penis was rapidly removed and affixed at the proximal base to a glass cover slip with ethyl cyanoacrylate gel (Super Glue). A drop of accelerant (Turbo Set I; Palm Labs Adhesives, Inc.) was applied to the glue bead to quickly position the penis in full moment cantilever formation. Body size (defined as width of prosoma, between coxae I and II) and penes were digitally photographed, and images were used to measure total penis length not fixed and determine the target 5% deflection to be achieved with the force transducer. Cover slips with attached penes were submerged in a polyacrylate box filled with room temperature Ringer's solution, and fixed to the side of the box using a 1/8" x 1/8" neodymium magnet to allow for easy repositioning.

Using a non-magnetic hook, force was applied to the distal third of each penis in the dorsal, ventral, and lateral aspects in order to achieve deflection at 5% of the free length. Deflection of each aspect was repeated three times, consisting of a work loop (penis rapidly displaced and returned) and a viscoelastic test (penis was displaced and held for three minutes). Displacement and force produced were logged as voltage changes every 50 milliseconds using Easylogger Dual Version 1.0 software (EasySync Ltd.).

Data analysis

Each force/displacement log was transformed to set baselines to zero. Then, voltages were converted from millivolts to milliNewtons (multiplied by a factor of

0.01 mV/mN) and millimeters (multiplied by a factor of 1/1150.7 or 0.000869 mV/mN). After plotting each sample work loop, we estimated the maximum slope from least squares regression with GraphPad Prism, v. 5.04 (GraphPad Software) to define stiffness, or spring constant (k) of the ascending displacement/force line, assuming the elasticity of the cuticle follows Hooke's law:

$$F = -kX$$

where F is the force required to bend the sample a given distance and X is the displacement. We additionally compared the area under the ascending (d_1) and descending (d_2) portions of the work loop. This ratio is defined as the structural resilience ratio, R:

$$R = \frac{d_2}{d_1}$$

Viscoelastic relaxation was approximated for samples by identifying the maximum experimental resistance achieved upon a vertical displacement of 5% of the penis length and determining the sampling time, in milliseconds, at which the resisting force relaxed to 90% of the maximum. This measure indicates the time-dependence to the strain of a material, and, along with resilience ratio, indicates the degree to which penes behave viscoelastically (Lakes, 2009). In the event that 90% force production was not reached during the sampling interval, the total log time for the test was taken as the relaxation sampling time. Initial test resistances and relaxation times were subsequently log-transformed to avoid potential heteroscedasticity between different bending directions (dorsal/ventral/lateral) and morphological groups (sacculate/non-sacculate). Mean values for all variables were established per specimen from three replicate tests per bending aspect, and from these, mean species values were calculated.

We utilized phylogenetic comparative methods to control variance due to shared evolutionary history and to describe the tempo and mode of evolution in penile stiffness, resilience ratio, relaxation times, and initial test resistances. To provide a historical framework for comparative analyses, we pruned a maximum clade credibility reconstruction from a previous Bayesian-likelihood analysis (Burns et.al. 2013) to include only the 10 taxa for which we had data. The *geiger* package (Harmon et al., 2008), utilized in the statistical programming software, R (R Development Core Team, 2013) was employed to evaluate evolutionary models for each trait, including the null model assumption of Brownian motion (random-walk), directional evolution (Brownian motion with a trend), Pagel's lambda (phylogenetic signal), kappa (punctuated equilibrium), and delta (time-dependent rates, comparable to early burst evolutionary model) (Pagel, 1999; 1997). Brownian motion was treated as the null model, with decreases in AICc based on model log-likelihood after correction for parameter number (ranging from 2—ancestral state and evolutionary rate—for standard Brownian motion to 3—ancestral state, rate, and an additional parameter for the trend, branch-length, and node-depth models) indicating a more complex model of character evolution to be suitable. Model probability was determined by AICc weights (Burnham and Anderson, 2004). *Geiger* was also employed to characterize sacculate and non-sacculate species by the three types of mechanical force traits measured using phylogenetic multiple analysis of variance (MANOVA) (Garland et al., 1993), in which the Wilk's Lambda test statistic was compared to those from 1 million data simulations on the phylogeny. To confirm assumptions of normality and homoscedasticity, we ran Shapiro-Wilk's and Levene's tests on each variable.

The R package *phytools* (Revell, 2012) was used to generate a principal components analysis for the four traits on all aspects, and specific regressions of stiffness, resilience ratio, initial test resistance, and 90% relaxation time between dorsal and ventral flexion were done with the *caper* package, in order to ascertain whether there is a preferred reinforcement surface as dorsal and ventral flexural resistance increases. We also examined the potential covariance between stiffness and initial test resistance. Lastly, *phytools* was employed to assess whether the loss of nuptial sacs promotes an increased evolutionary rate in mechanical reproductive traits. Additionally, reproductive traits are frequently said to evolve faster than somatic features, but this assumption is rarely tested (Huber, 2003). We used the *make.simmap* function in the R package *phytools* to construct 1000 stochastically-mapped phylogenies of sacculate and non-sacculate lineages. That is, in these trees, trait onset in conditioned by the instantaneous-transition matrix rather than from an *a priori* distribution, allowing each simulation to encapsulate a slightly different potential picture of the evolution of the trait binary. Using this distribution, we fit a noncensored

Brownian rate variation model (O’Meara et al., 2006) under restricted maximum likelihood to each mapped tree for body width and all mechanical force traits, allowing a maximum of 5000 iterations to reach convergence. Mapped trees were subsequently applied to reduced maximum likelihood to fit rates and log-likelihood scores of 1-rate and 2-rate models (function “brownieREML”), allowing up to 5000 iterations to reach convergence for each continuous trait. Model AICs and mean rates were calculated and compared for each variable and between body size and genital traits.

Results and Discussion

Principal Components Analysis

To explore the interrelationships among mechanical force variables associated with penile flexure, we performed a phylogenetic principal components analysis, where we selected a multivariate lambda model of evolution in order to account for variance in traits due to species relatedness without assuming Brownian motion (λ=6.9e-05, LogL λ=-427.58). Trait loadings (initial test resistance was not included in the analysis due to multicollinearity), and species scores on principal components 1 and 2 are plotted in Figure 5.3. Principal components 1 and 2 together account for nearly 75% of the variance in the data. Mechanical force values from all bending aspects load highly on PC1, particularly measures of relaxation time (PC1 loadings: dorsal=-0.92, ventral=-0.64, lateral=-0.85). Dorsal and ventral stiffness (PC1 loadings: 0.86 and 0.6 respectively) and dorsal and ventral resilience ratios (PC1 loadings: -0.81 and -0.71) also contribute heavily to

PC1. Lateral measures of these traits loaded more heavily on principal component 2 (PC2 loadings: lateral stiffness=0.29, lateral resilience ratio=-0.82) although lateral stiffness is best represented on principal component 3 (not pictured, PC3 loading: 0.88).

Species scores are fairly well defined by the 1st component axis alone, particularly when further classified by nuptial gift sac presence/absence (Fig 5.3: sacculate species identified by black circles, non-sacculate species by blue squares). Principal component 1 separates all members of the derived *calcar* group from all other species, indicating these three species have unusually high dorsal and ventral stiffness, resilience ratios, and relaxation times as compared to other species. These clusters form in spite of the removal of phylogenetic signal from the trait variance/covariance matrix. Other non-sacculate species included in the analysis, *L. vittatum* and *L. uxorium of the vittatum species-group,* tended to group with sacculate taxa. Principal component scores from the sacculate and *vittatum* group species were best defined by high lateral stiffness and low values for the other bending aspects, indicating greater dorsal and ventral compliance in these species. Principal components 1 and 2 and also indicate that the sacculate and *vittatum* species have low resilience ratios and shorter relaxation times than *calcar* group members.

Model Selection

Understanding the mode of evolutionary change for reproductive traits is essential for evaluating covariation in these traits, as well as simulating these traits to test macroevolutionary hypotheses. We used the fitContinuous function in the R package *geiger* to evaluate the Akaike information criteria of 5 potential models of evolution for each mechanical force trait measured. Model fitting AIC weights are summarized in Table 5.1. We found the majority of mechanical force traits were best modeled individually as Brownian (Table 5.1: higher AIC weights), suggesting traits evolve randomly as a function of the phylogenetic tree. This result was confirmed by the maximum likelihood estimates of Pagel's lambda, which were, or approached, 1 for several traits across the three bending aspects, including dorsal 90% relaxation, stiffness, and initial test resistance, ventral resilience ratio, and lateral viscoelasticity and test resistance. A lambda value of 1 is considered equivalent to a Brownian motion evolutionary model (Boettiger et al., 2011). Thus, contrasting with previously investigated measurements of relative biomechanical reproductive traits in male harvestmen [Chapter 4], mechanical force traits display relatively high phylogenetic signal, or correlation to phylogeny.

Two mechanical force traits, however, had lower AICc scores for the non-Brownian models. Lateral 90% relaxation time was best modeled by the kappa branch transformation (κ=6.6E-214, AICc=252.56) and lateral resilience ratio was best modeled by the lambda branch transformation (λ=0.715, AICc=4.06). For both of these traits, the Brownian model had the next highest AIC weight (Lateral 90% relaxation time: 0.27; Lateral resilience ratio: 0.31), indicating the alternative model may not be an improvement over Brownian motion. However, it may be meaningful that the traits best modeled by the more-complex functions were both derived from lateral bending. This is the bending aspect that we expected would change least between sacculate and non-sacculate groups, primarily due to the effects of natural selection promoting mechanisms of penile motion to resist penile fracture. That lateral traits are less likely to be simply modeled as a function of the phylogeny may suggest the additional input of mechanisms outside the realm of sexual selection in the evolutionary maintenance of the characters. Body size was additionally found to be best modeled by a lambda branch transformation with high probability (λ=3.81e-15, AICc=-11.04, $AICc_{wt}$=0.71); this result, as well as the low level of phylogenetic signal indicated by the value of Pagel's lambda, supports previous evaluations of body size evolution in leiobunine harvestmen (Burns et al., unpublished data).

Phylogenetic Regressions

We examined mechanical force trait analogues associated with bending along the dorsal and ventral axes to assess whether changes along the dorsoventral surfaces are correlated or if cuticular investment on one side of the penis is favored. Resistance was expected to increase particularly in non-sacculate, pregenital barrier-present species for which precopulatory conflicts are expected to be most common (Gavrilets, 2000). Based on the high probability of evolution by Brownian motion from the model selection results for most traits, we accounted for phylogeny in generalized linear models by setting lambda equal to 1.

We found that with the exception of penile cuticular resilience ratio (Adj. R^2=-0.0599, p=0.5), the same traits showed significant positive correlations when ventral and dorsal bending profiles were compared (Fig. 5.4). Dorsal increases in stiffness (Adj. R^2=0.3945, p<0.05), log-initial test resistance production (Adj. R^2=0.7727, p<0.001), and log-relaxation time (Adj. R^2=0.6622, p<0.01) were all significantly correlated to their ventral analogues. These results may indicate that fortification to the ventral penis is accompanied by dorsal fortification, which is expected given penes of most species are dorsoventrally flattened. However, plots, particularly of dorsoventral stiffness (Fig. 5.4A) and initial test resistance (Fig. 5.4C), suggest much of the correlation is carried by non-sacculate species, which display greater variance in values than their sacculate counterparts even after variance due to phylogenetic relationships is considered. We explored the evolutionary basis for this variation in subsequent analyses of group-level and evolutionary rate dynamics.

Mechanical Trait Differences Due to Morphological Phenotype

Group-level differences were investigated using phylogenetic multiple analysis of variance (MANOVA) for each set of trait values from dorsal, ventral, and lateral bending, using nuptial gift sac presence as the grouping variable. The Wilk's lambda test statistic and significance level were calculated for the data and for 1 million Brownian motion simulations based on the evolutionary variance/covariance matrix estimated from the data across the phylogeny. Thus, model significance indicated by the standard MANOVA is supported by the commonality of the actual data test statistic compared to a null distribution. Results from group means comparisons are summarized in Figure 5.5.

We found no significant difference between sacculate and non-sacculate stiffness (Wilk's λ=0.35, $F_{3,6}$=3.67, model p=0.082, phylogenetic p=0.65), resilience ratio (Wilk's λ=0.33, $F_{3,6}$=4.04, model p=0.069, phylogenetic p=0.68), or initial test resistance (Wilk's λ= 0.7, $F_{3,6}$=0.856, model p=0.512, phylogenetic p=0.19). Furthermore, high phylogenetic p-values in these models may indicate the same group means are achieved in most simulations, in which branches (lengths equivalent to relative time) are randomly rescaled to allow greater potential change along longer segments. The separation between non-sacculate species in the *vittatum* (i.e. *Leiobunum vittatum, L. uxorium*) and *calcar* (i.e. *L. calcar, L. euserratipalpe, L. nigropalpi*) groups is consistent with results from the principal components analysis (Fig. 5.3), where the *vittatum* group tended to cluster with the sacculate species.

A significant difference was found, however, in the relaxation times of the sacculate and non-sacculate species (Wilk's λ=0.26, $F_{3,6}$=5.77, model $p<0.05$) (Fig. 5.5D), indicating that, under displacement, non-sacculate took significantly longer to reach 90% of their initial resistance force. However, we found this result was not robust to data simulation (phylogenetic p=0.7815), suggesting the level of separation between group relaxation times was not particularly unique to the original dataset. The same result was found for all other data types. Tests of data normality and heteroscedasticity indicated that while data largely followed a normal distribution, (with the exception of ventral stiffness; W=0.8367, $p<0.05$)

there were significantly unequal variances between sacculates and non-sacculates for many traits, primarily from dorsal bending (stiffness: $F_{1,8}$=9.83, p<0.05; initial test resistance: $F_{1,8}$=16.7, p<0.01; 90% relaxation time: $F_{1,8}$=8.61, p<0.05). While the expectation of univariate normality is not ironclad for phylogenetic data, (Revell, 2009b) heteroscedasticity may be indicative of evolutionary or experimental issues. We hypothesize the lack of model significance as compared to the null distribution is reflected in the combined effects of a limited sample size, within-group variation, particularly in stiffness and initial test resistance, as evidenced by the large standard errors of the means, and, potentially, uncertainty in branch-length estimates. Experimental error may also play a role in the inflation of data variance. Repeated sampling could induce microscopic damage or internal friction to cuticular structures, reflected in mechanical trait values as hysteresis (Chamay, 1970). This would lead to decreased stiffness, resilience (greater work lost), and short relaxation times as sampling is replicated. A paired comparison of first and third replicates of stiffness, 90% relaxation time, and resilience ratios for all traits in all specimens revealed, however, although values differed in time, stiffness (dorsal: t=3.121, df=48, p<0.01; ventral: t=2.381, df=48, p<0.05; lateral: t=2.194, df=47, p<0.05), relaxation time (dorsal: t=3.3, df=53, p<0.001; ventral: t=2.880, df=48, p<0.01; lateral: t=2.07, df=54, p<0.05), and resilience (dorsal: t=2.925, df=48, p<0.01; ventral: t=2.520, df=48, p<0.01; lateral: t=1.666, df=47, p<0.05) were all increased in third sample replicates as opposed to first sample replicates. While the trend might suggest a random application of bending replicates would be a preferable experimental approach, these results indicate that the degree of displacement and number of bending replicates do not appear to induce elastic hysteresis in specimens.

Although phylogenetic simulation did not identify a significant difference in viscoelasticity between sacculate and non-sacculate species, we performed three follow-up phylogenetic univariate tests comparing means of dorsal, ventral, and lateral relaxation times. We found significantly longer non-sacculate relaxation times for dorsal (single dot contrast; $F_{1,8}=5.16$, $p<0.05$) and lateral (double dot contrast; $F_{1,8}=19.21$, $p<0.001$) bending, and a similar, although non-significant trend for higher non-sacculate ventral aspect relaxation ($F_{1,8}=0.639$, $p=0.78$). These results demonstrate significant differentiation of elastic responses in penile cuticle between sacculate and non-sacculate species, which could be a function of phylogeny or heteroscedasticity.

Estimating Rates of Change of Mechanical Force Traits

Earlier, we found some potential evidence that non-sacculate and sacculate leiobunine species differ in their penile mechanical traits, as well as evidence of much within-group trait variance (Fig. 5.1, Fig. 5.3). We wanted to test whether the diversification of male genitalia in *Leiobunum* into sacculate and non-sacculate lineages arose by chance or if this diversification reflects a fundamental divergence in the evolutionary rate of mechanical force traits. After fitting a noncensored Brownian rate variation model under restricted maximum likelihood to stochastically mapped trees for body width and all mechanical force traits, we found that no more than 0.9% of runs failed to converge for the simulations of any given trait. Non-converging simulations were removed from the final estimates of log-likelihood and trait rates. Using log-likelihood score per tree, we calculated mean AICs and AIC weights for the one- and two-rate competing models. Results are summarized in Table 5.2.

We found evidence supporting the 2-rate evolutionary model for five of the thirteen traits we examined. For these traits, including lateral stiffness, lateral resilience ratio, ventral relaxation time, and dorsal and ventral initial test resistance, the mean 2-rate model AIC was lower than the single rate model AIC. However, contrary to our expectations, rates of evolution were not always higher for the mechanical force traits of the non-sacculates species. Lateral stiffness and ventral relaxation time had higher rates for sacculate lineages, approximately four times the non-sacculate rate for the former and about twice the rate for non-sacculates in the latter case. There are several possible reasons for this. The variance for lateral stiffness in both phenotypes were very high, but standard deviation for sacculates (mean ± standard deviation: 320.026±191.004) exceeded that of non-sacculates (175.476±170.96) (Fig. 5.5A). It might be possible that data variance led to the estimation of a higher sacculate rate, but a Levene's test on these data demonstrated equality of variances between groups (Lateral stiffness: $F_{1,8}$=1.11, p>0.1; Ventral relaxation time: $F_{1,8}$=0.027, p>0.5). Alternatively, the synergy of the stochastic character maps and distribution of data at the tips of the trees could have increased the likelihood of a higher sacculate rate, especially if early or frequent transitions to non-sacculate state require compensation by way of an increased sacculate rate. This seems a better potential explanation for the higher sacculate evolutionary rates of these characters.

Lateral resilience ratio, dorsal initial test resistance, and ventral initial test resistance all had higher non-sacculate evolutionary rates. In some cases the ratios were especially extreme: 65 times higher for dorsal initial test resistance in non-sacculates, for example (Table 5.2). Again, as for lateral stiffness, the large rate increases likely are affected by high trait variance, which was also seen in resistance force (dorsal mean + SEM: 0.5813±0.1767; ventral: 0.9272±0.1695; lateral: 0.5557±0.1458; Fig. 5.5C). However, dorsal and ventral resistance force had low (at/below 20%) AIC weights for the null, one-rate model, whereas the one-rate model was far more competitive for lateral stiffness, lateral resilience ratio (sacculate mean + SD: 0.514±0.181; non-sacculate: 0.757±0.085), and ventral relaxation time (sacculate: 3.446±1.051; non-sacculate: 3.866±0.833; weights between 38-47%). Thus, our confidence in assigning separate rates of initial test resistance in sacculate and non-sacculate lineages, and in expecting a higher rate for non-sacculate lineages, is bolstered by these findings.

Conclusions

The Evolution of Penile Bending Resistance

We developed an experimental procedure to measure four mechanical force variables—stiffness, resilience ratio, in initial test resistance force, and relaxation time—associated with penile resistance to bending in three directions (dorsal, ventral and lateral), using specimens from 10 harvestmen species. An AIC approach was taken to assess the best-fitting model of evolution for each character. Contrary to reproductive biomechanical measures, such as relative genital muscle force and cuticular investment in reproductive structures, previously made in the same group of species [Chapter 4], strong phylogenetic signal was found for many mechanical force traits, favoring a Brownian motion interpretation of penile resistance evolution. We believe these results are due to the combinatory power of mechanical force traits to summarize information about penile shape and cuticular architecture (Rowe and Arnqvist, 2012). Just as a simple machine can be endlessly reconfigured to deliver the same force by altering effort, load size, or mechanical advantage, similar genital performance can be presumably achieved through a variety of mechanisms. Mechanical force variables appear to track all of these mechanistic changes in genital evolution, resulting in values that tend towards high similarity between taxa with shared ancestry.

We additionally found that the majority of mechanical force traits change across the phylogeny at higher rates than body size, confirming the conventional assumption that reproductive character evolution outpaces that of most somatic features. Although sexual selection may also have a function in body size evolution (Blanckenhorn, 2000), these results support the fast-rate assumptions of reproductive characters while simultaneously refuting the assumption that high evolutionary rate must yield a lack of phylogenetic correlation (Revell et al., 2008).

Ventral and dorsal bending resistance measures were found to be positively correlated after accounting for phylogeny. This is sensible given that the most successful penile prying motion would require high force and stiffness on either side of the lever axis, as well as the ability to continuously apply high forces over an extended period of time. This relationship may be due to correlated investments in cuticle on the dorsal and ventral penile surfaces (Vincent and Wegst, 2004) thus regulating both the size and shape of the penile cross-section (Amany and Prasini, 2009), but could additionally be influenced by penile shape. Males of some species of *Leiobunum* have pronounced penile curvature in the dorsoventral axis that could affect stiffness and resilience ratios (Fig. 5.1; *L. vittatum, L. calcar*), as pre-curved beam structures have an adjusted neutral axes and are expected to tolerate compression and tension differently than straight beams (Gonzalez and Llorca, 2005). Taxonomists have previously remarked on these curvatures, particularly among the *calcar* species group (Ingianni et al., 2011), as a potential adaptation to increase penile length (and thus muscular attachment for extrusion mechanisms, [Chapter 4]) under body size constraints. It is therefore unclear if dorsoventral bending resistance originates due to penile curvature, or in spite of it. Future work could explore the evolutionary implications of penile extrusion mechanisms by comparing muscle attachment and dorsal and ventral cuticular thickness at cross-section between species with and without penile curvature. A lack of evolutionary dependence between penes with increased extrusion muscle attachment and dorsoventral investment in species with curved penes would signal the ability of curved penes to develop without the additional requirement of increased cuticular investment to bolster the dorsoventral axis.

Morphological Phenotype: A Binary May Not Be Sufficient

Throughout the paper, we explored mechanical force trait responses based on discrete morphological phenotype, namely the presence or absence of penile sacs that deliver a fluid nuptial gift under a “female appeasement” mating system context. In species where nuptial gift sacs have been lost, we expected a correlated increase in stiffness, resilience ratio, 90% relaxation time, and initial test resistance in all bending directions. While with only five species of each phenotype we had few phylogenetic contrasts to make, we found significantly longer dorsal and lateral mean relaxation times during displacement of non-sacculate penes as compared to sacculate species (Fig. 5.5). However, these results were not robust with respect to data simulation across phylogeny, indicating the same degree of mean separation found between these groups is easily recovered under Brownian motion simulation. We also examined the potential for rate increases in mechanical force variables of non-sacculate lineages, expecting that variables associated with increasing antagonism in males would be best described with a two-rate model allowing for non-sacculate parameters to evolve at higher rates.

However, we found only two traits, dorsal and ventral initial test resistance, which were convincingly modeled with two rate parameters and displayed higher rates of change along non-sacculate lineages. There are two immediate possibilities as to why distinction between sacculate and non-sacculate species was so minimal. The first is that experimental error, combined with a small sample size, constituted too great a statistical hurdle to find significant differences in mean values. We found that at the smallest penile sizes (seen in *L. bracchiolum* and *L. uxorium* species), our force transducer was barely capable of registering a signal during dorsal and ventral bending. In ongoing work, a finer measurement apparatus would be well advised. Additionally, our species sample was not exhaustive of all non-sacculate species*,* or even all of *Leiobunum,* but simply included species easily collected in our vicinity in numbers to ensure within-species accuracy. It is doubtlessly helpful to all comparative trait studies that the largest sample possible be included to maximize statistical power and also to present the largest number of species contrasts when research questions are macroevolutionary in nature. Even the inclusion of one additional member of the *vittatum* group, the derived *L. crassipalpe* (Burns et al., 2012), might drastically alter these results by closing the gap between group variances. This species has penile features in common with the *calcar* group—elongated, thickened penes with dorsoventral curvature—as well as the group to which it belongs—e.g. the distal half to two-thirds of the penis is a thin cylinder, which the proximate base is much thicker, bearing the majority of the intrinsic muscle fibers (Burns et al., 2012; [Chapter 4]).

The second potential justification for the lack of mechanical trait differences between sacculate and non-sacculate *Leiobunum* relates the high phylogenetic signal we found in many traits analyzed here to group-level variance. In a phylogenetic principal components analysis (Fig. 5.3), computed using a maximum likelihood-lambda branch transformation to account for trait evolution via non-Brownian processes, we found a strong disparity in species scores, primarily on principal component 1, between non-sacculate taxa from the *vittatum* (*Leiobunum vittatum, L. uxorium*) and *calcar* (*L. nigropalpi, L. euserratipalpe, L. calcar*) species groups. *Calcar* group species tended to score alongside most trait loadings on PC1 whereas *vittatum* group species were nearly indistinguishable from the cluster of sacculate taxa scores. If principal component 1 is taken to constitute level of potential mating antagonism in harvestmen species with increases following the trait loadings into the negative x-axis, this distribution indicates *calcar* group males have greatly increased potential for coercivity relative to the non-sacculates examined. This group disparity is supported by the phylogeny (Fig. 5.1), as the *calcar* group is distal to all other included species. Other sources of variance exaggeration (e.g. due to small sample size or experimental error) may thus be magnified by phylogenetic effects, yielding a result that makes assessments of the true phylogenetic effects on group variance challenging to identify without increasing tree size to either 1) improve analytical power to identify group contrasts, or 2) properly assess phylogenetic signal (Blomberg et al., 2003) without the *calcar* group.

In phylogenetic regressions (Fig. 5.4) we find that even after accounting for sizable phylogenetic correlations *calcar* group species show strong evolutionary increases in penile bending resistance, whereas the *vittatum* group has greatly reduced stiffness (Figs. 5.4A) and lower initial test resistance (Figs.

5.4C) than even sacculate species. However, non-sacculate species appear to be united by their similar resilience ratios (Figs. 5.4B) and 90% relaxation times (Figs. 5.4D), particularly in the ventral and lateral bending directions. These within-group similarities were presumably enough to differentiate sacculate and non-sacculate relaxation times using phylogenetic MANOVA, but not other mechanical force variables.

Ultimately, it appears treating non-sacculates as a unified morphological phenotype may be problematic. Although all non-sacculate species included in this analysis are known to have females with sterno-opercular pregenital barriers, barrier morphology and function differ between females of the *vittatum* and *calcar* groups. In *vittatum* species, the internal surface of the genital operculum has two large cuticular apophyses that create an aperture for a peg-like sclerite on the sternum to oppose. *Calcar* group females utilize muscle inserted on an elongated lever arm on the sternum to pivot the sternum underneath the sclerotized anterior lip of the operculum. In a previous discriminant analysis performed using biomechanical reproductive characters from both males and females we found classification by the discrimination model was improved when the grouping variable was barrier presence, as opposed to nuptial gift sac presence [Chapter 4]. This was presumably because some leiobunine harvestmen species have sacculate males with barrier-present females (*Hadrobunus grandis;* [Chapter 4]) and some species have non-sacculate males, while their females have no pregenital barriers (*Leiobunum relictum*; [Chapter 4]), mean group membership does change slightly depending on grouping variable. It would seem to be that it is actually the female pregenital barrier presence that most reliably signals increases in precopulatory mating antagonism.

Given the correlation between these barriers and loss of nuptial gift sacs in males, and variation in male genital traits, we must conclude male morphology reflects a variety of sexual selection mechanisms at work, including female choice either for nuptial gift quality/access or for the mechanical signals provided by the penis and antagonistic coevolution to overcome female defenses, and male force responses as we have seen may be the result of evolutionary compromises to favor mating strategies that may themselves change across a breeding period. Ultimately, although members of the *vittatum* and *calcar* groups are united by their lack of penile sacs, results of our multivariate analysis support divergence in behavior and/or mechanistic function of penes during mating.

Tables

Table 5.1: Evolutionary model selection for body size and mechanical force traits. Akaike information criterion (corrected for small sample size) standardized weights for male body size and mechanical reproductive traits. Models included Brownian motion (random walk), Directional (Brownian motion with a trend), kappa (punctuational equilibrium), lambda (phylogenetic signal), and delta (time-dependence) (Pagel 1999; 1997). Unstandardized weights were calculated with the equation $AICc_{wt} = e^{\wedge((AIC_{minimum} - AIC_i)/2)}$ (Burnham and Anderson, 2004). Preferred model (greatest $AICc_{wt}$) is indicated with grayed box.

Trait	Brownian model $AICc_{wt}$	Directional model $AICc_{wt}$	kappa model $AICc_{wt}$	lambda model $AICc_{wt}$	delta model $AICc_{wt}$
Dorsal Stiffness	0.658522	0.0851997	0.070372	0.05973979	0.12616598
Ventral Stiffness	0.534888	0.0830429	0.048536	0.13488979	0.19864276
Lateral Stiffness	0.445955	0.0745462	0.061829	0.21716775	0.20050118
Dorsal Resilience Ratio	0.409787	0.0718894	0.162836	0.15530791	0.20017854
Ventral Resilience Ratio	0.572916	0.0768263	0.117286	0.11409458	0.11887667
Lateral Resilience Ratio	0.306954	0.0528567	0.143229	0.35960809	0.13735129
Dorsal 90% Relaxation	0.62159	0.1961796	0.056389	0.05638937	0.06945164
Ventral 90% Relaxation	0.584331	0.0851205	0.053601	0.10173979	0.17520706
Lateral 90% Relaxation	0.269506	0.0453424	0.440757	0.13772963	0.10666494
Dorsal Initial Test Resistance	0.621124	0.0866473	0.088256	0.05634711	0.14762585
Ventral Initial Test Resistance	0.405880	0.0719919	0.129344	0.17422450	0.21855872
Lateral Initial Test	0.652490	0.0823045	0.083922	0.05919261	0.12208979

Resistance					
Body Size	0.068336	0.0140848	0.151244	0.71218927	0.05414546

Table 5.2: Rate modeling for body size and mechanical force traits. Results of reduced maximum likelihood analysis of evolutionary rates of body size and mechanical force traits over 1000 trees mapped with presence/absence of nuptial gift sacs. The likelihoods of the 1-rate model (sacculate and non-sacculate rates equal) and 2-rate models (sacculate and non-sacculate rates unequal) were evaluated using AIC, calculated using the equation $AIC_i = (2*k) - (2 * \text{log-likelihood}_i)$. AIC weights were calculated with the equation $AIC_{wt} = e\verb|^|^{((AIC_{minimum} - AIC_i)/2)}$ (Burnham and Anderson, 2004) and standardized. Means do not include AIC/rates from runs with lack of convergence. For traits where model selection favored a single rate of evolution, sacculate and non-sacculate rates (white boxes) are equal. For traits where model selection favored separate rates of evolution for sacculate versus non-sacculate lineages, blue colored boxes indicate increased rates for non-sacculates. Grey boxes indicate increased rates for sacculate lineages. Blue boxes indicate increased rates for non-sacculate lineages.

Trait	**AIC-1 rate model**	**Mean AIC-2 rate model**	**AIC-1$_{wt}$**	**AIC-2$_{wt}$**	**Sacculate Rate**	**Non-sacculate Rate**
Dorsal Stiffness	105.0828	107.0631	0.729123	0.270877	435,399.1	435,399.1
Ventral Stiffness	107.7556	109.7029	0.725846	0.274154	585,956	585,956
Lateral Stiffness	127.1941	126.9194	0.465709	0.534291	9,389,668	2,375,247
Dorsal Resilience Ratio	-11.6476	-10.9024	0.592084	0.407916	1.014	1.014
Ventral Resilience Ratio	-2.63609	-1.88826	0.592405	0.407595	5.736	5.736
Lateral Resilience Ratio	3.946919	3.680836	0.466788	0.533212	1.747409	8.950095
Dorsal 90% Relaxation	-3.44285	0.579211	0.88195	0.11805	3.721	3.721
Ventral 90% Relaxation	-0.98595	-2.00657	0.37512	0.62488	3.333947	1.908435
Lateral 90% Relaxation	-8.40739	-8.09579	0.538871	0.461129	1.454	1.454

Dorsal Initial Test Resistance	68.15725	60.92392	0.026169	0.973831	215.2127	14,059.11
Ventral Initial Test Resistance	68.04747	64.89557	0.171371	0.828629	853.0332	11,586.65
Lateral Initial Test Resistance	72.07083	73.72307	0.695534	0.304466	11,114.72	11,114.72
Body Size	-5.71242	-4.18201	0.682483	0.317517	1.961	1.961

Figures

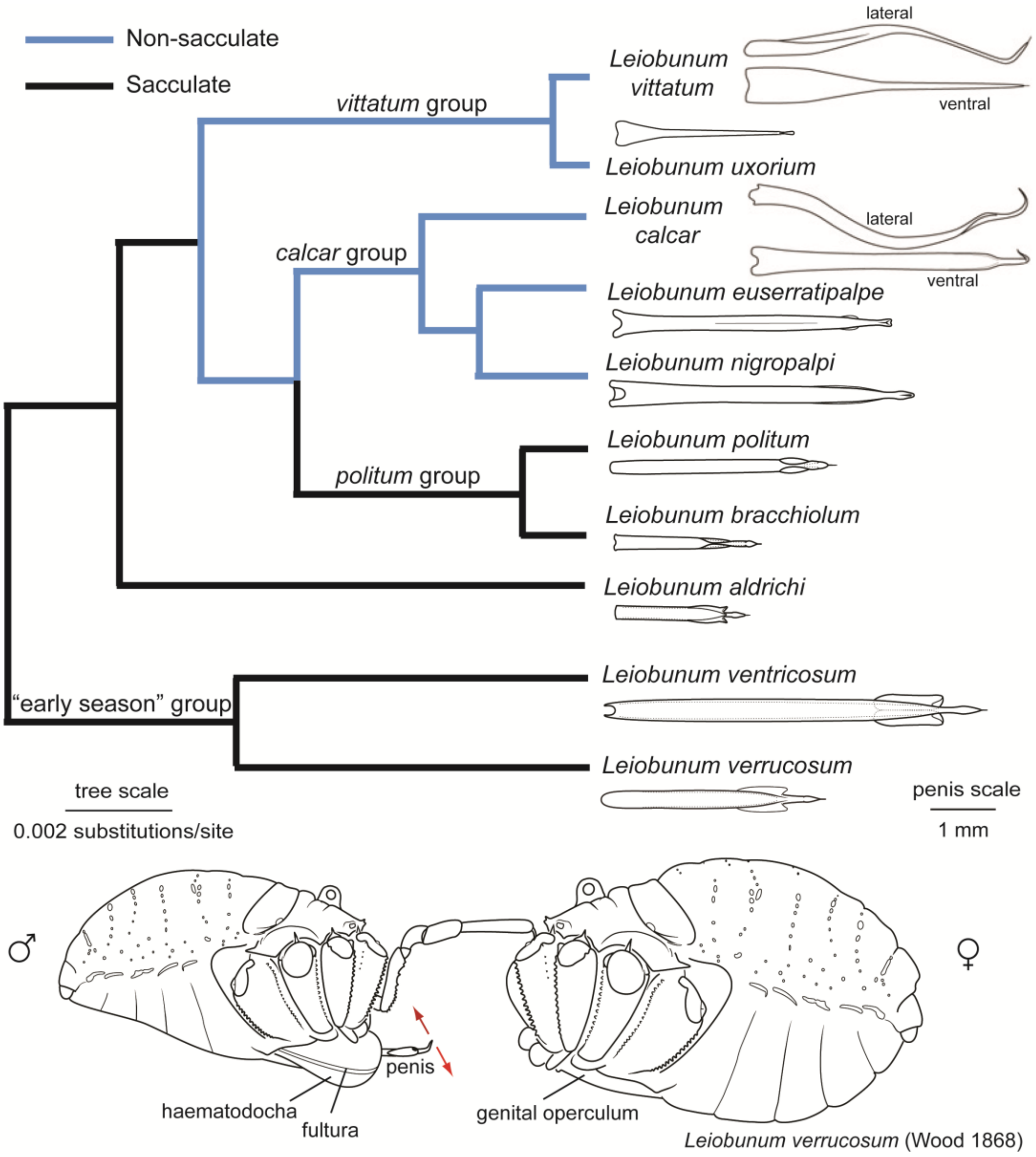

Figure 5.1: Male reproductive morphology and phylogeny of *Leiobunum sp.* Penes (to scale: bar = 1 mm) from 10 study species, arranged along the pruned maximum clade credibility tree (Burns et al., 2013). Tree scale is in substitutions per site. Sacculate taxa, found on black branches, include *Leiobunum verrucosum, L. ventricosum, L. aldrichi, L. politum,* and *L. bracchiolum.* Species constitute members of the “early-season” and *politum* species groups: all display the plesiomorphic feature of paired cuticular sacs on the distal penis. Non-sacculate taxa are identified by blue lineages. These include *Leiobunum vittatum* (lateral and ventral views) and *L. uxorium* (members of the *vittatum* group) and *L. calcar* (lateral and ventral views), *L. nigropalpi,* and *L. euserratipalpe* (all

members of the late season-maturing *calcar* group). We hypothesized these discrete classes should be highly correlated with genital functionality, such that kinetics might discriminate them. Inset shows a line drawing of *Leiobunum verrucosum* male encountering a female (legs removed for clarity), with penis extruded. Red arrows indicate axis of flexion occurring at glans-shaft joint.

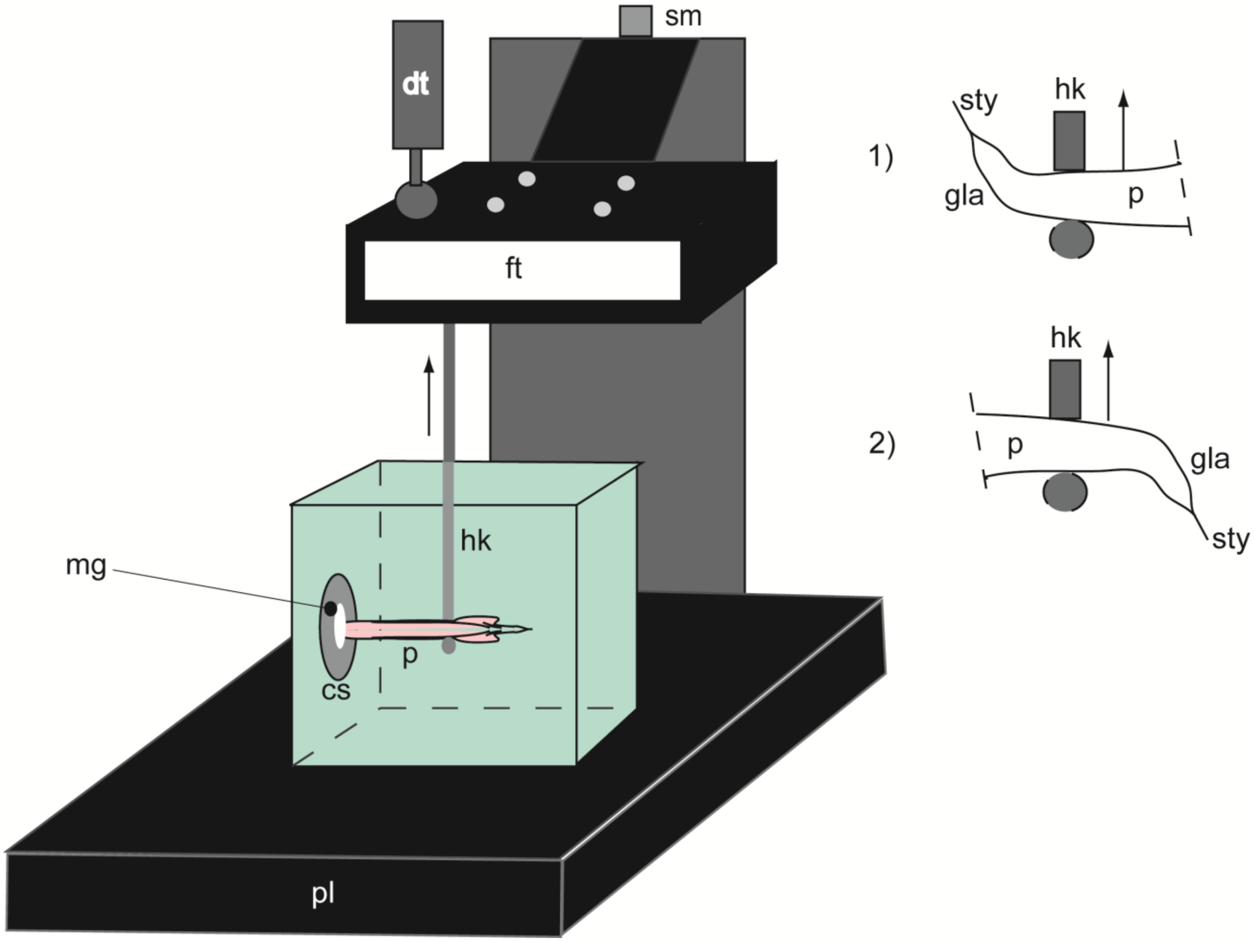

Figure 5.2: Force and displacement transducer experimental design. Apparatus consisted of an Aurora Scientific Inc. force transducer (ft), mounted vertically in contact with a Microstrain displacement transducer (dt) in order to simultaneously track position and force exerted by sample against the non-magnetic hook (hk). Penes (p) were mounted with cyanoacrylate to a glass coverslip (cs) in cantilevered position and displaced under Ringer's solution in the ventral (1), dorsal (2), and lateral (shown on apparatus) directions. Mg=magnet, Pl=platform, Sm=stepper motor, Gla=glans, Sty=penile stylus.

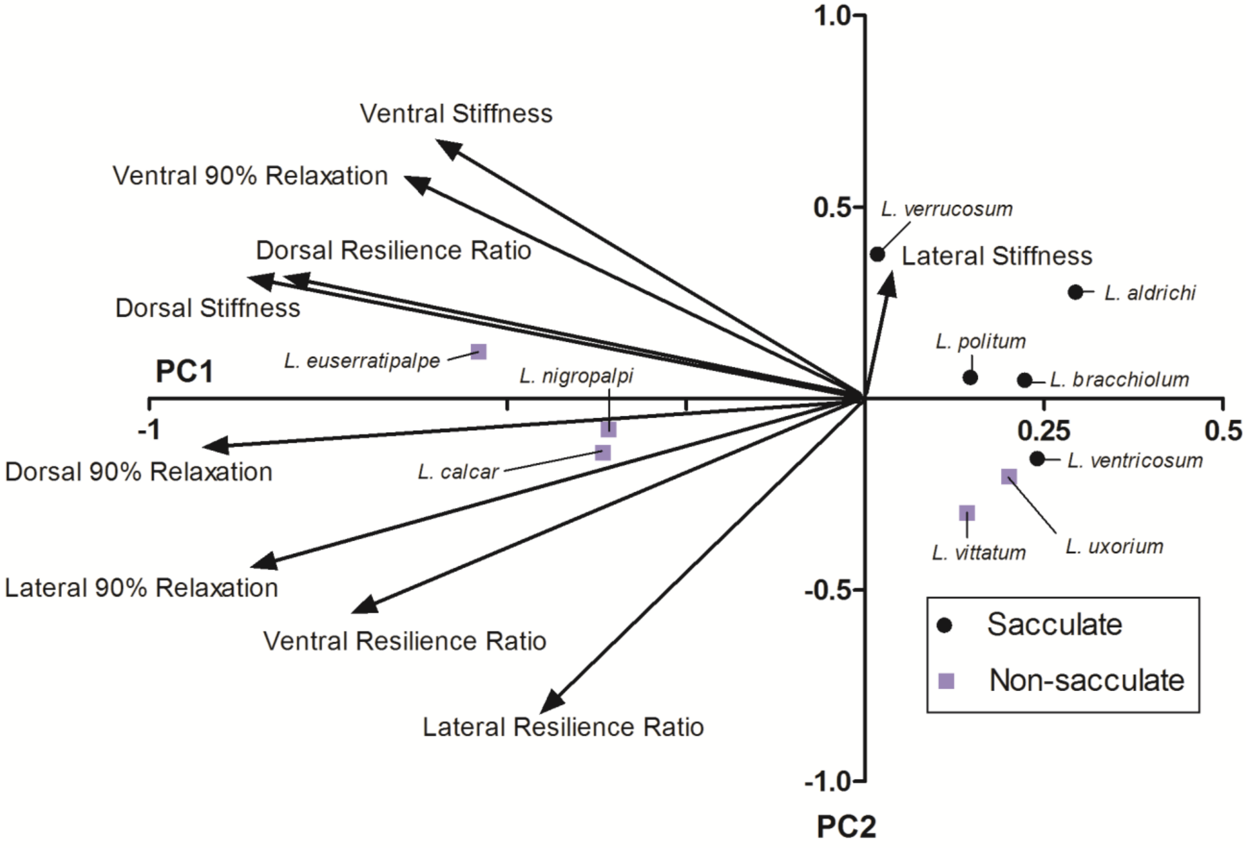

Figure 5.3: Phylogenetic principal components analysis of mechanical force data. A phylogenetic principal components analysis, using the maximum likelihood estimate lambda (λ=6.9e-05, LogL λ=-427.58) to remove variance due to shared species history, was applied to dorsal, ventral, and lateral stiffness, resilience ratio, and 90% relaxation time (initial test resistance data were removed from the analysis due to multicollinearity). Principal components 1 (x-axis) and 2 (y-axis) together account for 74.3% of the total data variance. Trait loadings appear as black arrows. Non-sacculate species are indicated with blue squares, sacculate species with black circles.

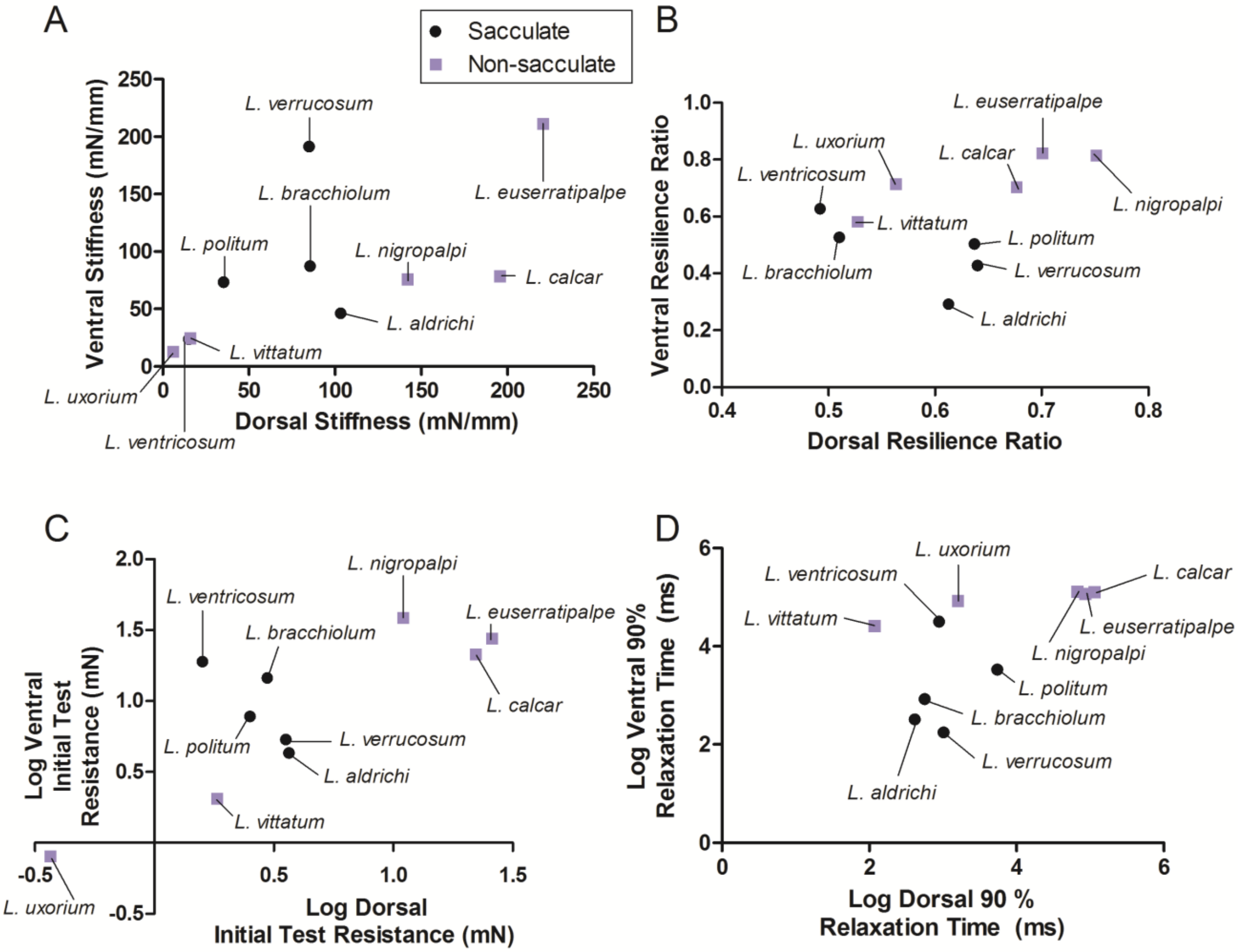

Figure 5.4: Phylogenetic regressions of mechanical force data from dorsal/ventral bending. Phylogenetic regressions of species means of dorsal versus ventral A) stiffness, B) resilience ratio, C) log-transformed initial test resistance, and D) log-transformed 90% relaxation time. In all figures, sacculate species values are identified with black circles, and non-sacculate species with blue squares. Although the relationship between dorsal and ventral resilience ratios was not significant (Adj. R^2=-0.0599, p=0.5), significant correlations were found between ventral and dorsal measures of stiffness (Adj. R^2=0.3945, $p<0.05$), initial test resistance (Adj. R^2=0.7727, $p<0.001$), and viscoelasticity (Adj. R^2=0.6622, $p<0.01$) indicating evolutionary increases in these ventral traits are significantly correlated to increases in dorsal analogues.

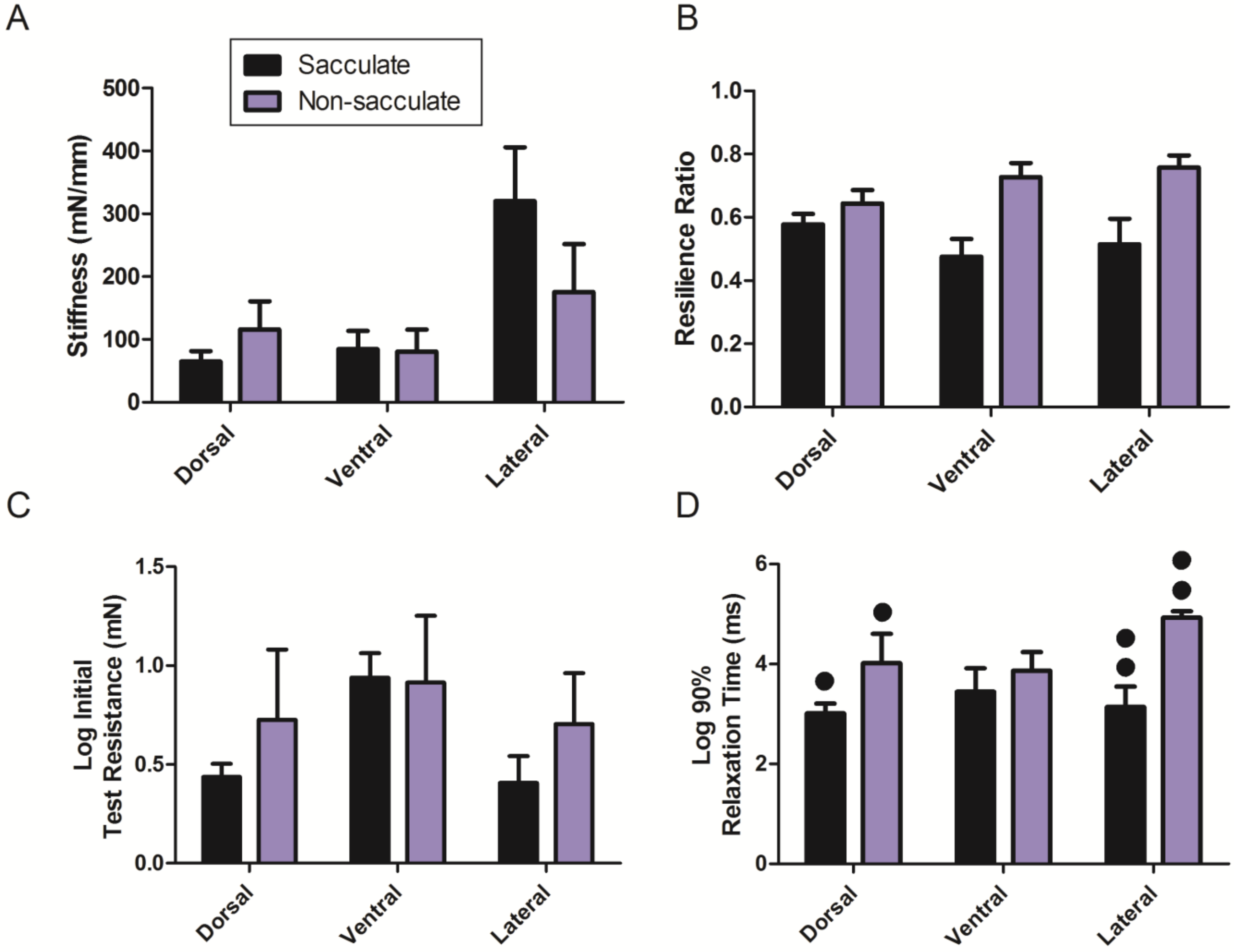

Figure 5.5: Phylogenetic MANOVA of mechanical force data. Bar graph results summarize four phylogenetic MANOVA tests comparing the A) stiffness, B) resilience ratio, C) initial test resistance, and D) 90% relaxation times (log-transformed) of penes displaced dorsally, ventrally, and laterally for sacculate and non-sacculate species. Bars are group means plus standard error for sacculate (black) and non-sacculate (blue) species for each of three bending aspects. MANOVA significance was determined by acquiring the Wilk's Lambda test statistic for actual data and 1 million data simulations over the phylogeny. Although simulations never recovered a significant p-value at α=0.05, the test for log-relaxation time was statistically significant (Approximate $F_{3,6}$=5.77, $p<0.05$) and subsequent phylogenetic univariate tests identified significantly lower relaxation times for non-sacculate species after dorsal bending (single dot comparison; $F_{1,8}$=5.16, $p<0.05$) and lateral bending (double dot comparison; $F_{1,8}$=19.21, $p<0.001$).

CHAPTER SIX: Dissertation Conclusions

Overview

At the beginning of my dissertation work, much research in the field of sexual selection was presented from the perspective that reproductive behaviors and structures evolve primarily due to the maintenance of a single mechanistic process, such as female choice (Eberhard, 1996; Kodric-Brown, 1990), good genes (Neff and Pitcher, 2005; Cameron et al., 2003), intrasexual or sexual conflict (Andersson and Simmons, 2006; Arnqvist and Rowe, 2005). More recently, we have seen a more nuanced approach to the treatment of sexual selection, particularly as sexual conflict is concerned. In 2012, Patricia L.R. Brennan and Richard O. Prum delivered a study on the limits of researching sexual conflict in the narrow sense: that is, with the expectation that conflict consists only of female attempts to avoid male-imposed mating costs. This paper played an influential role in forming my approach to the study of sexual selection mechanisms. We are now beginning to understand that the narrow “direct-benefits versus direct-harm” sense of sexual conflict may be just one mechanism among many in the evolution of reproductive diversity. Traits that originate in one context, such as non-adaptive random pleiotropy or male-male competition over females, may become useful, then maintained, in another context, such as intersexual competition or female choice (Bonduriansky, 2011; Armbruster, 2002; Berglund et al., 1996). Traits and behaviors that superficially appear to function in a threatening or coercive manner may instead be resultant of female preference for the delivery of mechanical signals/stimulation (Córdoba-Aguilar, 1999), or motor performance (Byers et al., 2010) as vigor and force production are generally honest signals of mate quality that are unlikely to be faked. In fact, taking a strict Darwinian aesthetic view of male features, traits may not have any adaptive utility at all beyond their preferred status with females (Prum, 2012).

My contributions to this discourse have been threefold. First, I have introduced a new potential model system to the field of sexual selection. The leiobunine harvestmen are a clade encapsulating many features useful for the study of sexual selection described in Andersson and Simmons (2006): diverse reproductive phenotypes, accessible genital structures with simple function, intriguing geographic distribution, and a phylogenetic tree that supports the parallel evolution of focal traits. Secondly, I have taken a novel approach to the field, implementing phylogenetic comparative methods, biomechanical, and kinetic characters to test hypotheses of character change based on varying mechanisms for sexual selection. Recent applications of comparative methods typically mention sexual selection only as a potential driver of speciation (Ng et al., 2013; Kraaijeveld et al., 2011), but investigation into the macroevolution of mating systems using a comparative species approach has not received a strong focus. Similarly, functional analysis of reproductive traits using biomechanical characteristics to enhance between-species comparability was heretofore an unknown practice, although others had called for this approach over attempts to interpret function from morphology (Garland, 2003). Lastly, the results of my dissertation work extrapolated to the field of sexual selection indicate the mutual exclusivity of selection mechanisms is unlikely—at last testing the assumptions indirectly made by other workers in the field (Berglund et al., 1996). What follows here is a summary of the chapters of my dissertation leading to this conclusion, followed by a prospectus for the future of mating system research in the leiobunine harvestmen.

Summary

My overarching goal in proposing this research project was to assess the functions of female choice and sexual conflict in the evolution of reproductive traits of the leiobunine harvestmen of eastern North America. I began this project by reconstructing the phylogeny of eastern North American leiobunine harvestmen [Chapter 2], validating several taxonomic groups first proposed by McGee (1970, 1977) and providing molecular evidence for the reassignment of others. While unsurprisingly the genus *Leiobunum* was not found to be monophyletic, my results supported the union of the leiobunine harvestmen, including the genera *Leiobunum, Hadrobunus,* and *Eumesosoma.*

Species groups within *Leiobunum* were distinguished largely by discrete reproductive morphologies in males and females. Males in the “early-season”, *Leiobunum politum,* and some *Hadrobunus* have penile nuptial gift sacs that deliver a fluid imbibed orally by the female prior to copulation. Females in these groups display no defensive armaments and termination of mating is accomplished by running away or adopting a face-down posture. However we discovered at least four species where these nuptial gift sacs were no longer present, in *Hadrobunus* species*, Leiobunum holtae,* and the *Leiobunum vittatum* and *Leiobunum calcar* species groups. In each of these species groups, females had evolved unique pregenital barriers formed by the sternal sclerite and genital operculum. This development was taken as a heuristic indicator of the effects of sexual conflict, a mechanism of sexual selection in which the fitness interests of the sexes differ with respect to mating rate, and, although character co-occurrence within species was not exactly 1:1 (two *Hadrobunus* species have females with pregenital barriers, while their males are sacculate, and one derived *vittatum* group species has non-sacculate males while females are barrier-less) parsimony supported the derived states of sac loss and barrier gain. In Chapter 3, a likelihood-based approach to compare models of binary trait change as either independent (barrier gain and sac loss occur as unique processes with separate rates) or dependent (barrier gain and sac loss occur as a concerted process). As a historical background we used a distribution of ultrametric trees that passed a topological filter based on the Bayesian likelihood tree from Chapter 2. We additionally employed stochastic character mapping to estimate the frequency and strength of correlation between male and female discrete traits for 100 replicates of each filtered tree.

Our results supported the dependent, correlated evolution of male and female morphology, although the lockstep of these changes made rate precedence of either male or female arms unclear. Under this model, male and female morphology formed reproductive syndromes, one indicative of the effects of female choice/appeasement (nuptial gift sacs), the other indicating an increase in the presence of coercion in mating (female barriers). These syndromes seemed likely particularly in view of the significant natural history and geography distinctions between species groups and the in and out-group. Non-sacculate phenotype is a purely temperate phenomenon; tropical leiobunines are all sacculate species. The most extreme non-sacculate phenotypes are additionally found among species that occur at high latitude and altitude, where breeding activity is minimized to late summer. Furthermore, many non-sacculate species overwinter as eggs and do not reach maturity until the summertime, contributing to the minimization of breeding period, whereas most sacculate species overwinter as sub-adults and mature in the early spring.

The research detailed in Chapter 3 supported the function of female choice and sexual conflict as mutually exclusive mechanisms, the effects of these shaping both morphology and mating system. However, with only two state options per sex and lacking species with useful intermediate stages, the potential for bias towards syndrome formation prompted a deeper investigation into the putative effects of female choice and sexual conflict. In Chapter 4, I used a multivariate comparative approach to assess the covariation of biomechanical traits related to male mating antagonism and female resistance, including genital muscle relative force, cuticular investment in reproductive structures, and penile resistance to bending, all features expected to increase with the strengthened effects of sexual conflict. If female choice and sexual conflict were truly mutually exclusive mechanisms, I expected to find conflict traits would have linear correlations and species with female pregenital barriers, an informational tag indicating the presence of sexual conflict at some level in the mating system, would be discriminated from species with nuptial gift sacs, identifying the presence of female choice, by their high scores upon linear combinations of these traits.

I found that biomechanical reproductive traits associated with the production, delivery, and defense/reception of large mechanical signals/coercive forces covaried within and between sexes, although significant single-variable linear correlations between male and female traits were only derived from comparisons of body size and male and female genital muscle relative force. While I found a strong correlation between combinations of male and female traits generated via canonical correlation analysis, species did not segregate into clusters based on nuptial sac or barrier presence, and discriminant analysis using both barrier and sac presence yielded several misclassified taxa, although barrier presence fared better as a grouping variable than sac presence, indicating its function as a heuristic marker of sexual conflict is justified. This indicated the presence of species intermediacy, not incorporated by a previously defined syndrome. Thus, my results support the simultaneous effects of female choice and sexual conflict in the evolution of reproductive diversity in the leiobunine harvestmen.

Results from chapter 4 underscored that while penile nuptial sac loss was correlated with female pregenital barrier presence, there was no implicit mechanical or behavioral basis for penile sac loss alone to signal the evolutionary transition of female appeasement to precopulatory antagonism. In

Chapter 5, I took a dynamic mechanical approach to understanding penile precopulatory function and evolution. I measured penile resilience, architectural stiffness, initial test resistance, and time to 90% relaxation of initial resistance as elicited through dorsal, ventral, and lateral bending in ten sacculate and non-sacculate species of *Leiobunum.* I used maximum likelihood and stochastic character mapping to fit evolutionary models of trait change and rate divergence between sacculate and non-sacculate lineages. In addition, I examined mean differences in kinetic traits between sacculate and non-sacculate species, expecting that if non-sacculate phenotype truly indicates the presence of sexual conflict, non-sacculate species will display greater penile resilience, stiffness, initial test resistance, and longer times to relaxation, as all of these traits should improve precopulatory antagonistic performance.

While in Chapter 4 I found most biomechanical traits measured in Chapter 4 had very low phylogenetic correlation, indicating other evolutionary processes may have diminished the signal of shared ancestry in the data, nearly every mechanical force traits conformed to a Brownian motion or “random-walk” model of evolution, indicating shared evolutionary history strongly predicts trait value. This may have been due to the unique ability of kinetic traits to encapsulate the effects of shape and cuticular architecture in penile bending response. However, results from phylogenetic principal components analysis and multivariate analysis of variance (MANOVA) indicated a large variance in non-sacculate species. Mean kinetic values in species of the non-sacculate *Leiobunum calcar* group were much greater than those of non-sacculates in the *L. vittatum* group.

Multivariate species scores for the *vittatum* group species were nearly indistinguishable from sacculates. These results were consistent with findings from Chapter 4 in that traits associated with precopulatory antagonism defined only a subset of non-sacculates, but this leaves a question as to the function of female pregenital barriers in a species group with non-sacculate males. Do penes and barriers have different or alternative functions in different species groups? I discuss this and hypotheses related to the ultimate causes of conflict in the following section.

Ongoing and Future Work

The successful use of a non-model organism in a broad macroevolutionary context engenders numerous follow-up questions available for on-going exploration. Primary among these inquiries is: what are the environmental and/or ecological components of the evolutionary mechanisms at play in this system? In Chapter 3, I hypothesized that summer maturation and distributions into temperate regions may play a role in decreasing breeding season, leading to an increase in selective pressure to mate with coercive strategies. Although eastern North American distribution and later maturation may not be the sole causes of mating system transition (two sacculate species, *L. aldrichi* and *L. politum,* mature in summer), the temperate phylogeography of the reproductive morphologies I have investigated should receive further study. A more precise species phenology, as well as an understanding of temporally mediated changes in mating strategy in males (i.e. whether precopulatory antagonism increases throughout the breeding season) and females (i.e. the degree to which postcopulatory choice may be enforced) will be necessary to approach these topics properly.

The chemical makeup of the nuptial gift issued from accessory glands in sacculate leiobunines is additionally unknown. There is no indication that production of this gift ceases when the sacs decrease in size and/or are lost (or, as for the sacs in *Hadrobunus grandis*, moved proximally to the base of the penis) —it does suggest, however, that availability of nuptial gift to females decreases, which implies an enhancement in the cost of gifts to the giver, with either females or larcenous males as the recipients. It is yet unclear how nuptial gift functions in non-sacculate mating. Future work could address the fitness benefits of nuptial gifts in an experimental manner as in Hall et al. (2008) by controlling delivery and volume of nuptial gift, in order to evaluate the fidelity of female mating responses, and plasticity of male mating strategies, with and without direct benefits.

Future efforts in comparative species approaches using the leiobunine harvestmen would do well to widen the phylogeny to increase the number of contrasts and tree length for identifying critical regions of trait rate shifts. *Hadrobunus* in particular has proved to be far more taxon-rich, and morphologically diverse, than previously known, and efforts are underway to describe and sequence these species (Shultz, 2012). Additional groups to incorporate in a future framework might include the Japanese *Leiobunum* of the Honshu and Hokkaido islands. Tsurusaki (1985, 1986, 2001) has described penile and pedipalpal features in males of the *curvipalpe* species group that parallel divergent features among the eastern North American leiobunines. This species group displays temperate species distribution and a form of facultative parthenogenesis, both of which may function in the origination of conflict between the sexes. Hedin et al. (2012) found that geography was better than taxonomy in uniting Sclerosomatidae, observing that relationships between Japanese and North American species suggested a boreotropic evolutionary history; thus the inclusion of additional western North American and Mesoamerican taxa could aid in forming the temporate leiobunines into a group ideal for the study of long-term mating system evolution across a phylogeographic backdrop.

Conclusions

Explaining the diversity of reproductive traits has been an enduring goal of evolutionary biologists, and over the course of my dissertation work, this research has gained theoretical momentum that experimental methods have yet to attain. I have contributed to this field, showing that gaining a better understanding of the evolutionary basis of mating system change requires a scope beyond single species studies, interpretive morphology, and individual mechanistic assumptions. The application of comparative methods has been integral to providing the historical framework upon which trait change. Efforts to increase phylogenetic contrasts and incorporate behavioral, geographic, and population-level approaches have the potential to revolutionize the field of evolutionary biology.

APPENDICES

Appendix 1

Table S2.1: Results of model fit testing by gene (MrModeltest (Nylander, 2004) and jModeltest (Posada, 2008)).

Gene	**MrModeltest Diagnosis**	**#Selections from Decision Trees**	**jModeltest Diagnosis**	**AIC (from jModeltest)**	**AIC for GTR+I+G**
ND1	GTR+I+G	4	TrN+I+G	22525.3871	22528.5274
tRNA Leu	F81+G	2 (GTR+G; 2)	N/A	N/A	N/A
16S	GTR+G	4	GTR+I+G	28142.9703	28142.9703
tRNA Val	GTR+G	2 (HKY+G; 2)	N/A	N/A	N/A
12S	GTR+G	2 (HKY+G; 2)	TIM2+I+G	8066.0820	8072.0332
28S	GTR+I+G	2 (GTR+I; 2)	TVM+G	4195.8440	4200.7477
EF1α	GTR+I+G	4	TIM2+G	7769.1907	7773.8117

Table S2.2: Bayesian posterior probabilities (BPP) and maximum likelihood (ML) bootstrap support values by node for additional analyses with models recommended by MrModeltest (Nylander, 2004) and jModelTest (Posada, 2008) (see Supplement 2.1) using concatenated data with 0 partitions and a GTR+I+G model, 3 partitions (mitochondrial DNA, 28S ribosomal DNA, and elongation factor 1 alpha) each with a GTR+I+G model, or 7 partitions, each with a GTR+I+G model.

Node	**BPP, 0 partitions**	**ML Bootstraps, no partitions**	**BPP, 3 partitions**	**ML bootstraps, 3 partitions**	**BPP, 7 partitions**	**ML bootstraps, 7 partitions**
1	.99	84	.55	79	.95	86
2	1.0	100	1.0	100	1.0	98
3	<0.5	<50	.95	<50	.64	<50
4	.99	51	1.0	67	.99	64
5	1.0	99	1.0	100	1.0	100
6	1.0	87	1.0	93	1.0	85
7	1.0	98	1.0	98	1.0	95
8	1.0	98	1.0	94	1.0	91
9	1.0	100	1.0	100	1.0	100
10	1.0	84	1.0	84	1.0	91
11	1.0	100	1.0	100	1.0	100
12	1.0	93	1.0	88	1.0	84
13	1.0	100	1.0	99	1.0	100

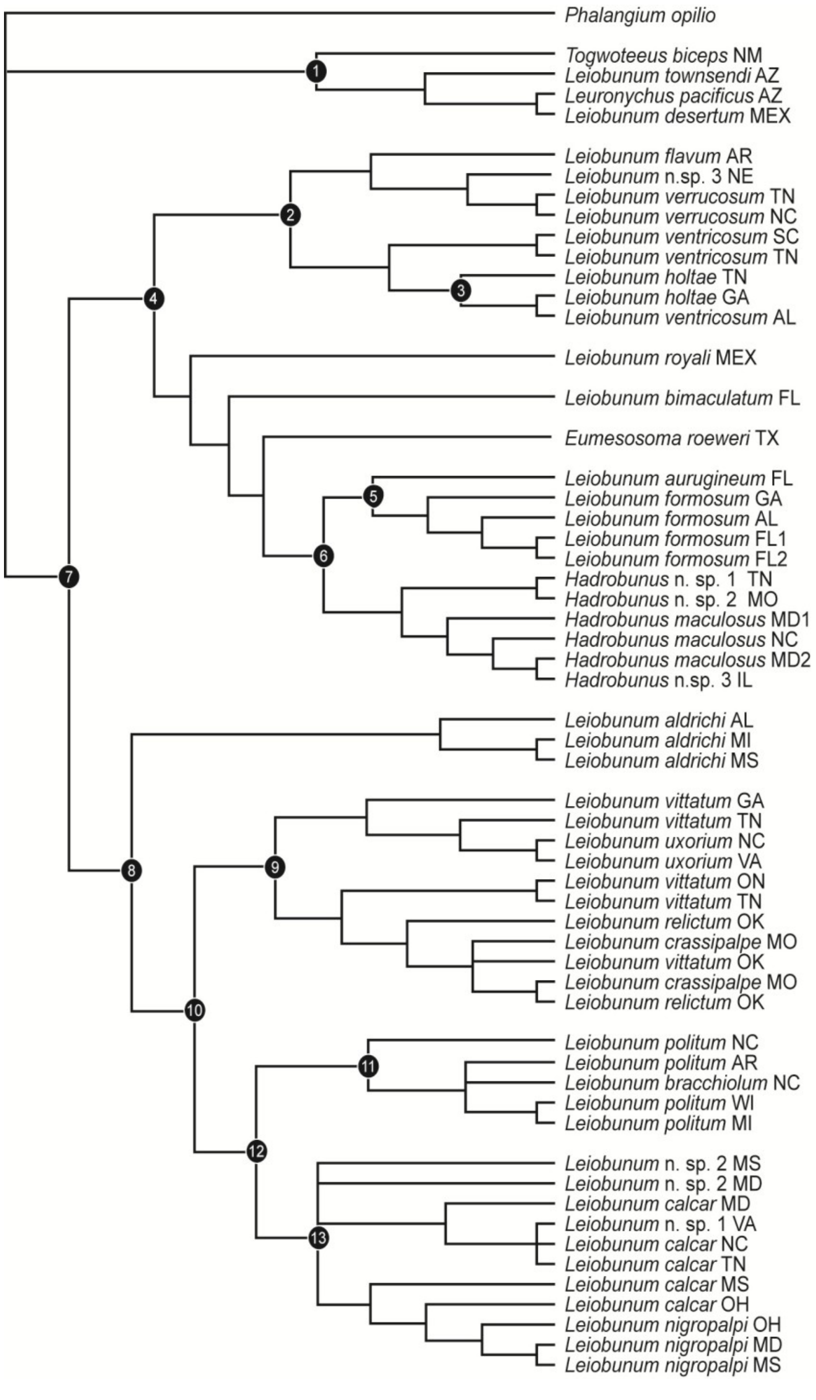

Figure S2.1: Topology with assigned nodes, corresponding to support values given in Table S2.2. Of special note are nodes that identify the major species groups reliably recovered in our analyses: Early-season group = Node 2; *Hadrobunus sp.* group = Node 6; *L. vittatum* group = Node 9; *L. politum* group = Node 11; *L. calcar* group = Node 13.

Appendix 2

Table S3.1: Taxon sampling for BEAST v1.7.1 phylogenetic reconstruction and reproductive trait evaluation. Accession numbers are for the GenBank genetic sequence repository; numbers GQ870643–GQ870668 and GQ872152–GQ872185 are derived from (Hedin et al., 2010). Columns 5 and 6 include relevant papers on species morphology (Shultz, 2008a, 2008b; McGhee, 1977, 1970) and/or numbers of male and female specimens analyzed for current study.

Species	Accession numbers	Sequence specimen locality	Morphological specimen locality	Male traits	Female traits
Eumesosoma roeweri	JQ432365, JQ432307, JQ432253	USA: TX: Wichita Co.	USA: TX: Travis Co., USA: TX: Wichita Co., USA: TX: Williamson Co.	6 specimens	5 specimens
Hadrobunus grandis	JQ432358, JQ432300, JQ432249	USA: FL: Alachua Co.	USA: FL: Alachua Co.	4 specimens; (Shultz, 2012)	5 specimens; (Shultz, 2012)
Hadrobunus n. sp. 3 IL	JQ432363, JQ432305	USA: IL: Johnson Co.	USA: IL: Johnson Co.	2 specimens	2 specimens
Hadrobunus n. sp. 1 TN	JQ432359, JQ432301, JQ432250	USA: TN: Sevier Co.	USA: TN: Blount Co., USA: WV: Monongalia Co.	6 specimens	5 specimens
Hadrobunus maculosus	JQ432360, JQ432302, JQ432361, JQ432362, JQ432303, JQ432304, JQ432251	USA: MD: Howard Co.	USA: MD: Garrett Co.	6 specimens	5 specimens
Hadrobunus n. sp. 2 MO	JQ432364, JQ432306, JQ432252	USA: MO: Ozark Co.	USA: KS: Douglas Co.	2 specimens	6 specimens
Leiobunum aldrichi	GQ870650, JQ432342, JQ432284, GQ872154, GQ870649,	USA: MI: Calhoun Co.	USA: OH: Stark Co.	5 specimens; (Shultz, 2008a)	5 specimens; (Shultz, 2008a)

	JQ432343, JQ432285, GQ872153, JQ432344, JQ432286, JQ432238				
Leiobunum bimaculatum	JQ432366, JQ432308	USA: FL: Jackson Co.	USA: VA: Nansemond Co., USA: MS: George Co., USA: GA: Toombs Co., USA: GA: Tyton Co.	2 specimens	6 specimens
Leiobunum bracchiolum	JQ432330, JQ432272, JQ432230	USA: NC: Guilford Co.	USA: MD: Frederick Co., USA: MD: Prince George's Co.	2 specimens	6 specimens
Leiobunum calcar	GQ870653, JQ432316, JQ432258, GQ872157, JQ432317, JQ432259, JQ432223, JQ432319, JQ432261, GQ870655, JQ432320, JQ432262, GQ872158, JQ432318, JQ432260	USA: MD: Frederick Co.	USA: NC: Madison Co., USA: MD: Garrett Co.	4 specimens; (Ingianni et al., 2011)	8 specimens; (Ingianni et al., 2011)
Leiobunum crassipalpe	JQ432331, JQ432273, JQ432332, JQ432274, JQ432231	USA: MO: Butler Co.	USA: MO: Butler Co.	2 specimens	5 specimens
Leiobunum euserratipalpe	JQ432321, JQ432263, GQ870656, JQ432322, JQ432264,	USA: MD: Montgomery Co.	USA: PA: Bucks Co.	5 specimens; (Ingianni et al., 2011)	7 specimens; (Ingianni et al., 2011)

	GQ872160				
Leiobunum flavum	JQ432353, JQ432295, JQ432245	USA: AR: Garland Co.	USA: AR: Garland Co.	5 specimens	3 specimens
Leiobunum formosum	JQ432354, JQ432296, JQ432356, JQ432298, JQ432247, JQ432355, JQ432297, JQ432246, JQ432357, JQ432399, JQ432248	USA: FL: Jackson Co.	USA: FL: Hernando Co., USA: VA: Dickerson Co., USA: VA: Northampton Co. , USA: FL: Liberty Co.	5 specimens	4 specimens
Leiobunum hoffmani	GQ870654, JQ432315, JQ432257, GQ872159	USA: VA: Grayson Co.	USA: VA: Grayson Co.	6 specimens; (Ingianni et al., 2011)	6 specimens; (Ingianni et al., 2011)
Leiobunum holtae	JQ432345, JQ432287, JQ432239, JQ432346, JQ432288, JQ432240	USA: TN: Cumberland Co.	USA: TN: Hamilton Co., USA: TN: Van Buren Co.	2 specimens	3 specimens
Leiobunum n. sp. 1 NE	JQ432352, JQ432294	USA: NE: Lancaster Co.	USA: NE: Lancaster Co.	5 specimens	5 specimens
Leiobunum nigropalpi	JQ432323, JQ432265, JQ432224, JQ432324, JQ432266, JQ432225, JQ432325, JQ432267, JQ432226	USA: MD: Frederick Co.	USA: MD: Garrett Co.	6 specimens; (Ingianni et al., 2011)	11 specimens; (Ingianni et al., 2011)
Leiobunum politum	JQ432326, JQ432268, JQ432227, JQ432327, JQ432269, JQ432228, JQ432328, JQ432270, JQ432229,	USA: AR: Lawrence Co.	USA: MO: Greene Co., USA: MO: Butler Co., USA: AR: Lafayette Co.	2 specimens; (McGhee, 1977)	4 specimens

	JQ432329, JQ432271				
Leiobunum potosum	JQ432370, JQ432312	MEXICO: Tlaxcala, Ixtacuixtla	MEXICO: Puebla, MEXICO: Guerrero	6 specimens	5 specimens
Leiobunum relictum	JQ432340, JQ432341, JQ432282, JQ432283, JQ432237	USA: OK: Comanche Co.	USA: OK: Comanche Co.	3 specimens	6 specimens
Leiobunum royali	JQ432367, JQ432309, JQ432254	MEXICO: Veracruz, Xalapa	MEXICO: Veracruz	5 specimens	6 specimens
Leiobunum townsendi	JQ432369, JQ432311	USA: AZ: Cochise Co.	USA: AZ: Cochise Co.	5 specimens	5 specimens
Leiobunum uxorium	JQ432339, JQ432281, JQ432235, JQ432338, JQ432280, JQ432236	USA: VA: Smythe Co.	USA: VA: King George Co., USA: PA: Lancaster Co., USA: MD: Howard Co., USA: PA: Cumberland Co.	3 specimens; (McGhee, 1977)	8 specimens
Leiobunum ventricosum	JQ432348, JQ432290, JQ432349, JQ432291, JQ432242, JQ432350, JQ432292, JQ432243	USA: TN: Blount Co.	USA: TN: Sevier Co., USA: TN: Knox Co., USA: KY: Whitley Co.	4 specimens; (McGhee, 1970)	4 specimens
Leiobunum verrucosum	JQ432351, JQ432293, JQ432244, JQ432347, JQ432289, JQ432241	USA: TN: Cumberland Co.	USA: KY: Whitley Co.	4 specimens; (Shultz, 2008b; McGhee, 1970)	5 specimens
Leiobunum vittatum	JQ432333, JQ432275, JQ432232, GQ870651, JQ432334,	USA: TN: Davidson Co.	USA: MO: Carter Co., USA: AR: Greene Co.,	5 specimens; (McGhee, 1970)	4 specimens

	JQ432276, GQ872155, JQ432335, JQ432277, JQ432233, JQ432336, JQ432278, JQ432234, GQ870652, JQ432337, JQ432279, GQ872156				
Leuronychus pacificus	JQ432368, JQ432310, JQ432253	USA: AZ: Cochise Co.	USA: AZ: Cochise Co., USA: CA: San Diego Co., USA: CA: Los Angeles Co., USA: CA: Orange Co.	4 specimens	3 specimens
Togwoteeus biceps	JQ432371, JQ432313	USA: NM: Taos Co.	USA: NV: White Pine Co., USA: NM: Taos Co.	5 specimens	2 specimens

Appendix 3

Table S4.1: Taxon sampling for molecular phylogenetic reconstruction and reproductive trait evaluation. Accession numbers are for the GenBank genetic sequence repository; numbers GQ870643–GQ870668 and GQ872152–GQ872185 are derived from Hedin et al., 2010. Columns 5 and 6 list numbers of male and female specimens analyzed for biomechanical variables, except for penile section modulus (column 7). Columns 8 and 9 indicate female pregenital barrier and penile nuptial gift sac presence, grouping variables used in testing for continuous or clustered species distributions.

Species	GenBank Accession numbers	Molecular specimen locality	Morphological specimen locality	Male morphological traits	Female morphological traits	Penile section modulus samples	Barrier present?	Penile Sacs present?
Eumesosoma roeweri	JQ432365, JQ432307, JQ432253	USA: TX: Wichita Co.	USA: TX: Travis Co., USA: TX: Wichita Co., USA: TX: Williamson Co.	6 specimens	5 specimens	3 specimens	No	Yes
Hadrobunus grandis	JQ432358, JQ432300, JQ432249	USA: FL: Alachua Co.	USA: FL: Alachua Co.	4 specimens	5 specimens	1 specimens	Yes	Yes
Hadrobunus n. sp. 3 IL	JQ432363, JQ432305	USA: IL: Johnson Co.	USA: IL: Johnson Co.	2 specimens	2 specimens	0 specimens	Yes	Yes
Hadrobunus n. sp. 1 TN	JQ432359, JQ432301, JQ432250	USA: TN: Sevier Co.	USA: TN: Blount Co., USA: WV:	6 specimens	5 specimens	4 specimens	Yes	No

			Monongalia Co.					
Hadrobunus maculosus	JQ432360, JQ432302, JQ432361, JQ432362, JQ432303, JQ432304, JQ432251	USA: MD: Howard Co.	USA: MD: Garrett Co.	6 specimens	5 specimens	5 specimens	Yes	No
Hadrobunus n. sp. 2 MO	JQ432364, JQ432306, JQ432252	USA: MO: Ozark Co.	USA: KS: Douglas Co.	2 specimens	6 specimens	3 specimens	No	Yes
Leiobunum aldrichi	GQ870650, JQ432342, JQ432284, GQ872154, GQ870649, JQ432343, JQ432285, GQ872153, JQ432344, JQ432286, JQ432238	USA: MI: Calhoun Co.	USA: OH: Stark Co.	5 specimens	5 specimens	2 specimens	No	Yes
Leiobunum	JQ432366,	USA: FL:	USA: VA:	2 specim	6 specim	2 speci	No	Yes

bimaculatum	JQ432308	Jackson Co.	Nansemond Co., USA: MS: George Co., USA: GA: Toombs Co., USA: GA: Tyton Co.	ens	ens	mens		
Leiobunu bracchiol	JQ432330, JQ432272, JQ432230	USA: NC: Guilford Co.	USA: MD: Frederick Co., USA: MD: Prince George’s Co.	2 specimens	6 specimens	2 specimens	No	Yes
Leiobunum calcar	GQ870653, JQ432316, JQ432258, GQ872157, JQ432317, JQ432259, JQ432223, JQ432319, JQ432261, GQ870655, JQ432320,	USA: MD: Frederick Co.	USA: NC: Madison Co., USA: MD: Garrett Co.	4 specimens	8 specimens	4 specimens	Yes	No

	JQ432262, GQ872158, JQ432318, JQ432260							
Leiobunum crassipalpe	JQ432331, JQ432273, JQ432332, JQ432274, JQ432231	USA: MO: Butler Co.	USA: MO: Butler Co.	2 specimens	5 specimens	2 specimens	Yes	No
Leiobunum euserratipalpe	JQ432321, JQ432263, GQ870656, JQ432322, JQ432264, GQ872160	USA: MD: Montgomery Co.	USA: PA: Bucks Co.	5 specimens	7 specimens	3 specimens	Yes	No
Leiobunum flavum	JQ432353, JQ432295, JQ432245	USA: AR: Garland Co.	USA: AR: Garland Co.	5 specimens	3 specimens	3 specimens	No	Yes
Leiobunum formosum	JQ432354, JQ432296, JQ432356, JQ432298, JQ432247,	USA: FL: Jackson Co.	USA: FL: Hernando Co., USA: VA: Dickerson Co., USA: VA:	5 specimens	4 specimens	6 specimens	Yes	No

	JQ432355, JQ432297, JQ432246, JQ432357, JQ432399, JQ432248		Northampton Co. , USA: FL: Liberty Co.					
Leiobunum hoffmani	GQ870654, JQ432315, JQ432257, GQ872159	USA: VA: Grayson Co.	USA: VA: Grayson Co.	6 specimens;	6 specimens;	3 specimens	Yes	No
Leiobunum holtae	JQ432345, JQ432287, JQ432239, JQ432346, JQ432288, JQ432240	USA: TN: Cumberland Co.	USA: TN: Hamilton Co., USA: TN: Van Buren Co.	2 specimens	3 specimens	2 specimens	Yes	No
Leiobunum n. sp. 1 NE	JQ432352, JQ432294	USA: NE: Lancaster Co.	USA: NE: Lancaster Co.	5 specimens	5 specimens	4 specimens	No	Yes
Leiobunum nigropalpi	JQ432323, JQ432265, JQ432224, JQ432324, JQ432	USA: MD: Frederick Co.	USA: MD: Garrett Co.	6 specimens	11 specimens	4 specimens	Yes	No

	266, JQ432225, JQ432325, JQ432267, JQ432226							
Leiobunum politum	JQ432326, JQ432268, JQ432227, JQ432327, JQ432269, JQ432228, JQ432328, JQ432270, JQ432229, JQ432329, JQ432271	USA: AR: Lawrence Co.	USA: MO: Greene Co., USA: MO: Butler Co., USA: AR: Lafayette Co.	2 specimens	4 specimens	1 specimen	No	Yes
Leiobunum potosum	JQ432370, JQ432312	MEXICO: Tlaxcala, Ixtacuixtla	MEXICO: Puebla, MEXICO: Guerrero	6 specimens	5 specimens	2 specimens	No	Yes
Leiobunum relictum	JQ432340, JQ432341, JQ432282, JQ432283,	USA: OK: Comanche Co.	USA: OK: Comanche Co.	3 specimens	6 specimens	2 specimens	No	No

	JQ432237							
Leiobunum royali	JQ432367, JQ432309, JQ432254	MEXICO: Veracruz, Xalapa	MEXICO: Veracruz	5 specimens	6 specimens	2 specimens	No	Yes
Leiobunum townsendi	JQ432369, JQ432311	USA: AZ: Cochise Co.	USA: AZ: Cochise Co.	5 specimens	5 specimens	2 specimens	No	Yes
Leiobunum uxorium	JQ432339, JQ432281, JQ432235, JQ432338, JQ432280, JQ432236	USA: VA: Smythe Co.	USA: VA: King George Co., USA: PA: Lancaster Co., USA: MD: Howard Co., USA: PA: Cumberland Co.	3 specimens	8 specimens	2 specimens	Yes	No
Leiobunum ventricosum	JQ432348, JQ432290, JQ432349, JQ432291, JQ432242, JQ432350, JQ432292, JQ432243	USA: TN: Blount Co.	USA: TN: Sevier Co., USA: TN: Knox Co., USA: KY: Whitley Co.	4 specimens	4 specimens	8 specimens	No	Yes

Leiobunum verrucosum	JQ432351, JQ432293, JQ432244, JQ432347, JQ432289, JQ432241	USA: TN: Cumberland Co.	USA: KY: Whitley Co.	4 specimens	5 specimens	2 specimens	No	Yes
Leiobunum vittatum	JQ432333, JQ432275, JQ432232, GQ870651, JQ432334, JQ432276, GQ872155, JQ432335, JQ432277, JQ432233, JQ432336, JQ432278, JQ432234, GQ870652, JQ432337, JQ432279, GQ872156	USA: TN: Davidson Co.	USA: MO: Carter Co., USA: AR: Greene Co.,	5 specimens	4 specimens	3 specimens	Yes	No

Leuronychus pacificus	JQ432368, JQ432310, JQ432253	USA: AZ: Cochise Co.	USA: AZ: Cochise Co., USA: CA: San Diego Co., USA: CA: Los Angeles Co., USA: CA: Orange Co.	4 specimens	3 specimens	1 specimens	No	Yes
Togwoteeus biceps	JQ432371, JQ432313	USA: NM: Taos Co.	USA: NV: White Pine Co., USA: NM: Taos Co.	5 specimens	2 specimens	1 specimens	No	Yes

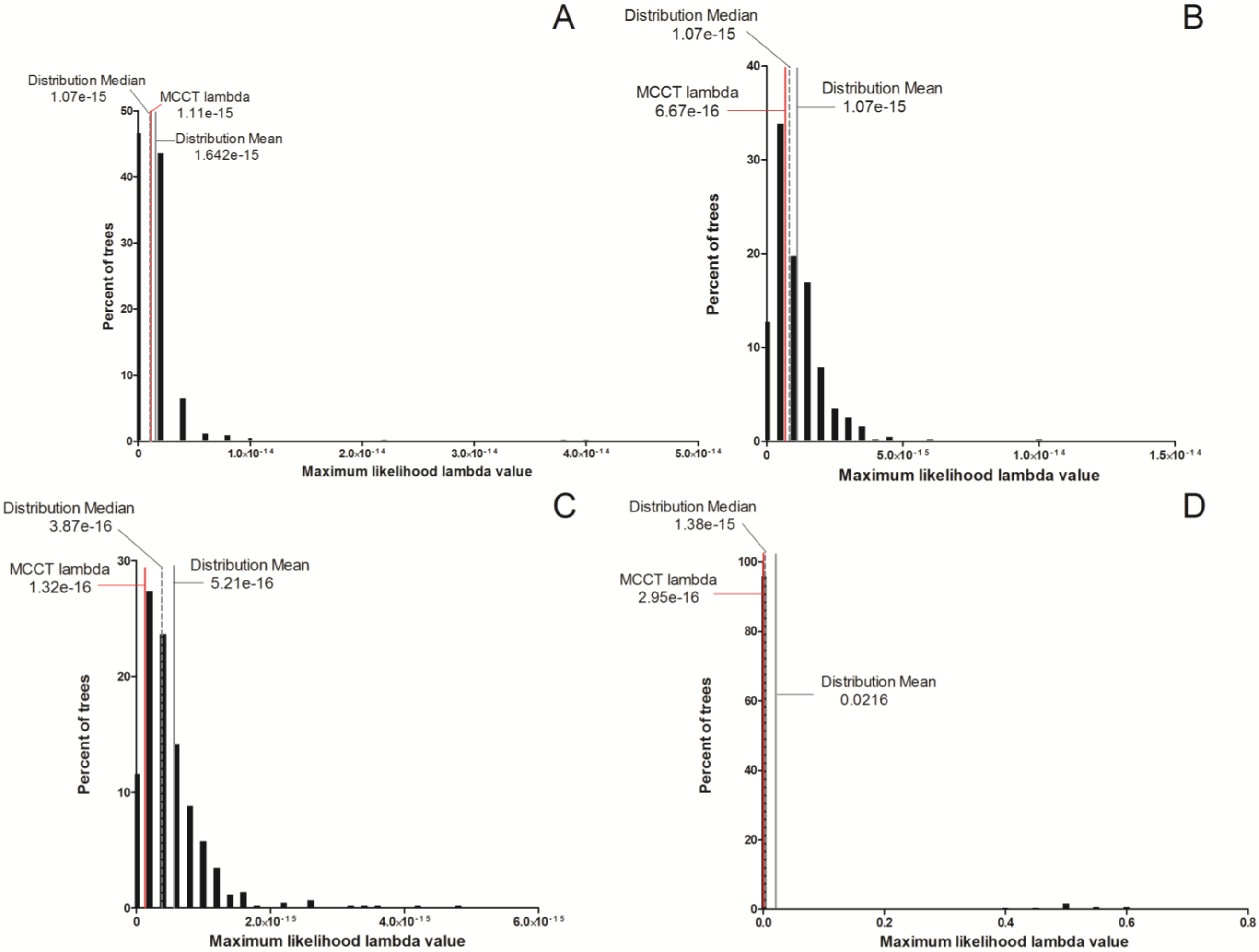

Figure S4.1: Frequency distribution of maximum likelihood estimates of lambda for filtered posterior distribution of trees (n=431). Plots are for reproductive traits where the maximum likelihood estimate of lambda from the maximum clade credibility tree (solid red line) was significantly lower than the distribution mean (solid gray line) and median (dotted gray line). A) Female body size. B) Intrinsic penile muscle relative force C) Penile cuticular mass D) Section modulus (Z_y). See Table 4.2 for values for all traits included in comparative methods.

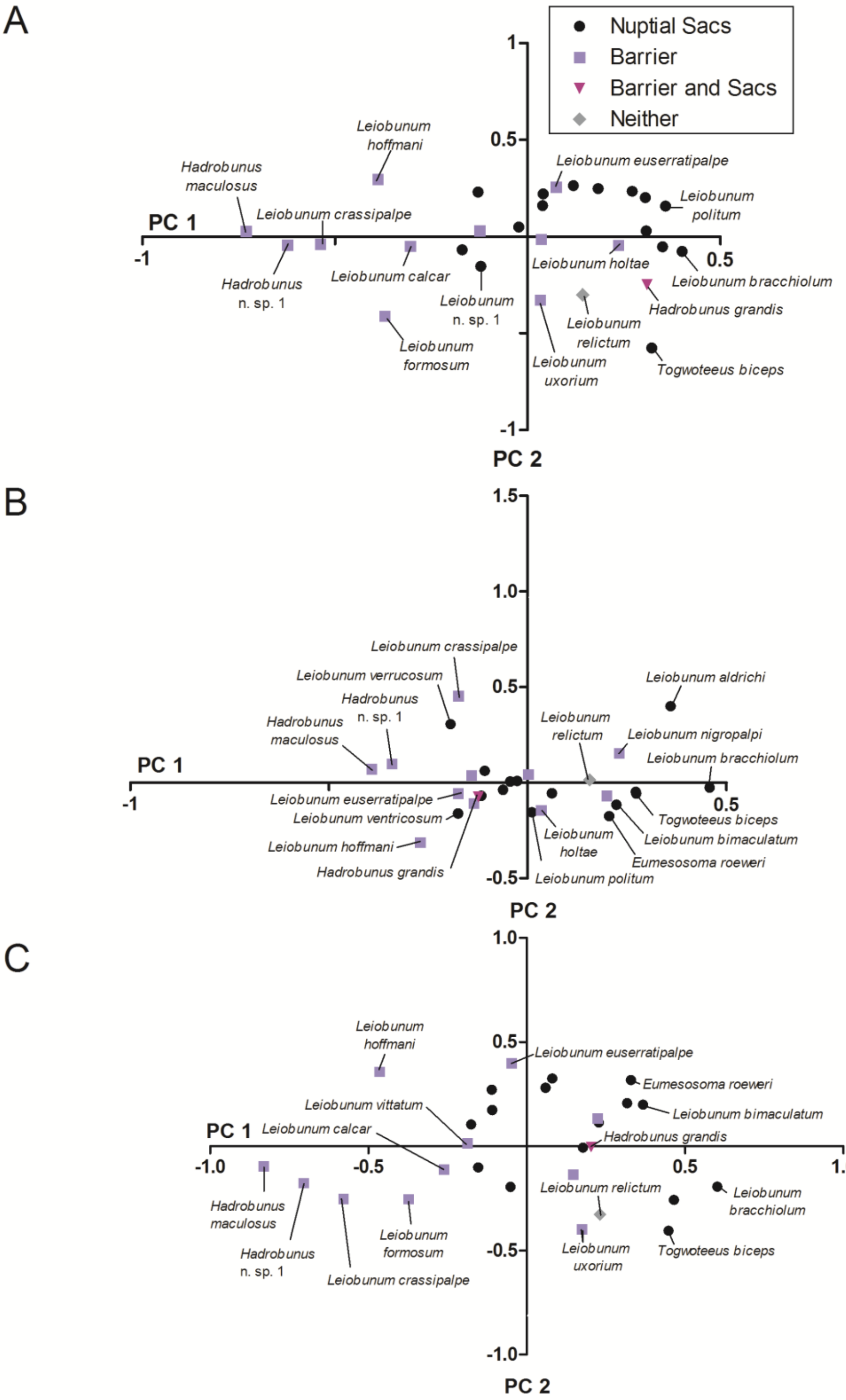

Figure S4.2: Principal components graphs without variable loading vectors. A-C) Phylogenetic principal components analyses of (A) male, (B) female, and (C) all reproductive traits. Morphological distinction was applied to each species score: either antagonistic (female pre-genital barrier present) or female enticement-based (nuptial gift sac present), and was applied to each species score. *Hadrobunus grandis*—sacculate, barrier present—was indicated with violet triangles; *Leiobunum relictum*—non-sacculate, barrier absent—was indicated in light gray diamonds.

Appendix 4

Table S5.1: Taxon sampling for molecular phylogenetic reconstruction and mechanical force trait evaluation. Accession numbers are for the GenBank genetic sequence repository; numbers GQ870643–GQ870668 and GQ872152–GQ872185 are derived from Hedin et al., 2010. Column 5: penile nuptial gift sac presence, grouping variable used in testing for rate and trait mean differences. Column 6: numbers of male specimens analyzed for mechanical force traits.

Species	GenBank Accession numbers	Molecular specimen locality	Kinetic specimen locality	Penile nuptial gift sac presence	# specimens
Leiobunum aldrichi	GQ870650, JQ432342, JQ432284, GQ872154, GQ870649, JQ432343, JQ432285, GQ872153, JQ432344, JQ432286, JQ432238	USA: MI: Calhoun Co.	USA: MD: Frederick Co.	Present	2 specimens
Leiobunum bracchiolum	JQ432330, JQ432272, JQ432230	USA: NC: Guilford Co.	USA: MD: Montgomery Co.	Present	2 specimens
Leiobunum calcar	GQ870653, JQ432316, JQ432258, GQ872157, JQ432317, JQ432259, JQ432223, JQ432319, JQ432261, GQ870655, JQ432320, JQ432262, GQ872158, JQ432318, JQ432260	USA: MD: Frederick Co.	USA: TN: Carter Co.	Absent	9 specimens
Leiobunum euserratipalpe	JQ432321, JQ432263, GQ870656,	USA: MD: Montgomery Co.	USA: MD: Frederick Co., USA:	Absent	10 specimens

	JQ432322, JQ432264, GQ872160		MD: Montgomery Co.		
Leiobunum nigropalpi	JQ432323, JQ432265, JQ432224, JQ432324, JQ432266, JQ432225, JQ432325, JQ432267, JQ432226	USA: MD: Frederick Co.	USA: MD: Montgomery Co., USA: TN: Washington Co., USA: VA: Fairfax Co.	Absent	6 specimens
Leiobunum politum	JQ432326, JQ432268, JQ432227, JQ432327, JQ432269, JQ432228, JQ432328, JQ432270, JQ432229, JQ432329, JQ432271	USA: AR: Lawrence Co.	USA: MD: Montgomery Co.	Present	6 specimens
Leiobunum uxorium	JQ432339, JQ432281, JQ432235, JQ432338, JQ432280, JQ432236	USA: VA: Smythe Co.	USA: MD: Montgomery Co.	Absent	8 specimens
Leiobunum ventricosum	JQ432348, JQ432290, JQ432349, JQ432291, JQ432242, JQ432350, JQ432292, JQ432243	USA: TN: Blount Co.	USA: TN: Washington Co.	Present	5 specimens
Leiobunum verrucosum	JQ432351, JQ432293, JQ432244, JQ432347, JQ432289, JQ432241	USA: TN: Cumberland Co.	USA: MD: Montgomery Co., USA: TN: Washington Co.	Present	3 specimens
Leiobunum vittatum	JQ432333, JQ432275, JQ432232,	USA: TN: Davidson Co.	USA: MD: Montgomery Co.	Absent	4 specimens

	GQ870651, JQ432334, JQ432276, GQ872155, JQ432335, JQ432277, JQ432233, JQ432336, JQ432278, JQ432234, GQ870652, JQ432337, JQ432279, GQ872156				

References

Akaike H (1974) A new look at the statistical model identification. *IEEE Trans Autom Contr* 19: 716-723.

Albo MJ, T Bilde, G Uhl (2013) Sperm storage mediated by cryptic female choice for nuptial gifts. *Proc R Soc B* 280: e20131735 doi:10.1098/rspb.2013.1735.

Allen CE, BJ Zwaan, PM Brakefield (2011) Evolution of sexual dimorphism in Lepidoptera. *Annu Rev Ento* 56: 445-464.

Alonzo SH, T Pizzari (2013) Selection on female remating interval is influenced by male sperm competition strategies and ejaculate characteristics. *Phil Trans R Soc B* 368: 20120044.

Alonzo SH, RR Warner (2000) Female choice, conflict between the sexes and the evolution of male alternative reproductive behaviors. *Evol Ecol Res* 2: 149–170.

Amany A, D Pasini (2009) Material and shape selection for stiff beams under non-uniform flexure. *Mat Design* 30: 1110-1117.

Andersson M, LW Simmons (2006) Sexual selection and mate choice. *Tr Ecol Evol* 21: 296-302.

Andersson M (1994) *Sexual Selection.* Princeton University Press, Princeton, NJ. 599 pp.

Armbruster WS, J Lee, AG Baldwin (2009) Macroevolutionary patterns of defense and pollination in Dalechampia vines: Adaptation, exaptation, and evolutionary novelty. *Proc Nat Acad Sci* 106: 18085–18090.

Armbruster S (2002) Can indirect selection and genetic context contribute to trait diversification? A transition-probability study of blossom-colour evolution in two genera*. J Evol Biol* 15: 468-486.

Arnqvist G, L Rowe (2005) *Sexual Conflict*. Princeton University Press, Princeton, NJ. 360 pp.

Arnqvist G, L Rowe (2002) Antagonistic coevolution between the sexes in a group of insects. *Nature* 415: 787-789.

Arnqvist G, M Edvardsson, U Friberg, T Nilsson (2000) Sexual conflict promotes speciation in insects. *Proc Nat Acad Sci USA* 97(19): 10460-10464.

Arnqvist G (1998) Comparative evidence for the evolution of genitalia by sexual selection. *Nature* 393: 784-786.

Arnqvist G (1992) Pre-copulatory fighting in a water strider: inter-sexual conflict or mate assessment? *Anim Behav* 43(4): 559-567.

Bailey NW, AJ Moore (2012) Runaway sexual selection without genetic correlations: social environments and flexible mate choice initiate and enhance the Fisher process. *Evol* 66: 2674–2684.

Barker D, M Pagel (2005) Predicting functional gene links using phylogenetic-statistical analysis of whole genomes. *PLoS Comp Biol* 1: 24-31.

Beaulieu JM, DC Jhuwueng, C Boettiger, BC O'Meara (2012) Modeling stabilizing selection: Expanding the Ornstein-Uhlenbeck model of adaptive evolution. *Evol* 66: 2369-2383.

Berglund A, A Bisazza, A Pilastro (1996) Armaments and ornaments: an evolutionary explanation of traits of dual utility. *Biol J Linn Soc* 58: 385-399.

Bergsten J, KB Miller (2007) Phylogeny of diving beetles reveals a coevolutionary arms race between the sexes. *PLoS ONE* 2(6): e522. doi: 10.1371/journal.pone.0000522.

Bertin A, DJ Fairbairn (2005) One tool, many uses: precopulatory sexual selection on genital morphology in *Aquarius remigis*. *J Evol Biol*18(4): 949-961.

Bishop SC (1949a) The Phalangida (Opiliones) of New York with special reference to the species of the Edmund Niles Huyck Preserve, Rensselaerville, New York. *Proc Rochester Acad Sci* 9, 159–235.

Bishop SC (1949b) The function of the spur on the femur of the palpus of the male, Leiobunum calcar (Wood) (Arachnida: Phalangida). *Entomol News* 60, 10–11.

Blanckenhorn WU (2000) The evolution of body size: what keeps organisms small? *Quart Rev Biol* 75: 385-407.

Blest AD, G Pomeroy (1978) The sexual behaviour and genital mechanics of three species of Mynoglenes (Araneae: Linyphiidae). *J Zool* 185: 319-340.

Blomberg SP, T Garland, AR Ives (2003) Testing for phylogenetic signal in comparative data: behavioral traits are more labile. *Evol* 57: 717-745.

Boettiger C, G Coop, P Ralph (2011) Is your phylogeny informative? Measuring the power of comparative methods. *Nat Prot* 6: 46-55.

Boggs CL (1995) Male nuptial gifts: phenotypic consequences and evolutionary implications. In: Leather SR, Hardie J, editors. *Insect Reproduction*. Boca Raton: CRC Press. pp. 215–242.

Bollback JP (2006) SIMMAP: Stochastic character mapping of discrete traits on phylogenies. *BMC Bioinf* 7: 88.

Bond JE, DA Beamer, MC Hedin, P Sierwald (2003) Gradual evolution in male genitalia in a sibling species complex of millipedes (Diplopoda: Spirobolida: Rhinocricidae: *Anadeobolus*). *Invert Syst* 17: 711-717.

Bonduriansky R (2011) Sexual selection and conflict as engines of ecological diversification. *Am Nat* 178: 729-745.

Bonduriansky R, SF Chenoweth (2008) Intralocus sexual conflict. *Tr Ecol Evol* 24(5): 280-288.

Boughman JW (2002) How sensory drive can promote speciation. *Tr Eco Evol* 17: 571–577.

Brennan PLR, RO Prum (2012) The limits of sexual conflict in the narrow sense: new insights from waterfowl biology. *Phil Trans R Soc B* 367: 2324-2338.

Brennan PL, RO Prum, KG McCracken, MD Sorenson, RE Wilson, et al. (2007) Coevolution of Male and Female Genital Morphology in Waterfowl. *PLoS ONE* 2(5): e418. doi: 10.1371/journal.pone.0000418.

Burnham KP, DR Anderson (2004) Multimodal inference: Understanding AIC and BIC in model selection. *Sociol Meth Res* 33: 261-304.

Burns MM, M Hedin, JW Shultz (2013) Comparative analyses of reproductive structures in harvestmen (Opiliones) reveal multiple transitions from courtship to precopulatory antagonism. *PLoS ONE* 8(6): e66767. doi:10.1371/journal.pone.0066767.

Burns MM, M Hedin, JW Shultz (2012) Molecular phylogeny of the leiobunine harvestmen of eastern North America (Opiliones: Sclerosomatidae: Leiobuninae). *Mol Phylo Evol* 63: 291–298.

Byers J, E Hebets, J Podos (2010) Female mate choice based upon male motor performance. *Anim Behav* 79: 771-778.

Calsbeek R, B Sinervo (2002) Uncoupling direct and indirect components of female choice in the wild. *Proc Nat Acad Sci* 99: 14897–14902, doi: 10.1073/pnas.242645199.

Cameron E, T Day, L Rowe (2003) Sexual conflict and indirect benefits. *J Evol Biol* 16: 1055-1060.

Cayetano L, AA Maklakov, RC Brooks, R Bonduriansky (2011) Evolution of male and female genitalia following release from sexual selection. *Evol* 65: 2171-2183.

Chamay A (1970) Mechanical and morphological aspects of experimental overload and fatigue in bone. *J Biom* 3: 263-264.

Chapman T (2010) Sexual conflict and sex allocation. *Biol Lett* 5(5): 660-662.

Chapman T (2006) Evolutionary conflicts of interest between males and females. *Curr Biol* 16: R744–R754.

Chapman T, G Arnqvist, J Bangham, L Rowe (2003) Sexual conflict. *Tr Ecol Evol* 18(1): 41-47.

Cheverud JM, M Dow, W Leutenegger (1985) The quantitative assessment of phylogenetic constraints in comparative analyses: sexual dimorphism in body weight among primates. *Evol* 39:1335-1351.

Coddington JA, SF Larcher, JC Cokendolpher (1990) The systematic status of Arachnida, exclusive of Acari, in North America north of Mexico, pp. 5-20. In: *Systematics of the North American Insects and Arachnids: Status and Needs*, M Kosztarab, CW Schaefer, eds. Virginia Agricultural Experiment Station Information Series 90-1. Virginia Polytechnic Institute & State University: Blacksburg VA.

Cokendolpher JC (1980) Replacement name for Mesosoma Weed, 1892, with a revision of the genus (Opiliones, Phalangiidae, Leiobuninae). *Occas Pap Mus Texas Tech Univ* 66, 1–19.

Cokendolpher JC (1981) Status of Leiobunum serratipalpe Roewer (Opiliones, Leiobunuidae). *J Arachnol* 9, 112–113.

Cokendolpher JC, VF Lee (1993) *Catalogue of the Cyphopalpatores and Bibliography of the Harvestmen (Arachnida, Opiliones) of Greenland, Canada, USA, and Mexico.* Vintage Press, Lubbock, TX.

Cooper N, W Jetz, RP Freckleton (2010) Phylogenetic comparative approaches for studying niche conservatism. *J Evol Biol* 23: 2529–2539.

Córdoba-Aguilar A (1999) Male copulatory sensory stimulation induces female ejection of rival sperm in a damselfly. *Proc R Soc B* 22: 779-784.

Cordero C, WG Eberhard (2003) Female choice of antagonistic male traits: a critical review of some current research. *J Evol Biol* 16: 1-6.

Cornwallis CK, T Uller (2010) Towards an evolutionary ecology of sexual traits. *Tr Ecol Evol* 25(3): 145-152.

Cosentino CC, BL Roman, IA Drummond, NA Hukriede (2010) Intravenous Microinjections of Zebrafish Larvae to Study Acute Kidney Injury. *J Vis Exp* 42: e2079. doi:10.3791/2079.

Cothran RD (2004) Precopulatory mate guarding affects predation risk in two freshwater amphipod species. *Anim Behav* 68: 1133–1138.

Crosby CR, SC Bishop (1924) Notes on the Opiliones of the southeastern United States with descriptions of new species. *J Elisha Mitchell Sci Soc* 40, 8–26.

Curtis DJ, G Machado (2007) Ecology. In: Pinto-da-Rocha R, Machado G, Giribet G, editors. *Harvestmen: The Biology of Opiliones*. Cambridge: Harvard University Press. pp. 280-309.

Daly M, M Wilson (1983) *Sex, Evolution, and Behavior.* Wadsworth Publishing Company, Belmont, CA.

Darwin C (1871) *The Descent of Man and Selection in Relation to Sex*. J. Murray, London, UK.

Davidovits P (2008) Chapter 1. *Physics in Biology and Medicine, Third edition*. Academic Press. p. 10.

Davis NM (1934) A revision of the genus *Leiobunum* (Opiliones) of the United States. *Am Midl Nat* 15:662-705.

De Villemereuil P, JA Wells, RD Edwards, SP Blomberg (2012) Bayesian models for comparative analysis integrating phylogenetic uncertainty. *BMC Evol Biol* 12: 102.

Drummond AJ, MA Suchard, D Xie, A Rambaut (2012) Bayesian phylogenetics with BEAUti and the BEAST 1.7. *Mol Biol Evol* 29: 1969-1973.

Drummond AJ, A Rambaut (2007) BEAST: Bayesian evolutionary analysis by sampling trees**.** *BMC Evol Biol* 7**:** 8.

Drummond AJ, SYW Ho, MJ Phillips, A Rambaut (2006) Relaxed phylogenetics and dating with confidence. *PLoS Biol* 4: e88.

Eberhard WG (2010) Evolution of genitalia: theories, evidence, and new directions. *Genetica* 138: 5-18.

Eberhard WG (2004a) Rapid divergent evolution of sexual morphology: comparative tests of antagonistic coevolution and traditional female choice. *Evol* 58: 1947-1970.

Eberhard WG (2004b) Male-female conflict and genitalia: failure to confirm predictions in insects and spiders. *Biol Rev* 79: 121-186.

Eberhard WG, C Cordero (2003) Female choice of sexually antagonistic male adaptations: a critical review of some current research. *J Evol Biol*16: 1-6.

Eberhard WG (1996) Female control: sexual selection by cryptic female choice. Princeton: Princeton University Press. pp. 472.

Eberhard WG (1993) Copulatory courtship and genital mechanics of three species of *Macrodactylus* (Coleoptera Scarabaeidae Melolonthinae). *Ethol Ecol Evol* 5: 19-63.

Eberhard WG (1985) *Sexual Selection and Animal Genitalia.* Harvard University Press, Cambridge, MA and London, England.

Edgar AL (1966) Phalangida of the great lakes region. *Am Midl Nat* 75, 347–366.

Eldakar OT, DS Wilson, MJ Dlugos, JW Pepper (2010) The role of multilevel selection in the evolution of sexual conflict in the water strider *Aquarius remigis. Evol* 64: 3183-3189.

Emlen DJ (2001) Costs and the diversification of exaggerated animal structures. *Science* 291: 1534–1536.

Fedorka KM, TA Mousseau (2004) Female mating bias results in conflicting sex-specific offspring fitness. *Nature* 42: 65-67.

Felsenstein J (2012) A comparative method for both discrete and continuous characters using the threshold model. *Am Nat* 179: 145–159.

Felsenstein J (2004) Variants of parsimony. In: Felsenstein J. *Inferring Phylogenies*. Sunderland: Sinauer Associates, Inc. pp. 73–84.

Felsenstein J (1985) Phylogenies and the Comparative Method. *Am Nat* 125(1): 1-15.

Foerster K, T Coulson, BC Sheldon, JM Pemberton, TH Clutton-Brock et al. (2006) Sexually antagonistic genetic variation for fitness in red deer. *Nature* 447: 1107-1110.

Friberg U, TA Lew, PG Byrne, WR Rice (2005) Assessing the potential for an ongoing arms race within and between the sexes: selection and heritable variation. *Evol* 59: 1540–1551.

Fricke C, J Perry, T Chapman, L Rowe (2009.) The conditional economics of sexual conflict. *Biol Lett* 5(5): 671-674.

Gage MJG (2012) Complex sperm evolution. *Proc Nat Acad Sci* 109: 4341–4342.

Gage, MJG (2004) Evolution: sexual arms races. *Curr Biol* 14: R378–R380.

Garland T, AF Bennett, EL Rezende (2005) Phylogenetic approaches in comparative physiology. *J Exp Biol* 208: 3015-3035.

Garland T (2003) Chapter 3: Selection experiments: an under-utilized tool in biomechanics and organismal biology. In: VL Bels, JP Gasc, A Casino, eds. *Vertebrate Biomechanics and Evolution*. Oxford: BIOS Scientific Publishers Ltd. pp.23-56.

Garland T, AW Dickerman, CM Janis, JA Jones (1993) Phylogenetic analysis of covariance by computer simulation. *Syst Biol* 42: 265-292.

Gasparini C, A Devigili, A Pilastro (2011) Cross generational effects of sexual harassment on female fitness in the guppy. *Evol* 66: 532–543.

Gavrilets S, TI Hayashi (2005) Speciation and sexual conflict. *Evol Ecol* 19: 167-198.

Gavrilets S (2000) Rapid evolution of reproductive barriers driven by sexual conflict. *Nature* 403: 886-889.

Gay L, E Brown, T Tregenza, D Pincheira-Donoso, PE Eady et al. (2011) The genetic architecture of sexual conflict: male harm and female resistance in *Callosobruchus maculatus*. *J Evol Biol* 24: 449-456.

Goloboff PA, JS Farris, KC Nixon (2008) TNT, a free program for phylogenetic analysis. *Cladistics* 24, 774–786.

González C, J Llorca (2005) Stiffness of a curved beam subjected to axial load and large displacements. *Int J Sol Struct* 42: 1537-1545.

Gwynne DT (2008) Sexual conflict over nuptial gifts in insects. *Annu Rev Entomol* 53: 83–101.

Hall MD, LF Bussière, J Hunt, R Brooks (2008) Experimental evidence that sexual conflict influences the opportunity, form, and intensity of sexual selection. *Evol* 62: 2305-2315.

Hall TA (1999) BioEdit: a user-friendly biological sequence alignment editor and analysis program for Windows 95/98/NT. *Nucl Acids Symp Ser* 41, 95–98.

Harvey PH, MD Pagel (1991) *The Comparative Method in Evolutionary Biology.* Oxford University Press, New York, NY.

Harmon LJ, JT Weir, CD Brock, RE Glor, W Challenger (2008) GEIGER: investigating evolutionary radiations. *Bioinformatics* 24:129-131.

Head ML, J Hunt, MD Jennions, R Brooks (2005) The Indirect Benefits of Mating with Attractive Males Outweigh the Direct Costs. *PLoS Biol* 3(2): e33. doi: 10.1371/journal.pbio.0030033

Hedin M, N Tsurusaki, R Macías-Ordóñez, JW Shultz (2012) Molecular systematics of sclerosomatid harvestmen (Opiliones, Phalangioidea, Sclerosomatidae): geography is better than taxonomy in predicting phylogeny. *Mol Phylo Evol* 62: 224–236.

Hedin M, S Derkarabetian, M McCormack, C Richart, JW Shultz (2010) The phylogenetic utility of the nuclear protein-coding gene EF-1a for resolving recent divergences in Opiliones, emphasizing intron evolution. *J Arachnol* 38: 9-20.

Hendry CR, TJ Guiher, RA Pyron (2014) Ecological divergence and sexual selection drive sexual size dimorphism in new world pitvipers (Serpentes: Viperidae). *J Evol Biol* 27: 760–771. doi: 10.1111/jeb.12349.

Hone DWE, MJ Benton (2005) The evolution of large size: how does Cope's Rule work? *Tr Ecol Evol* 20: 4-6.

Hosken DJ, P Stockley (2004) Sexual selection and genital evolution. *Tr Ecol Evol* 19: 87-93.

Huber BA (1993) Genital mechanics and sexual selection in the spider *Nesticus cellulanus* (Araneae: Nesticidae). *Can J Zool* 71: 2437-2447.

Huber BA (2003) Rapid evolution and species-specificity of arthropod genitalia: fact or artifact? *Org Divers Evol* 3: 63-71.

Huber BA, WG Eberhard (1997) Courtship, copulation, and genital mechanics in *Physocyclus globosus* (Aranaeae, Pholcidae). *Can J Zool* 75: 905-918.

Huelsenbeck JP, R Nielsen, JP Bollback (2003) Stochastic mapping of morphological characters. *Syst Biol* 52: 131–158.

Huelsenbeck JP, F Ronquist (2001) MRBAYES: Bayesian inference of phylogeny. *Bioinformatics* 17: 754–755.

Huelsenbeck JP, JP Bollback (2001) Empirical and hierarchical Bayesian estimation of ancestral states. *Syst Biol* 50: 351–366.

Huelsenbeck JP, B Rannala, JP Masly (2000) Accomodating phylogenetic uncertainty in evolutionary studies. *Science* 288: 2349-2350.

Huk T, W Winkel (2008) Testing the sexy son hypothesis—a research framework for empirical approaches. *Behav Ecol* 19: 456–461.

Hunt G, K Roy (2006) Climate change, body size evolution, and Cope's Rule in deep-sea ostracodes. *Proc Nat Acad Sci* 103: 1347-1352.

Ingianni E, CR McGhee, JW Shultz (2011) Taxonomy of the Leiobunum calcar species-group (Opiliones, Sclerosomatidae, Leiobuninae). *J Arachnol* 39: 454–481.

Jagadeeshan S, RS Singh (2006) A time-sequence functional analysis of mating behavior and genital coupling in *Drosophila*: role of cryptic female choice and male sex-drive in the evolution of male genitalia. *J Evol Biol* 19: 1058-1070.

Jeffreys H (1961) The Theory of Probability. New York: Oxford University Press. pp. 432.

Klingenberg CP, J Marugán-Lobón (2013) Evolutionary covariation in geometric morphometric data: analyzing integration, modularity, and allometry in a phylogenetic context. *Syst Biol* 62: 591-610.

Kodric-Brown A (1990) Mechanisms of sexual selection: insights from fishes. *Ann Zool Fennici* 27: 87-100.

Koene JM, H Schulenburg (2005) Shooting darts: co-evolution and counter-adaptation in hermaphroditic snails. *BMC Evol Biol* 5(25): 1-13.

Kokko H, R Brooks, MD Jennions, J Morley (2003) The evolution of mate choice and mating biases. *Proc R Soc Lond B* 270: 653-664.

Kraaijeveld K, FJL Kraaijeveld-Smit, ME Maan (2011) Sexual selection and speciation: the comparative evidence revisited. *Biol Rev* 86: 367-377.

Krivickas LS, DJ Dorer, J Ochala, WR Frontera (2011) Relationship between force and size in human single muscle fibres. *Exper Physiol* 96: 539-547.

Lakes RS (2009) *Viscoelastic Materials.* Cambridge: Cambridge University Press, pp. 457.

Larkin MA, G Blackshields, NP Brown, R Chenna, PA McGettigan et al. (2007) Clustal W and Clustal X version 2.0. *Bioinf* 23: 2947-2948.

Leonard JL (2010) Introduction: Celebrating and Understanding Reproductive Diversity. In: Leonard J, A Córdoba-Aguilar (eds.) *The Evolution of Primary Sexual Characters in Animals.* Oxford University Press, pp.1-8.

Lewis SM, CK Cratsley, JA Rooney (2004) Nuptial gifts and sexual selection in Photinus fireflies. *Integr Comp Biol* 44: 234–237.

Losos JB, RE Glor (2003) Phylogenetic comparative methods and the geography of speciation. *Tr Eco Evol* 18: 220–227.

Löytynoja A, MC Milinkovitch (2003) A hidden Markov model for progressive multiple alignment. *Bioinformatics* 19**:**1505–1513.

Macdonald AJ (2001) Appendix 2: Stress and Strain. In: *Structure and Architecture.* Reed Educational and Professional Publishing Ltd., pp. 134-139.

Machado G, R Macías-Ordóñez (2007) Reproduction. In: Pinto-da-Rocha R, G Machado, G Giribet (eds.). *Harvestmen: The Biology of Opiliones.* Cambridge: Harvard University Press. pp. 414–454.

Macías-Ordóñez R, G Machado, A Pérez-González, JW Shultz (2010) Genitalic evolution in Opiliones. In: Leonard J, A Córdoba-Aguilar, (eds.). *The Evolution of Primary Sexual Characters in Animals.* Oxford University Press. pp. 285–306.

Maddison WP, DR Maddison (2011) Mesquite: a modular system for evolutionary analysis. Version 2.75 http://mesquiteproject.org.

Maklakov AA, G Arnqvist (2009) Testing for direct and indirect effects of mate choice by manipulating female choosiness. *Curr Biol* 19: 1903–1906.

Maklakov AA, T Bilde, Y Lubin (2005) Sexual conflict in the wild: elevated mating rate reduces female lifetime reproductive success. *Amer Nat* 165: 38–45.

Martins EP, TF Hansen (1997) Phylogenies and the comparative method: a general approach to incorporating phylogenetic information into the analysis of interspecific data. *Amer Nat* 149:646-667.

Masly JP (2012) 170 years of ‘‘lock-and-key’’: genital morphology and reproductive isolation. *Int J Evol Biol* DOI: 10.1155/2012/247352.

Mayr E (1963) Animal Species and Evolution. Cambridge: Harvard University Press.pp. 811.

McGhee CR (1977) The politum group (bulbate species) of Leiobunum (Arachnida: Phalangida: Phalangidae) of North America*. J Arachnol* 3: 151–163.

McGhee CR (1970) The Sacculate and Lanceolate Groups of the Genus Leiobunum (Arachnida: Phalangida, Phalangiidae) in the Eastern United States. Ph.D. Dissertation. Blacksburg, Virginia Polytechnic Institute and State University. pp. 186.

McGill BJ, JS Brown (2007) Evolutionary game theory and adaptive dynamics of continuous traits. *Ann Rev Ecol Evol Sys* 38: 403-435.

McLachlan G (2004) Discriminant analysis and statistical pattern recognition. Hoboken: John Wiley and Sons. pp. 447.

Muller MN, SM Kahlenberg, ME Thompson, RW Wrangham (2007) Male coercion and the costs of promiscuous mating for female chimpanzees. *Proc R Soc B* 274: 1009–1014.

Nandy B, V Gupta, N Udaykumar, MA Samant, S Sen, NG Prasan (2014) Experimental evolution of female traits under different levels of intersexual conflict in *Drosophila melanogaster. Evol* 68: 412-425.

Neff BD, TE Pitcher (2005) Genetic quality and sexual selection: an integrated framework for good genes and compatible genes. *Mol Ecol* 14: 19-38.

Newton MA, AE Raftery (1994) Approximate Bayesian inference with the weighted likelihood bootstrap. *J Roy Stat Soc B* 56: 3–48.

Ng J, EL Landeen, RM Logsdon, RE Glor (2013) Correlation between *Anolis* lizard dewlap phenotype and environmental variation indicates adaptive divergence of a signal important to sexual selection and species recognition. *Evol* 67: 573-582.

Nylander JA (2004) MrModeltest v2. Program distributed by the author. Evolutionary Biology Centre, Uppsala University. http://www.abc.se/~nylander/mrmodeltest2/mrmodeltest2.html

O'Meara BC, C Ané, MJ Sanderson, PC Wainwright (2006) Testing for different rates of continuous trait evolution using likelihood. *Evol* 60: 922-933.

Pagel M, A Meade (2006) Bayesian analysis of correlated evolution of discrete characters by reversible-jump Markov chain Monte Carlo. *Amer Nat* 167: 808–825.

Pagel M, A Meade (2004) A Phylogenetic Mixture Model for Detecting Pattern-Heterogeneity in Gene Sequence or Character-State Data. *Syst Biol* 53: 571-581.

Pagel M, A Meade, D Barker (2004) Bayesian estimation of ancestral character states on phylogenies. *Syst Biol* 53: 673–684.

Pagel M (1999) Inferring the historical pattern of biological evolution. *Nature* 401:877-884.

Pagel M (1997) Inferring evolutionary processes from phylogenies. *Zoo Scripta 26*: 331-348.

Pagel M (1994) Detecting correlated evolution on phylogenies: a general method for the comparative analysis of discrete characters. *Proc R Soc Lond B* 255: 37–45.

Paradis E (2006) *Analysis of Phylogenetics and Evolution with R.* Use R! series. Springer, New York, NY. 386 pp.

Paradis E, J Claude, K Strimmer (2004) APE: analyses of phylogenetics and evolution in R language. *Bioinformatics* 20: 289–290.

Parker GA, CM Lessells, LW Simmons (2013) Sperm competition games: a general model for precopulatory male-male competition. *Evol* 67: 95-109.

Parker GA (2006) Sexual conflict over mating and fertilization: an overview. *Phil Trans R Soc B* 361: 235-259.

Parker GA (1979) Sexual selection and sexual conflict. In: Blum MS, Blum NA (eds.). *Sexual selection and reproductive competition in insects*. Academic Press, New York, NY. pp. 123–166.

PischeddaA, AK Chippindale (2006) Intralocus sexual conflict diminishes the benefits of sexual selection. *PLoS Biol* 4(11): 2099-2103.

Pomiankowski A, Y Iwasa (1998) Runaway ornament diversity caused by Fisherian sexual selection. *Proc Nat Acad Sci* 95: 5106–5111.

Posada D (2008) jModelTest: Phylogenetic Model Averaging. *Mol Biol Evol* 25: 1253-1256.

Pizzari T, RS Snook (2003) Perspective: Sexual conflict and sexual selection: Chasing away paradigm shifts. *Evol* 57(6): 1223-1236.

Prum RO (2012) Aesthetic evolution by mate choice: Darwin's *really* dangerous idea. *Phil Trans R Soc B* 367: 2253-2265.

R Development Core Team (2013) R: A language and environment for statistical computing. R Foundation for Statistical Computing. Vienna, Austria. ISBN 3-900051-07-0. Available: http://www.R-project.org.Accessed 2013 May 15.

Raftery AE, MA Newton, JM Satagopan, P Krivitsky (2007) Estimating the Integrated Likelihood via Posterior Simulation Using the Harmonic Mean Identity (with Discussion). In: Bernardo JM, ed. *Bayesian Statistics 8*. Oxford University Press, New York, NY. pp. 1–45.

Rambaut A (2009) FigTree v. 1.3.1. Molecular Evolution, Phylogenetics, and Epidemiology. Available: http://tree.bio.ed.ac.uk/software/figtree/. Accessed 2013 November 15.

Rambaut A, AJ Drummond (2007) Tracer v. 1.5. Molecular Evolution, Phylogenetics, and Epidemiology. Available: http://beast.bio.ed.ac.uk/ Tracer.Accessed 2013 May 15.

Rasband WS (2012) ImageJ, U. S. National Institutes of Health, Bethesda, Maryland, USA, http://imagej.nih.gov/ij/. Accessed 2014 March 16.

Reinhold K (2004) Modeling a version of the good-genes hypothesis: female choice of locally adapted males. *Org Div Evol* 4: 157–163.

Revell LJ (2012) phytools: An R package for phylogenetic comparative biology (and other things). *Methods Ecol Evol* 3: 217-223. doi:10.1111/j.2041-210X.2011.00169.x

Revell LJ (2009a) Size-correction and principal components for interspecific comparative studies. *Evol* 63: 3258-3268.

Revell LJ (2009b) Phylogenetic signal and linear regression on species data. *Meth Ecol Evol* 1: 319-329.

Revell LJ, AS Harrison (2008) PCCA: A program for phylogenetic canonical correlation analysis. *Bioinf* 24: 1018-1020.

Revell LJ, LJ Harmon, DC Collar (2008) Phylogenetic signal, evolutionary process, and rate. *Sys Biol* 57(4): 591-601.

Rice WR, AD Stewart, EH Morrow, JE Linder, N Orteiza et al. (2006) Assessing sexual conflict in the *Drosophila melanogaster* laboratory model system. *Phil Trans Roy Soc B* 361(1466): 287-299.

Rönn J, M Katvala, G Arnqvist (2007) Coevolution between harmful male genitalia and female resistance in seed beetles. *Proc Nat Acad Sci USA* 104(10): 921-925.

Roewer CF (1923) *Die Weberknechte der Erde, Systematische Bearbietung de bisher bekannten Opiliones.* Gustav Fischer, Jena.

Ronquist F, JP Huelsenbeck (2003) MRBAYES 3: Bayesian phylogenetic inference under mixed models. *Bioinf* 19:1572-1574.

Rowe L, G Arnqvist (2012) Sexual selection and the evolution of genital shape and complexity in water striders. *Evol* 66: 40-54.

Sánchez V, BE Hernández-Baños, C Cordero (2011) The Evolution of a Female Genital Trait Widely Distributed in the Lepidoptera: Comparative Evidence for an Effect of Sexual Coevolution. *PLoS ONE* 6(8): e22642. doi: 10.1371/journal.pone.0022642.

Sakaluk SK, PJ Bangert, A Eggert, C Gack, LV Swanson (1995) The gin trap as a device facilitating coercive mating in sagebrush crickets. *Proc R Soc Lond B* 261: 65-71.

Schmitz L, R Motani (2011) Nocturnality in dinosaurs inferred from scleral ring and orbit morphology. *Science* 332: 705-708.

Schultz TR, GA Churchill (1999) The role of subjectivity in reconstructing ancestral character states: A Bayesian approach to unknown rates, states, and transformation asymmetries. *Syst Biol* 48: 651–664.

Shapiro AM, AH Porter (1989) The lock-and-key hypothesis: evolutionary and biosystematic interpretation of insect genitalia. *Annu Rev Entomol* 34: 231–245.

Shultz JW (2012) The identity of *Hadrobunus grandis*: reassignment of *Leiobunum aurugineum* to *H. grandis* and *H. nonsacculatus* new species (Opiliones: Sclerosomatidae: Leiobuninae). *J Arachnol* 40: 269-303.

Shultz JW (2010) A new species of Hadrobunus (Opiliones: Sclerosomatidae: Leiobuninae) from the southeastern United States. *J Arachnol* 38, 572–580.

Shultz JW (2008a) Skeletomuscular anatomy of the harvestmen Leiobunum aldrichi (Weed, 1893) (Arachnida: Opiliones: Palpatores) and its evolutionary significance. *Zool J Linnean Soc* 128: 401–438.

Shultz JW (2008b) Leiobunum nigripes is a junior synonym of Leiobunum verrucosum (Opiliones, Sclerosomatidae). *J Arachnol* 36: 184–186.

Shultz JW (2005) Preliminary analysis of mating in Leiobunum nigripes (Opiliones) and diversification of male reproductive structures in Leiobunum. *Am Arachnol* 72:11.

Shultz JW (2000) Skeletomuscular anatomy of the harvestman *Leiobunum aldrichi* (Weed, 1893) (Arachnida: Opiliones) and its evolutionary significance. *Zool J Linn Soc* 128: 401–438.

Simmons LW (2014) Sexual selection and genital evolution. *Austral Entomol* 53: 1-17.

Simmons LW (2001) Sperm competition and its evolutionary consequences in the insects. Princeton University Press, Princeton, NJ. pp. 448.

Siva-Jothy MT (2006) Trauma, disease and collateral damage: conflict in cimicids*. Philos Trans R Soc Lond B* 361: 269–275.

Snook RR (2005) Sperm in competition: not playing by the numbers. *Tr Ecol* Evol 20: 46–53.

Song H, SR Bucheli (2010) Comparison of phylogenetic signal between male genitalia and non-genital characters in insect systematics. *Cladistics* 26: 23–35.

Soto IM, VP Carreira, JJ Fanara, E Hasson (2007) Evolution of male genitalia: environmental and genetic factors affect genital morphology in two *Drosophila* sibling species and their hybrids. *BMC Evol Biol* 7 (77): 1-11.

Suchard MA, RE Weiss, JS Sinsheimer (2001) Bayesian selection of continuous time Markov Chain evolutionary models. *Mol Biol Evol* 18: 1001–1013.

Swofford DL (2002) PAUP*. Phylogenetic Analysis Using Parsimony (*and Other Methods). Version 4. Sinauer Associates, Sunderland, MA.

Szekely T, GH Thomas, IC Cuthill (2006) Sexual Conflict, Ecology, and Breeding Systems in Shorebirds. *BioScience* 56(10): 801-808.

Tallamy DW, MB Darlington, JD Pesek, BE Powell (2003) Copulatory courtship signals male genetic quality in cucumber beetles. *Proc R Soc Lond B* 270: 77–82.

Tanabe T, T Sota (2013) Both male and female novel traits promote the correlated evolution of genitalia between the sexes in an arthropod. *Evol* 68: 441-452.

Tazzyman SJ, RM Seymour, A Pomiankowski (2012) Fixed and dilutable benefits: female choice for good genes or fertility. *Proc R Soc B* 279: 334-340.

Thornhill R, KP Sauer (1991) The notal organ of the scorpionfly (*Panorpa vulgaris*): an adaptation to coerce mating duration. *Behav Ecol* 2(2): 156-164.

Trivers RL (1972) Parental investment and sexual selection. In: Campbell B (ed.). *Sexual selection and the descent of man*. Aldine, Chicago, IL. pp. 136–179.

Tsurusaki N (2001) High incidence of gynandromorphs in a tetraploid parthenogenetic (probably facultative) harvestman, *Leiobunum globosum* (Arachnida, Opiliones). *Zool Sci* 18: 47.

Tsurusaki N (1986) Parthenogenesis and geographic variation of sex ratio in two species of *Leiobunum* (Arachnida, Opiliones). *Zool Sci* 3: 517-532.

Tsurusaki N (1985) Geographic variation of chromosomes and external morphology in the *montanum*-subgroup of the *Leiobunum curvipalpe*-group (Arachnida, Opiliones, Phalangiidae) with special reference to its presumable process of radiation (taxonomy). *Zool Sci* 2: 767-783.

Vahed K (2007) All that glisters is not gold: sensory bias, sexual conflict, and nuptial feeding in insects and spiders. *Ethology* 113(2):105-127.

Van Valen L (1973) A new evolutionary law. *Evolutionary Theory* 1: 1—30.

Venables WN, BD Ripley (2002) *Modern Applied Statistics with S.* Fourth Edition. Springer, New York. ISBN 0-387-95457-0

Venditti C, A Meade, M Pagel (2010) Phylogenies reveal new interpretation of speciation and the Red Queen. *Nature* 463: 348-352.

Venditti C, A Meade, M Pagel (2006) Detecting the Node-Density Artefact in Phylogeny Reconstruction. *Syst Biol* 55: 637-643.

Vincent JFV, UGK Wegst (2004) Design and mechanical properties of insect cuticle. *Arth Struc Dev* 33: 187-199.

Wedell N, C Kvarnemo, CM Lessells, T Trengenza (2006) Sexual conflict and life histories. *Anim Beh* 71: 999-1011.

Weir JT, DJ Wheatcroft, TD Price (2012) The role of ecological constraint in driving the evolution of avian song frequency across a latitudinal gradient. *Evol* 66: 2773-2783.

Wong BBM, U Candolin (2005) How is female mate choice affected by male competition? *Biol Rev* 80: 559–571.

Xie W, PO Lewis, Y Fan, L Kuo, M Chen (2011) Improving marginal likelihood estimation for Bayesian phylogenetic model selection. *Syst Biol* 60: 150–160.

Zatz C, R Werneck, R Macías-Ordóñez, G Machado (2011) Alternative mating tactics in dimorphic males of the harvestman Longiperna concolor (Arachnida: Opiliones). *Behav Ecol Sociobiol* 65: 995–1005.

Zwickl DJ (2006) Genetic algorithm approaches for the phylogenetic analysis of large biological sequence datasets under the maximum likelihood criterion. Ph.D. dissertation, The University of Texas at Austin.